University of Southern Queensland

FACULTY OF HEALTH, ENGINEERING AND SCIENCES

ENG4111 and ENG4112 Research Project

Towards two-dimensional infiltration measurement in complex and variable soil environments

A dissertation submitted by

Ned Skehan

In fulfilment of the requirements of
ENG4111 and ENG4112 Research Project

Towards the degree of
Bachelor of Engineering (Honours) (Agricultural)

Submitted October 2016

Abstract

The measurement of the infiltration rate in soil science has traditionally been a reasonable, but qualitative assessment of the physical characteristics of the soil. Monitoring how the infiltration rate changes over time gives insight into how the physical characteristics such as soil structure, changes. Quantifying this change is useful when assessing how mine site rehabilitation soils settle in the years following the burial of mining waste rock. The actual technique for measuring the infiltration rate is currently done as a point measurement, which is statistically unreliable for an average reading when the environment has a high level of variability within its physical characteristics. It was theorised that Electrical Resistivity Tomography (ERT) has the capability to quantify the infiltration variability that exists in complex soil environments which contains features including mining waste rock, textural variations, and structural anomalies such as varying degrees of compaction. This research investigated the use that a time lapsed measurement of soil moisture change over a two-dimensional transect has when attempting to track a wetting front through a soil profile. The project is broken into two distinct stages, developing a methodology for tracking a wetting front and applying the method to a variable soil to assess the accuracy. The first stage involves creating software protocols and inversion corrections that allow measurements of soil moisture to be corrected for time due to the ERT measuring in a successive technique with a specific order. As these corrections are developed and the order of measurement is known, the soil moisture across a two-dimensional transect can be measured repeatedly at a known time interval, allowing the quantification of the soil moisture rate of change, or the infiltration rate at every point along that transect. Once this method is developed, it is replicated on a variable soil, which contains a large buried rock, a textural change and a compacted region.

An irrigation system was developed to deliver the equivalent of an 8mm/hr rainfall event, and this was run while the ERT ran continuously, collecting a two-dimensional image of the profile every 60min. For the experiment on a variable profile, an anthropogenic soil was made, with buried features such as a rock, logs and a compacted section, with a texture change as the overburden. The same experimental procedure was then applied to this profile. Due to Terrameter malfunction an older model Terrameter SAS4000 was used to collect the variable profile data sets, which provided complications in analysis.

It was found that the ERT does have the capacity to locate stochastic variability in the underground pedology and geology, but does not deliver an infiltration rate accurate enough for scientific research. This is due to the ERT measuring at fixed depths, 13cm apart. The inversion software offers an improvement to this 13cm depth increment, however a lack of data density from the ERT prevented this improvement from being useful. Although the infiltration rate itself could not be parameterised explicitly from the data into minimum, maximum, and average infiltration rates, it was possible to identify that approximately 10% of the 5m wide irrigated section had a very high (relative to the profile) infiltration rate, while approximately 38% had a low rate, with two categories in between.

University of Southern Queensland

Faculty of Health, Engineering and Sciences

ENG4111 & ENG4112 Research Project

Limitations of Use

The Council of the University of Southern Queensland, its Faculty of Health, Engineering and Sciences, and the staff of the University of Southern Queensland, do not accept any responsibility for the truth, accuracy or completeness of material contained within or associated with this dissertation.

Persons using all or any part if this material do so at their own risk, and not at the risk of the Council of the University of Southern Queensland, its Faculty of Health, Engineering and Sciences or the staff of the University of Southern Queensland.

This dissertation reports an educational exercise and has no purpose or validity beyond this exercise. The sole purpose of the course pair entitled “Research Project” is to contribute to the overall education within the student’s chosen degree program. This document, the associated hardware, software, drawings, and any other material set out in the associated appendices should not be used for any other purpose: if they are so used, it is entirely at the risk of the user.

Certification

I certify that the ideas, designs and experimental work, results, analysis and conclusions set out in this dissertation are entirely my own effort, excepts where otherwise indicated and acknowledged.

I further certify that the work is original and has not been previously submitted for assessment in any other course or institution, except where specifically stated.

Ned Skehan

Student Number: 0061057365

_____

Signature

_____

Date

Acknowledgements

First thanks must go to my supervisor Dr John Bennett for his guidance and support through this project. His encouragement and resourcefulness whenever I came to him with a problem ensured the project remained on schedule and motivation was maintained. Plenty of time was spent discussing how the Terrameter can best be manipulated for infiltration measurement.

Thanks to David West and Will McCarthy from Agtronics for tackling this honours year with me head on, and with enthusiasm that ensured the project was seen through to completion for all of us.

Thanks to my family for listening to me try and explain what I was doing throughout the year, their patience and support as I used my explanation to them, to better understand complex phenomena myself was instrumental to my understanding of the topic.

Thanks to the NCEA for providing the Terrameter and all associated measuring equipment that goes with it. It is a sought after unit, so having loan of it for the better part of 6 months was extremely generous.

Thanks to Jenny Foley for a short notice loan of their Terrameter when a malfunction threatened the completion of the final experiment.

Finally, thanks to the University of Southern Queensland for allowing me the opportunity to undertake a thesis and contribute to the knowledge base within my chosen area.

Table of Contents

List of Figures

List of Tables

1.0 Introduction

1.1 Project overview

With the global population predicted to surpass 9.7 billion by 2050 (Nations, 2015), human reliance on the soil resource is paramount to our continued existence. In accordance with this, there is a requirement for the most efficient use of the soil system possible, so that we maximise food and energy production, without unduly degrading the soil resource. Quality of life and future development goals, globally, are contingent on this.

Critical then to this is the capacity to measure and analyse changes in a system, as well as to be able to describe/account for the complexities inherent within the system. Accurately, or at least sufficiently, monitoring changing components within the soil system provides managers' crucial information to take corrective action across a landscape or field, ensuring environmental degradation is limited, while production requirements are optimised. Soil physical properties describe the capability of a soil to provide a physical medium for plants to take hold and thrive within, whereby production is controlled by the soil hydraulic system, which in turn, governs water (infiltration), nutrient and solute dynamics.

Measurement of infiltration provides a sound indicator of soil physical properties describing numerous dynamic mechanisms, and more importantly a means to identify soil profile complexities. It is not a quantitative measurement of one aspect such as porosity, texture or structure, but a qualitative measurement of the overall system; it is a good indicator of whether a soil has the capacity to successfully host a plant. Reynolds et al (2002) detail the physical quality of a 'good' soil as one that is strong enough to hold plants upright, resist compaction and erosion; while being weak enough to allow roots and soil biology to have unrestricted movement and growth. This definition relies on the soil physical properties being of an adequate standard. Thus, it stands that the speed at which water moves into and throughout the profile would be an appropriate measure of the soil quality. By extension of this, it would also allow a means to identify zones of high, low and variable infiltration, which is in essence providing a description of the profile complexity and variability. However, this requires adequate resolution of infiltration measurement in the dimensions of interest (1, 2 or 3 dimensions throughout time), which is a function of measurement technique and the associated logistics.

Infiltration measurement method is traditionally taken with a standard infiltrometer, such as those described in Hillel (2003). There are a number of different variants of these tools; however they all follow the same concept of providing an elevated head over a single point and timing the duration for water to infiltrate the soil profile. This is a simple, cost effective and reasonably accurate measurement approach; however, it has the drawback of being a spatial point measurement. Under an arbitrary surface area of soil, there is always going to be an element of variation as the underlying pedology, and subsequent underlying geology, changes with the inclusions of physical obstructions such as rocks, right through to natural texture changes, and anthropogenic soil influences such as machinery compaction, depth to saprolitic layer, parent material and

rock outcrops. Using an infiltrometer at an arbitrary point may not be representative, as a whole, of the underground pedological and geological features. To overcome this, a large number of measurements must be completed to understand the minimum and maximum (variation) and average infiltration rates of an area. This becomes a very time-consuming and laborious task over large areas. Additionally, the basic infiltrometer takes near surface measurements. Hence, depth based infiltration, and the ability to visualise this, would require significant excavation. Thus, proximal sensing methods would be of benefit.

Near surface infiltration measurement may suffice for an intensive farming situation where the soil physical properties are reasonably homogenous with area and depth; i.e. not a highly variable and complex environment. However, the accuracy and applicability of this approach for highly variable and highly complex environments decreases as the variability and complexity increases. Such environments will become increasingly common in Australia, as open cut mine sites cease production and seek to reclaim and release land for agricultural production.

Within a mine site rehabilitation project, the interburden such as in Figure 1 that is used to fill the void left by the mining process consists of weathered rock such as sandstone and mudstone, amongst others, all in varying shapes and sizes. When these are replaced into the soil profile, they create stochastic variation where the occurrence and location of the rocks create a highly variable environment that is unable to be predicted by current means. Additionally, the soil profile is applied back over these interburden layers as in Figure 2. Hence, near surface point infiltration measurements become redundant as it measures only the replaced soil, and fails to provide information on the interburden. Additionally, the consequence of a point source is inept explanation of an unknown level of site variability with depth. This gives rise to the requirement for a new method of measurement that will account for the soil variation caused by standard rehabilitation practices.

Figure 1 Example of Interburden at New Acland mine demonstrating varying shapes and sizes of coarse fragments. Interburden on the front left and front right are from two sources, but will eventually be placed in the same soil profile.

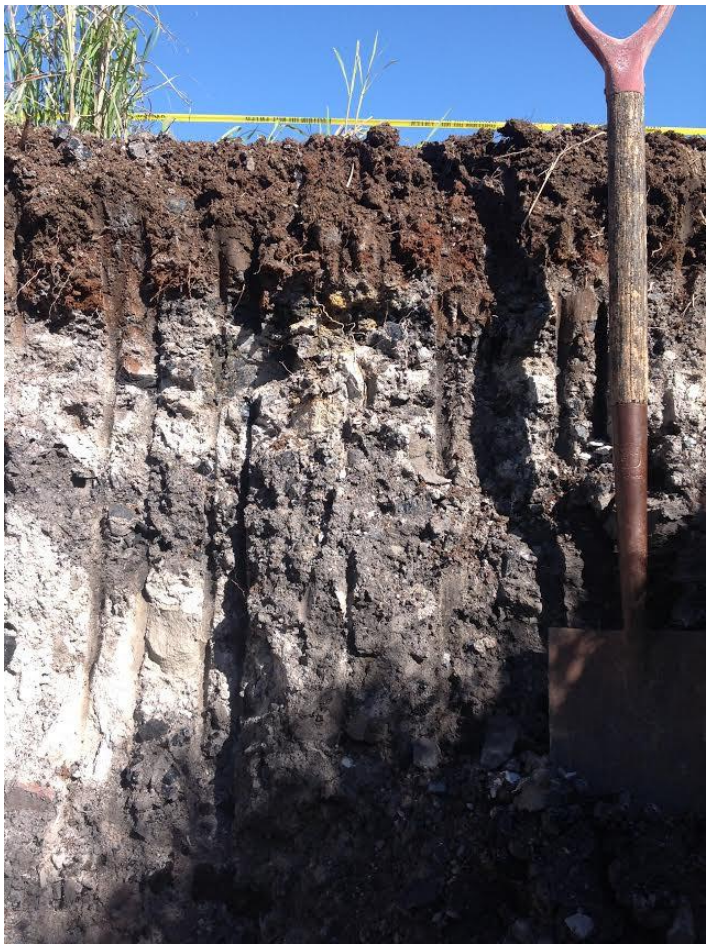

Figure 2 Soil profile of buried interburden with ≈30cm of soil as overburden. Note the heterogentiy of interburden colour (source) and coarse fragments.

With conditions for stochastic variability (e.g mine site rehabilitation) becoming more common, it is suggested that a two dimensional transect proximal imaging technique that identifies how the infiltration varies spatially should be developed. Statistically, this transect will provide a much higher chance of recognising the minimum, maximum and average infiltration rates across its length. In this case the absolute infiltration rate is of less value than understanding the level of stochastic variation. Subsequently, if the level of stochastic variation can be quantified, then the ability to account for this using a parameterised stochastic function within a soil hydraulic model (e.g. HYDRUS) is realised. HYDRUS uses a finite element mesh to model soil water dynamics within geometric parameters prescribed by the user. One of these input parameters is stochastic variability, where the expected variability parameters such as minimum, maximum, average and distribution can be randomly placed in the geometry. Hence, the ability to parametrise the stochastic variability, and account for this within HYDRUS, would effectively provide a tool to model complex and variable soil environments. Therefore, the primary issue becomes how to obtain a transect of infiltration data that parametrises the stochastic variability.

For this project, it is anticipated that Electrical Resistivity Tomography (ERT) will provide the means to locate infiltration variability, and possibly hydraulic conductivity over this

transect, using an ABEM Terrameter LS available from the National Centre for Engineering in Agriculture (NCEA). This technology is used extensively in geophysical studies to map rock formations or underground water (French & Binley, 2004; Greve, Acworth, & Kelly, 2008; Herman, 2001; M. Loke & Lane, 2004), which was the basis for its design. However, recent investigations have focussed on the application of this technology to soil science in the context of (Afshar, Abedi, Norouzi, & Riahi, 2015; Clément, Descloitres, Günther, Ribolzi, & Legchenko, 2009; Daily, Ramirez, LaBrecque, & Nitao, 1992; Garré et al., 2013). The ERT works as a computer with a power source and an array of electrodes, 64 for this project. In a prescribed order, the computer allocates DC current to these electrodes which transmits into the soil, where the soil features prevent some current from moving through them, dependent on their electrical conductivity. The current that is lost is measured on another prescribed electrode as a voltage drop, and through the use of Ohm's laws, is converted into an apparent resistivity reading. Using different combinations of electrodes allows the recording of information at various depths and locations along the transect line. With a data set of apparent resistivity at a range of locations within the two dimensional transect collected, it needs to be inverted into an actual resistivity reading using the software package RES2DINV. This gives a two dimensional transect image of the electrical resistivity throughout the profile, rather than a two dimensional transect image of the apparent resistivity's which are only relative to each other within the same soil profile.

Thus, changes in soil density, inclusion of variable rock fragments, complex cumulative fragment architectures, and changes in profile moisture content should all provide different resistivity responses. Hence, the aim of this project is to determine the capability of the ERT to parameterise variable and complex soil profile stochastic infiltration along a two dimensional transect, in order to inform future infiltration modelling of such environments.

1.2 Project objectives

Based on the aim of this work, the specific objectives of the project are as follows:

1. Develop a measurement method for an infiltration scenario that can be used in a highly variable soil environment that will at least locate the variability extremes, and potentially identify three parameters, the minimum, maximum and average infiltration rate, as well as the distribution of the infiltration variability.
2. Determine the method in which Terrameter LS measures so that the order of measurement may be manipulated to suit data analysis in a time-lapse situation.
3. Evaluate the strengths and limitations of this technology when measuring infiltration variability.

From the identified objectives, there are three distinct phases of the dissertation. The first is thoroughly understanding the function of the Terrameter so that it may be manipulated to suit the temporal and spatial resolution required for infiltration measurement. The second is taking a base line measurement and running the Terrameter continuously during irrigation with the correct settings and manipulated

protocols to collect the changing resistivity data on a fixed time-lapse. The third is data inversion and analysis so that a time lapse map of resistivity change, or infiltration will be produced.

The Terrameter is essentially a computer that assigns a direct current (DC) current through two current electrodes, and measures the voltage drop. The voltage drop is determined when the current reaches two other electrodes, in line with the current electrodes and between them, known as the potential electrodes; Ohm's law is subsequently used to calculate the resistivity. Different combinations of these electrodes give readings at various locations on the 2 dimensional transect, both along the transect, and at various depths, with the map of which being known as a 'pseudosection'. Four electrodes, in line and equally spaced, are required for measurement. The greater the spacing, the greater the point depth measurement. In a 64 pin line, any four pins with equidistance spacing can be used to provide a 2D depth based resistivity profile. Which electrodes are selected and in what order, is controlled by an .xml file that is supplied by the user and it is this file that can be manipulated to suit the situation required. Once the correct settings and files have been developed, a baseline type measurement is taken to identify the current state of electrical resistance in the soil, usually due to existing moisture or geographical features (ABEM, 2012). In this case, a drip irrigation line is then set up to apply water at a slow, controlled and known rate. As this occurs, the Terrameter is set to run continuously through its protocol so that as it finishes one cycle. It begins again until the soil water moves to a depth that cannot be measured, or until the soil moisture reaches an impermeable horizon, this being dependent on the environment, or until the experiment is terminated.

Resistivity 2D Inversion (RES2DINV) software will then be used to invert the apparent resistivity data into an actual resistivity data set that will determine where the soil moisture is changing at various locations throughout the profile. This enables data to be graphed in their respective time-lapsed intervals in a program such as Microsoft Excel or Matlab. The process of inversion and analysis is to be developed as part of this research project, so it will be subject to change as strengths and limitations of various methods are discovered and tested.

1.3 Assessment of consequential effects

The consequential effects of this research project can be split into two subsections, those that are contributed to by the project work itself, and those that eventuate from the resulting methodologies that will be developed.

The primary impact of the project work itself is the potential removal of soil cores to assess soil moisture. It is recognised that the samples taken remain in the whole ownership of the landowner and they must be returned to the site at the conclusion of analysis and kept free from all manner of chemical, physical and biological contamination whilst in the care of the project staff on the university premises. The landowners have been consulted and are aware of the processes required.

There is also the requirement to dig a pit to bury rocks and create compaction to simulate a variable soil environment. The excavation site has been recommended by the landowners with the agreement that the buried material will be removed and top soil replaced at the conclusion of the project. They are aware that it will be degraded to some extent but are understanding and willing for the excavation to take place and have offered to use their own machinery to complete the operation. The excavation site is within 200m of a natural waterway and over a known underground water source so care must be taken to ensure contamination by rubbish and chemicals is minimized. The water that will be used for the infiltration tests will be taken from the bore that exists in the underground water source, without any chemical additions. This will prevent foreign liquids from entering the natural waterways.

The soil is of a coarse texture which means the placement of electrodes will likely encounter contact issues due to air gaps from the porosity within the soil, potentially reducing the effectiveness of the measurement technique. To resolve this, a mixture of water, salt, and bentonite will be used to run down the small electrode hole at each electrode to improve contact. The solution that is added to the system will not be able to be removed. However, whilst the salinity of the mixture is high, the amount for each pin is very small, meaning subsequent dilution due to rainfall will render the salinity effects as inconsequential. The landowners are aware of this and are confident that the salinity levels required for the project will not hinder plant growth.

The consequential impacts of the project results are likely to include providing options to measurement techniques. The project aims to identify the potential that ERT brings to quantifying soil infiltration variability. This does not replace previous techniques, but seeks to provide new options to researchers and others interested in soil/water interactions. If the project proves a success, it should be noted that uptake of the proposed method requires ERT equipment, which is a very large economic investment.

2.0 Literature Review

2.1 Introduction

The past several decades have seen the human population increase at a significant rate, with the primary driver being the mechanisation of food production which has enabled more people to survive from the same arable land area. This increasing population however, has also become very energy dependent with mine sites, to some extent, competing with agriculture for use of the natural resources. As mining companies only have a certain amount of resource to extract, once a mines life has been completed, the land is usually rehabilitated to previous use, as an anthropogenic soil. Such sites, together with some other marginal agricultural soils, are renowned for being highly variable in their physical and chemical make-up leading to challenging measurement.

Within the area of soil science research, some of the methods for soil data capture are relatively dated, one of which is the measurement of soil water infiltration rates, or the hydraulic conductivity of a soil. As this is a natural process, it is, like all things in nature, highly dependent on a large range of factors such as soil texture, soil structure, geological features, ion balances and compaction. This variability can often happen over quite short distances which makes measurement potentially inaccurate if the equipment is limited to a point style measurement. For this reason it is aimed that the existing technique of Electrical Resistivity Tomography (ERT) could be used to measure the change in soil water content across the length of a 2D transect of the soil profile, as opposed to a single point along that distance. Understanding the extent of the variability across this transect is very important as an input parameter for existing infiltration models. Quantifying the extremes of variability leads to more accurate outputs from existing models. With the current measurements of hydraulic conductivity, measuring the absolute minimum and maximum conductivity rates becomes labour intensive as many samples must be collected to ensure statistical confidence.

Therefore the scope of this literature review will be to identify and discuss current empirical formulas used in infiltration calculations, discuss existing 2D measurement techniques for soil moisture profiles, and discuss current uses of ERT in agriculture and identify where similar research has already been completed.

2.2 Background research in infiltration

Infiltration is the term given to the process where water enters the soil at a specific rate, usually measured as distance/time (Hillel, 1980). (Horton, 1941; Zhang, 2011) note that initial moisture content, rainfall intensity, soil texture and soil structure are the leading determinates in controlling the water infiltration rate of a soil. In order to include these factors, a number of empirical models have been developed to determine infiltration rates and total infilled volume after a given time. These models will be the focus in this section of the literature review. They will be discussed and compared.

1. Darcy's Law

$$f = K\left[\frac{h_0 - (-\psi - L)}{L}\right]$$

Where

$$K = Hydraulic\ Conductivity$$
$$h_0 = Depth\ of\ ponded\ water$$
$$\psi = Wetting\ front\ soil\ suction$$
$$L = Depth\ of\ subsurface\ ground$$

(Mays, 2010)

Darcy's equation above forms the basis of describing movement of water through soil. It is stating that the infiltration rate is proportional to the hydraulic gradient (Kirkham, 1972). Darcy's law is considered a governing principle from which a range of models were derived. The earliest being Richards (1931) who uses Darcy's law along with conservation of mass equations to develop two infiltration equations. Solving these however is challenging without the use of computer software due to the equations requiring iterative solutions (Ross, 1990). Researchers such as Ross (1990) are developing efficient models to solve these equations. Darcy's law applies to saturated flow in a non-swelling porous media.

2. Richards Equation

$$\frac{\partial \theta}{\partial t} = \frac{\partial}{\partial z}\left[K(h)\left(\frac{\partial h}{\partial z} - 1\right)\right]$$

Where

$$h = Pressure\ head\ (m)$$
$$\theta = Volumetric\ water\ content\ \left(\frac{m^3}{m^3}\right)$$
$$K = Hydraulic\ conductivity\ (ms^{-1})$$
$$z = Depth\ (m)(positive\ downwards)$$
$$t = Time\ (s)$$

The Richards equation was developed in 1931 in response to the Darcy equation being limited to saturated flow. Richards (1931) explains that unsaturated flow follows the laws of hydrodynamics where the primary drivers are gravity and the liquids pressure gradient force. With these two forces acting on a liquid in the soil, Richard developed a partial derivative equation that described the flux of water through the vadose zone that requires an iterative solution due to dependence on K and θ (Varado, Braud, Ross, & Haverkamp, 2006). The Richards equation itself has no explicit solution, however it has formed the basis of a number of different models that have created numerical solutions through different mathematical methods (Brebbia & Walker, 2013; Hornung & Messing, 1981; Neuman, 1973; Pan, Warrick, & Wierenga, 1996; Redinger, Campbell, Saxton, &

Papendick, 1984; Ross, 1990; Simunek, Huang, & Van Genuchten, 1998; Zarba, Bouloutas, & Celia, 1990; Zienkiewicz & Parekh, 1970).

3. Green-Ampt

$$F(t) = Kt + \psi\Delta\theta \ln\left[1 + \frac{F(t)}{\psi\Delta\theta}\right]$$

Where

$$K = Hydraulic\ Conductivity\ \left(\frac{cm}{hr}\right)$$
$$\psi = Wetting\ front\ soil\ suction\ (cm)$$
$$\theta = Water\ content$$
$$F = Volume\ already\ infiltrated$$

As F is on both sides of the equation, it must be estimated initially (usually the larger solution of $Kt\ or\ \sqrt{2\psi\Delta\theta KT}$), solved on the right hand side, then the solution used for the second iteration. This is repeated until LHS=RHS. Once the F has been found at the required time, it may be subbed into the corresponding infiltration rate equation.

$$f(t) = K\left[\frac{\psi\Delta\theta}{F(t)} + 1\right]$$

Where

$$f(t) = Infiltration\ rate$$

(Mays, 2010)

The Green-Ampt model is a difficult equation to work with considering it is still an iterative solution; however it has the benefit of having definitive parameters that can all be determined experimentally, and in some instances, empirical values for the soil type can be assumed without the need for experimenting. With this, the Green-Ampt has become popular in computer modelling as the computer has the power to complete iterations in a timely manner.

Limitations of the Green-Ampt model primarily revolve around the assumptions that it makes regarding the initial moisture content being uniform throughout the profile; having an initial ponded head of water; a constant hydraulic conductivity and a constant suction at the wetting front (King, Arnold, & Bingner, 1999). These all rely on the soil being homogenous with no variation in soil physical properties, which is unlikely to exist in a natural environment. Mohammadzadeh-Habili and Heidarpour (2015) identify a range of conditions that occur in different layered situations, such as when piston flow occurs over preferential flow and vice versa. They also identified that the hydraulic conductivity cannot be determined for lower layers when the upper layer has a lower permeability. These are reasonable limitations of the Green-Ampt model, however it still remains an efficient and accurate model in the situation of excess rainfall and flood irrigation whilst under ponded head conditions.

4. Horton

$$f_t = f_c + (f_0 - f_c)e^{-kt}$$

Where

$$f_t = Infiltration\ capacity\ \left(\frac{depth}{time}\right)\ at\ time\ t$$
$$f_c = Infiltration\ rate\ of\ saturated\ soil$$
$$f_0 = Infiltration\ rate\ of\ unsaturated\ soil$$
$$k = Decay\ constant\ specific\ to\ the\ soil$$

(Horton, 1941)

Horton's model can also be modified to suit a volumetric measurement rather than the infiltration rate that is shown above.

Horton's model is the most common selection for most hydrologists since it incorporates a saturated or steady state infiltration rate which is different to the initial or unsaturated rate. Zhenghui et al. (2003) notes that this difference is due to factors influencing the properties of the surface soil and how the initial moisture is adsorbed, rather than the preferential or matric flow that occurs at depth. The advantage of using Horton over Kostiakov, is that there is an initial finite condition, f_0 (Hillel, 1980). The limitation of the Horton model is the time consuming application of using field-gathered measurements as the constants in the empirical equation (Hillel, 1980). The Horton model itself is a simplification of the Richards equation where the soil water diffusivity (D) and the hydraulic conductivity (K) are assumed not to be a function of the soil moisture, when in fact they are. However by making this assumption, the Horton equation becomes solvable making it simple to use.

5. Kostiakov

$$f(t) = akt^{a-1}$$

Where 'a' and 'k' are empirical values.

(Kostiakov, 1932)

Much like Horton's model, integrating Kostiakov's equation will give a volumetric solution, rather than an instantaneous rate.

Instead of needing to resolve the equations repeatedly, approximate models were developed to require a certain selection of input parameters, in order to deliver the closest approximation possible. These have been developed for field application because of their ease of use. However in accordance with their simplicity, there are certain assumptions that limit their accuracy, such as an even and consistent wetting front to the depth of the profile which is more correct for sandy soils compared to clay soils (Kutilek, 1988).

The Kostiakov equation is an empirical equation that was the best curve fit available from measured field data (Turner, 2006). Fox, Phelan, and Criddle (1956) developed a type of test function that allowed the values of 'a' and 'k' to be determined. In addition, their function presented as a linear solution if the Kostiakov equation could be applied, and nonlinear if it were an incorrect fit (Naeth, Chanasyk, & Bailey, 1991).

The Kostiakov equation was found to be more accurate than the Philip model for irrigated fields where the spatial variability in the infiltration data was larger (Ghosh, 1980), but less accurate for semi-arid rangelands, typically those found throughout the United States and Australia (Gifford, 1976). This finding led Gifford (1976) to believe that the constants used in the Kostiakov equation were more comparable to vegetation indices rather than factors influencing the soil conditions.

6. Philip

$$f(t) = \frac{S}{2} t^{-\frac{1}{2}} + C_a$$

Where

$$S = Sorptivity$$
$$C_a = Constant$$

(Philip, 1957)

The C_a constant is a value dependant on the initial water content, and the application rate (Turner, 2006).

The Philip model was developed as a solution to the Richards equations that used Darcy's law as a fundamental (Turner, 2006). The solution is provided for horizontal and vertical infiltration under a range of conditions. It can be seen that although different methods have been taken, the Philip model is quite similar to the Kostiakov equation previously discussed. Youngs (1968) developed a number of solutions to estimate accurately, the sorptivity factor and the C_a term. The methodology followed for this estimation is beyond the scope of this literature review. The Philip equation is limited to a homogenous soil under ponded conditions with uniform initial moisture content, and is subsequently limited much like the Green-Ampt model, but without the need for an iterative solution.

7. Holtan

$$f_p = GIaSA^{1.4} + f_c$$

Where

$$SA = Available\ storage\ in\ A\ horizon$$
$$GI = Growth\ index\ of\ crop\ (\%\ from\ maturity)$$
$$a = A\ constant\ of\ surface\ connected\ porosity$$
$$f_c = The\ steady\ state\ infiltration\ rate\ estimation$$

SA is calculated as:

$$SA = (\theta_s - \theta_i)d$$

Where

$$\theta_s = Saturated\ water\ content\ of\ the\ soil$$
$$\theta_i = Actual\ volumetric\ water\ content$$
$$d = Depth\ of\ A\ horizon$$

(Holtan, 1971)

The Holtan model is based on empirical values that are readily available to the public, regarding a whole range of soil types commonly farmed for agriculture (Turner, 2006). It is based on the concept that the governing factors in the infiltration rates are the current volume of water in the soil, the volume of water at saturation, and other influences in the A horizon such as root activity and preferential flow paths (Rawls, Ahuja, Brakensiek, & Shirmohammadi, 1993).

There are comprehensive tables available for substitution of variables into the initial Holtan equation; however the challenge occurs when deciding what depth to calculate SA to as this becomes quite subjective (Ortiz-Reyes, 1979). It is also noted that the Holtan equation makes no reference to time, as it makes the infiltration rate a function of water storage (Turner, 2006). There are methods making reference to time but they include solving another water storage equation simultaneously and this is out of the scope of this review.

All these methods have their strengths and weaknesses, the challenge lies in selecting the correct equations for the situation at hand. The scope of this project is to locate and quantify infiltration variability, not to develop an infiltration model as these are already in abundance, and widely accepted as being adequately developed. It is intended that an accurate understanding of the infiltration variability will provide the means for an increased level of accuracy within existing models.

2.3 Variable infiltration environments

The aforementioned models and formulas for measuring soil water infiltration are filled with empirical values, constants, and variables that are specific to a certain soil in a particular environment. They are all point style calculations that are accurate for their given purpose, however using them in an environment where the infiltration will vary considerably due to geological features, compaction and textural changes requires a multitude of measurements combined with interpolation and extrapolation to achieve an accurate average and a comprehensive understanding of the variability parameters. These variable environments exist and are made up of a range of impermeable features.

2.3.1 Causes of variability

Consider the following Figure 3.

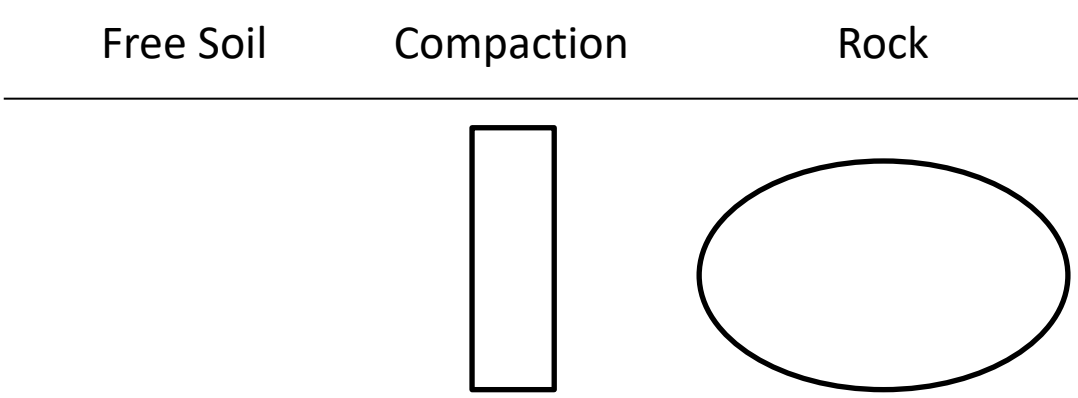

Figure 3 Infiltration variability factors

Under the free soil condition, the infiltration rate will be purely dependent on the texture, organic matter, initial moisture content, and porosity (Morin & Benyamini, 1977). Under the compaction condition, the infiltration rate will be dependent on the same factors, but lower due to a reduction in soil porosity. And under the rock condition, the infiltration rate will be limited to the permeability of the rock, which is dependent on the extent of fracturing and the resulting pore network.

Brouwer, Prins, Kay, and Heibloem (1988) identify common soil infiltration rates as follows:

- Clay 1-5 mm hr^{-1}
- Clay loam 5-10 mm hr^{-1}
- Loam 10-20 mm hr^{-1}
- Sandy Loam 20-30 mm hr^{-1}
- Sand < 30 mm hr^{-1}

These values are derived from a saturated flow experiment on soils that were not cultivated, conducted by researchers from the Food and Agriculture Organisation (FAO). They were not collected from various data sets around the world, however they were measured on soils that were classed according to the Soil Map of the World produced by the FAO and United Nations Educational, Scientific and Cultural Organisation (UNESCO), which is quite similar to the USDA Soil Taxonomy. Although the infiltration rate is highly dependent on a range of factors, the above rates give a reasonable ball park figure. They are suitable for the purpose of comparison with compaction and rock features.

Douglas and Crawford (1993) found that under a severe trafficking situation in a sandy loam grassland system, infiltration was reduced by as much as 76%, with recorded values of 26.9 mm hr^{-1} down to 6.3 mm hr^{-1} due to a reduction in the macro pore volume. Ryan, Monroe, Kacemi, and Monem (1990) found that under compacted clay, soil infiltration was reduced by 60% in the 0-15cm range, 80% in the 15-30cm range, and 55% in the 30-205cm range, all to values less than 2 mm hr^{-1}, with 0.5 mm hr^{-1} at depth using a 'conventional' tractor.

Caputo and Carlo (2011) examined infiltration rates on a hard sedimentary, fractured limestone rock and a soft sedimentary rock, calcarenite. They report that under laboratory conditions where preferential flow paths such as cracks and fissures are excluded, the limestone had an infiltration rate of 0.875 mm hr^{-1} which they attribute to the rock porosity. The calcarenite was found to have an infiltration rate of 20 mm hr^{-1} however they note that cracks and fissures were not excluded due to the aggregate arrangement being crumbly with large preferential flow paths networked throughout the sample.

These three different situations are represented graphically to demonstrate their comparison in Figure 3.

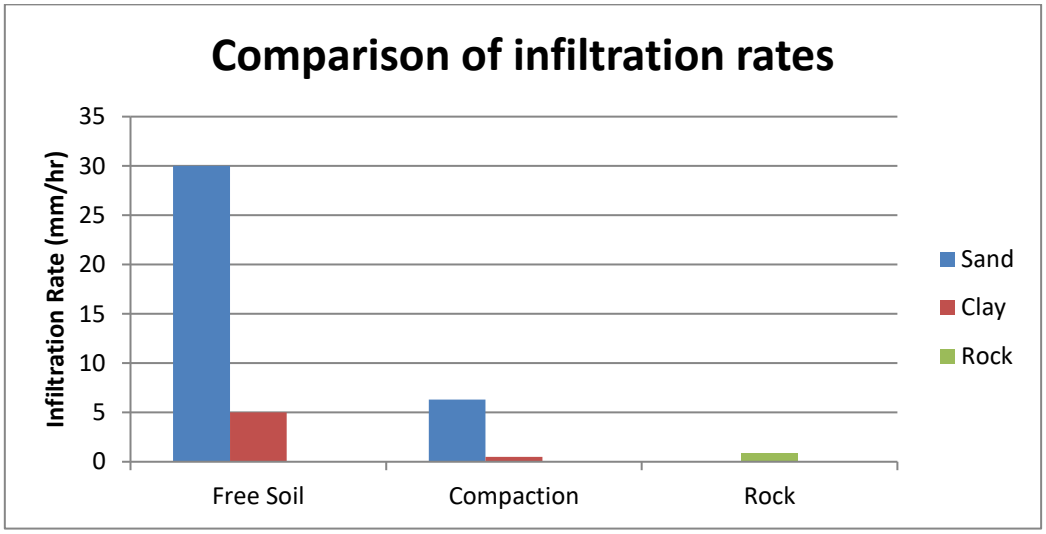

Figure 4 Comparison of infiltration rates

Although the above graph is a collection of various datasets in different locations collected for different research purposes, the point it makes is that as soon as rock and compaction are introduced, the infiltration rate of that profile becomes highly varied. Understanding where these disruptions occur and in what area of the profile is important when quantifying the average infiltration rate and the variability parameters as they will be highly influenced by these features.

Assume a 2D transect of 10m, with a random distribution of compaction and rock features throughout it. Taking a series of infiltration measurements with a traditional ring infiltrometer from the surface will require a very narrow spacing to ensure accuracy. However this becomes problematic as the water introduced to the system from each test may influence the adjacent sites if for instance, the water meets a rock and begins to flow laterally around the surface. If that spacing is widened to avoid this scenario, there is a likely chance that features will be missed. Statistically this is a very complicated situation as there may be a reading of 30 mm hr^{-1}, followed immediately by a 0.5 mm hr^{-1} measurement. This makes curve fitting very difficult as there will be large error bars and inaccurate averages associated with the infiltration rates.

2.3.2 Unsaturated and saturated flow

The infiltration rate that is officially recorded from an experiment is very important as it is dependent on the soil properties, and as the soil moisture content increases throughout the trial, the properties will change from unsaturated to saturated. Such change directly affects the infiltration rate as reviewed in the previous models and equations.

In saturated flow, both the micro and macro pores are filled with water and transmission through the profile is driven by large differences in pressure and gravity (Singer & Munns, 2006). Movement in a coarse-grained soil under this condition can be quite fast if there is no stratification between horizons and there is a ponded head on the surface. When the soil is unsaturated, the macro pores have been emptied by gravity and the surface area of the pore network becomes the critical factor with respect to how much water is retained and the ease of its movement (Oades, 1984). The water that remains becomes tightly held in thin films around the interior surface of the pore network. This hinders soil water movement considerably as hydraulic friction is increased as the width of the water film is decreased (Singer & Munns, 2006). This means that movement is no longer driven singularly by gravity, but by a potential gradient (ψ) consisting of gravity (ψ_g), pressure (ψ_p), matric potential (ψ_m), and solute (osmotic influence) (ψ_s) (Singer & Munns, 2006). The addition of a matric and solute potential create a higher infiltration rate than under a saturated situation.

The change from being driven by gravity and pressure, to a potential gradient occurs over a different time period for all soils. However the trends are the same. Consider Figure 55. As the cumulative infiltration increases, which is equal to the soil moisture, the infiltration rate decreases as the matric and solute potentials are equilibrated and gravity and pressure become the driving factors. As the infiltration rate decreases, it approaches an asymptote that is termed the “basic infiltration rate” (Walker, 1989).

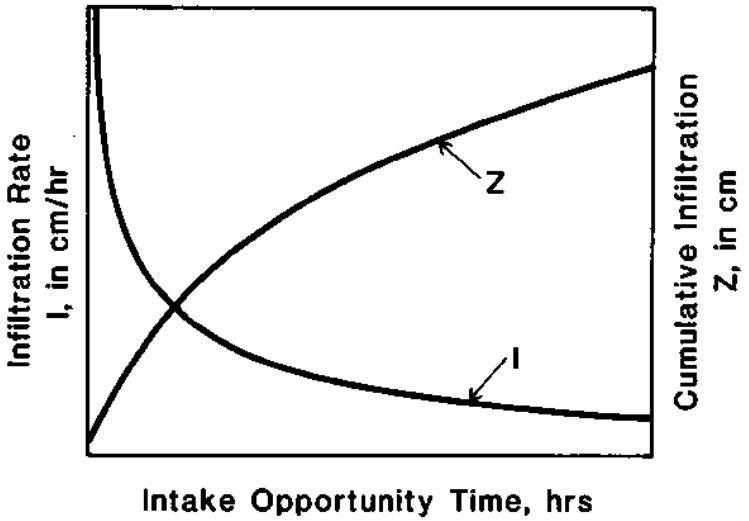

(Walker, 1989)

Figure 5 Infiltration change with time

2.4 2D Measurement of soil moisture profiles

Soil moisture measurement can be performed through a variety of methods. These methods are generally classified into three categories, the direct measurement, indirect measurement, and soil water potential measurement (Organization, 2014). Each of these have their own limitations and benefits which creates a framework of questions that allows the correct measurement technique to be selected based on the requirements and limitations of the specific project. For instance, broad scale measurement, site specific measurement or destructive measurement methods all contribute to the preferred measurement technique chosen. These measurement techniques are broken into three categories and consist of the following (Organization, 2014).

1) It is determined whether the measurement needs to quantify soil water or soil water potential. Gravimetric soil water is important for compaction type projects such as machinery in agriculture or civil construction sites, but soil water potential is important to agronomy in agriculture due to the plants physically creating a negative pressure in order to suck water from the soil. Water in the soil is not available to plants if the suction required is beyond the wilting point of the plant.
2) Direct vs indirect methods. Direct measurement is destructive as the sample needs to be removed from the environment and taken to a laboratory. Thus, if a broad scale understanding is required from this method, there is a need for a large area of representative soil that can provide a multitude of samples to achieve an accurate result. This involves a lot of labour and is destructive to the environment. The alternative is an indirect measurement where equipment is placed in the soil to measure a soil property that is known to strongly influence the moisture status, such as conductivity.
3) Understanding the applicability of each method in terms of the regional resources such as labour to undertake sampling, the quality of the equipment available such as a laboratory or measurement instruments, and the knowledge base of the people involved when using advanced equipment or undertaking data processing.

2.4.1 Direct measurement and interpolation

Direct measurement refers to the physical removal of a sample from the soil environment and quantifying water content as gravimetric moisture content and involves large amounts of time, labour, and is destructive to the test site. Currently, oven drying is the only truly direct measurement of the gravimetric moisture content.

Oven drying

Oven drying of soils is the most widely accepted method of determining the soil moisture as a percentage of the dry weight, known as the gravimetric water content. There is a standard associated with the testing method making it a consistent and accurate method for measuring soil moisture. Within that standard, there are three different methods regarding fine, medium and coarse-grained soils. Each method requires a minimum amount of soil to be dried in a thermostatically-controlled oven for

a certain amount of time (Australia, 1990). Once the standard has been followed, there is a formula to be completed to calculate the moisture content as a percentage of the soil's dry weight.

$$MC\% = \left(\frac{W_2 - W_3}{W_3 - W_1}\right) * 100$$

Where

$$W_1 = Weight\ of\ tin\ (g)$$
$$W_2 = Weight\ of\ moist\ soil + tin\ (g)$$
$$W_3 = Weight\ of\ dried\ soil + tin\ (g)$$

This method is limited to obtaining a spatial point measurement of the soil moisture, so when measuring the variation over a 2D transect, regular samples need to be taken and the values between them interpolated. This is a very time consuming method as drying takes approximately three days and samples have to be weighed before and after drying. Although each measurement is accurate, in a highly variable soil the statistical chances of collecting data on each end of the variability spectrum is so slight that there is no literature identifying how many samples are required to confidently understand the variation in different soil conditions. Wang, Engman, and Ungar (2010) used oven dried samples at 50m spacings for a long transect as a ground proofing technique to test airborne moisture instruments and noted that no quantitative assessment was made when investigating the variability parameters.

This inability to quantify the variability parameters makes creating a 2D transect of infiltration over any distance, an inefficient and expensive operation when using the oven drying method.

2.4.2 Indirect measurement techniques

Indirect measurement techniques enable repeated measurements of a sample without disturbing the soil for each sample thus the soil is left in the environment and monitored as the volumetric moisture content, independent of the soil physical properties such as soil density (Organization, 2014).

Soil water dielectrics

The dielectric constant is sometimes known as the permittivity and is a ratio of the electrical forces that exist in the soil medium between two electrodes, and the forces that would exist if it were a vacuum (Hanson & Peters, 2000). It is generally around 2-4 for a dry soil, and around 81 for water, indicating that as the moisture of the soil increases, so does the dielectric constant. It is also useful for negating the effects that texture have on the electrical properties of a soil as the dielectric constant of water is approximately 20-40 times larger making it far more influential than the soil properties. This holds until the moisture content is very low as soil properties will have more of an impact due to the dielectric constant becoming more closely aligned with that of dry soil. Currently, there are two methods to determine this constant: a capacitance probe which utilises frequency domain reflectometry, and time domain reflectometry.

Capacitance probes measure the dielectric constant of a soil by creating an oscillating electrical field between two rings within a tube. This field extends through the wall of the capacitor, usually made of PVC, and into the soil medium. The frequency of this oscillation changes with the moisture in the soil medium and this is what is monitored and related back to the dielectric constant, and subsequently the volumetric soil moisture (Dirksen, 1999). Capacitance probes are widely used and regarded as an accurate means of determining soil moisture given that they are calibrated correctly. T. J. Jackson (1990) notes that the most consistent and accurate method of calibrating a capacitance probe is using it in a liquid of known dielectric properties. This method will give results with less variability than most dielectric models will predict.

Time-domain reflectometry is quite similar to a capacitance probe; however instead of measuring the change in the oscillation frequency, it measures the magnitude of a return pulse from the end of a transmission line. This electromagnetic pulse is generated by a pair of parallel rods that push it along a transmission line into the soil, part of which is adsorbed, and part reflected. In the soil, the return wave is due to a step decrease meaning the reflection has the opposite signal to the generated wave (Hoekstra & Delaney, 1974; Topp, Davis, & Annan, 1980). The intensity of this return wave can be measured and related to volumetric soil moisture.

Radiological methods

Radiological measurements of soil water occur via two methods. The first and most commonly used involves quantifying and understanding how high energy neutrons interact with hydrogen atoms in the soil, generally being in the soil water. The second is usually reserved for laboratory measurement due to gamma radiation being more dangerous to work with and involves quantifying the attenuation of a gamma wave as it moves through the soil environment.

Fast neutron attenuation is completed using a neutron moisture meter, an instrument consisting of an aluminium access tube which is lowered into the soil with a fast neutron emitter and a slow neutron counter. The neutron is emitted at a high energy, the value of which depends on the source, and sends it into the soil environment. Energy is lost from these neutrons as they strike atoms of the same weight, primarily hydrogen (Brady & Weil, 1984). This reduces the velocity of the neutron by a factor of up to 500. These slower neutrons then enter the ‘slow’ neutron counter, usually a helium tube which emits a photon for each ‘slow’ neutron that strikes it. This photon strikes a thin wire in the access tube and creates an electrical signal that is recorded. The number of ‘slow’ neutrons that is recorded is approximately proportional to the number of hydrogen atoms in the soil and since most of the hydrogen exists in the form of water, the volumetric soil water can be calculated for a given sphere of influence. This sphere of influence is measurable, and is dependent on the dryness or wetness of a soil, dryer being a larger sphere (E. L. Greacen, 1981; Visvalingam & Tandy, 1972). Neutron moisture meters require delicate calibration which should be done in the soil. Once set, they can provide repeatable data at the same depth whenever required throughout a project or season. The technique is limited however due to the interference of hydrogen in the clay and organic fractions of the soil. E. Greacen, Correll, Cunningham, Johns, and

Nicolls (1981) found that incorrect calibration of a specific test site generated errors from soil hydrogen influence to affect results by up to 40%. They note that other minerals exist that have tendencies to absorb neutrons such as Boron and Iron, however they conclude that while calibration is difficult, when done correctly, neutron scattering techniques are a reliable and repeatable method of soil water measurement.

Gamma wave attenuation techniques have largely been reserved for laboratory measurements since dielectric techniques became available for field use. The method of gamma-ray attenuation involves propagating a gamma wave along a thin layer of soil approximately 25cm under the surface. The scattering and absorption of these waves is driven by the density of the medium the wave encounters, so assuming the dry density of the medium remains unchanged, the change in density will come from a change in water content. This provides the grounds for measuring the soil moisture as a function of a change in saturated density (Susha Lekshmi, Singh, & Shojaei Baghini, 2014). The limitation of this technique in a field situation arises when the dry density changes, which can be influenced by plant roots pushing into the top 25cm, as well as compaction from machinery or livestock on the surface.

Soil water potential

Measuring the soil water potential is done with three different instruments, tensiometers, resistance blocks and psychrometers. These are all similar in that they use a porous material to measure a negative pressure.

Tensiometers consist of a small ceramic cup on the end of a sealed plastic tube. When saturated and placed in the soil, the water will move from the ceramic into the soil matrix to achieve equilibrium. This water movement from the ceramic outwards creates a negative pressure through the plastic tube which is registered on a recording instrument at the top (Marthaler, Vogelsanger, Richard, & Wierenga, 1983).

Resistance blocks consist of a small block of porous material where two electrodes are placed a known distance apart. As the soil water moves into the ceramic block to reach equilibrium, the electrodes measure the resistance between them. As they are dependent on an electrical current, salinity will influence results and must be taken into account (Werner, 1995).

Psychrometers are primarily used for laboratory measurements and require extensive calibration when used in the field. They work via a thermocouple inside a porous chamber that is cooled to condense water. As this water is then evaporated there is a change in temperature and a current is produced along a wire which is measured by a meter (Merrill & Rawlins, 1972).

2.4.3 Other geophysical techniques

The measurement of soil moisture has taken a technological leap over the last two decades in line agricultural technology development in general. The uptake of Global Position Systems (GPS) use, satellite imagery and remote sensing has facilitated the development of a range of new soil moisture measurement methods. They will be discussed in this section and classified as geophysical techniques as they are widely

adopted across a broad range of industries such as agriculture and mining, and government compliance agencies.

Ground penetrating radar

Ground penetrating radar (GPR) uses electromagnetic waves at frequencies between 50MHz and 1200MHz, depending on the depth required (Lunt, Hubbard, & Rubin, 2005). The mechanism consists of a transmitter and a receiver which propagates a wave at the desired frequency between the pair. The wave splits into three sections, the airwave that travels directly to the receiver, the ground wave which travels at the ground surface, and a reflection wave that travels through the soil to a certain depth and is reflected to the receiver. This reflection wave is manipulated by subsurface contrasts, with the primary contrast usually being soil moisture, unless there are major geological features buried within the reflection depth (Powers, 1997). Chan and Knight (1999); Martinez and Byrnes (2001); Van Dam and Schlager (2000) all showed that the driver of the reflection variation in a shallow surface, commonly at depths associated with agriculture, was volumetric water content because soil texture changes were not able to produce such large contrasts, and water was the only material in the soil environment that had a high enough dielectric constant to create the manipulation in the reflection wave. Huisman, Sperl, Bouten, and Verstraten (2001) found that existing calibration equations such as Topp's equation that are used for calibrating time domain reflectometry equipment can be directly used to calibrate GPR data. The only limitation that Huisman, Snepvangers, Bouten, and Heuvelink (2002) found when mapping spatial variation was that heavier textured soil increased the inaccuracy of the volumetric moisture reading, and this was to be expected due to the conductivity of clay particles. GPR has been proven to be an efficient method of collecting soil moisture data for larger areas as the resolution of large scale changes is captured and represented well on the variogram of the data when compared to time domain reflectometry (Huisman et al., 2002). This is due to time domain reflectometry being overly sensitive to changes in soil properties such as compaction, while GPR averages such influences over a larger area. This suggests that one technique is not better than the other, but that each are suited to different situations.

Microwave and thermal infrared

Microwave (MV) sensors have been the primary source of data for satellite based soil moisture readings since the 1980's. These measurements have typically come from passive and active microwave sensors (Fang, Hain, Zhan, & Anderson, 2016; R. D. Jackson, 1982; Njoku & Li, 1999; Owe, De Jeu, & Walker, 2001). These datasets are usually available as a purchasable product from space agencies around the world. The theory of how the sensor actually collects the data is the same across agencies; however the models that the data is fed into to give soil moisture readings vary, meaning that very rarely do the same datasets provide the same result of the actual soil moisture. The benefit of using active and passive MV's comes to the fore when cloud cover is an issue, as long as it is not precipitating (Fang et al., 2016). Fang et al. (2016) notes however that the MV data is largely distorted when vegetation is moderate to heavy, but suggests that thermal infrared (TIR) data has the potential to overcome vegetation, but is devalued by cloud cover. Each technique has their own benefits and limitations.

Electromagnetic induction

Electromagnetic induction (EM) techniques have been used for the last 30 years when identifying the spatial variability of soil moisture. EM measures the bulk conductivity of a soil by transmitting a magnetic field from one end of the device, and sensing the return field through a receiver coil. Depending on how far these coils are apart, the magnetic field will reach to a specific depth. The magnetic field that is induced produces 'eddy currents' throughout the soil profile to the known depth and induces a magnetic field within the soil. The strength of this secondary field is measured by the receiver and is dependent on the bulk conductivity of the soil to the nominated depth (Schneider, 2016). Kachanoski, Wesenbeeck, and Gregorich (1988) showed that the bulk electrical conductivity read by EM methods was responsible for 96% of the spatial variability in the soil moisture when ground proofed over locations with a range of volumetric soil moisture readings, and a range of different textures.

2.4.4 ERT as used in geophysical applications

ERT is used within the industry of geophysics through the direct current resistivity application to mapping subsurface geological features, locating groundwater sources and monitoring ground water pollution. ERT is used in engineering to locate subsurface features such as mineshafts, cavities, geological fault lines, underground permafrost, etc. and in archaeology to map buried ancient buildings (J. M. Reynolds, 2011). This resistivity method is based on Ohm's laws. An electrical current I (ampere) is passed through a medium of length L (metres). The material has a resistance R (ohm) which causes a voltage drop V (volt) across this length, presuming the material is homogenous within this range (L) (Caputo & Carlo, 2011). Ohm's first law in the form of a vector for current flow through a continuous media is given a:

$$J = \sigma E \tag{1}$$

Where

$$J = Current\ Density$$
$$\sigma = media\ conductivity$$
$$E = Electric\ field\ intensity$$

M. Loke and Lane (2004) note that more commonly, the medium resistivity is used and is the reciprocal of σ, meaning $\left(\rho = \frac{1}{\sigma}\right)$. The electrical field intensity (E) is not useful, however the electric field potential is, and the pair are related in equation (2).

$$E = -\nabla\Phi \tag{2}$$

It can be noted that the flux has been introduced with equation (2) which is a measure of the electrical flow through a unit area.

Combining these equations creates an equation for the current density (the flow of charge per time, over a cross sectional area), which is dependent on the conductivity and the flux over a given field.

$$J = -\sigma\nabla\Phi \tag{3}$$

In most resistivity surveys, the current originates from an electrode in the ground which is a point source located at (x_s, y_s, z_s) that influences an elemental volume (ΔV). Dey and Morrison (1979) investigated a numerical solution to solving 3D potential distributions around a point source of current and introduced the empirical function, the Dirac delta function (δ) in order to remove dimensions from the current density to form a relationship with current itself. This leads to the equation (4)

$$\nabla . J = \left(\frac{I}{\Delta V}\right) \delta(x - x_s)\delta(y - y_s)\delta(z - z_s) \tag{4}$$

When equations (4) and (3) are combined, the following is produced.

$$-\nabla \cdot [\sigma(\mathrm{x,y,z})\nabla\Phi(\mathrm{x,y,z})] = \left(\frac{I}{\Delta V}\right) \delta(x - x_s)\delta(y - y_s)\delta(z - z_s) \tag{5}$$

This is the equation that provides a graphical solution to the potential distribution in the ground resulting from a point current source (M. Loke & Lane, 2004). The numerical solution to this equation comes in the form of forward modelling equations that have been developed for a variety of different cases by different researchers.

Equation (5) is a complicated equation but can be graphically displayed for ease of understanding in Figure 6.

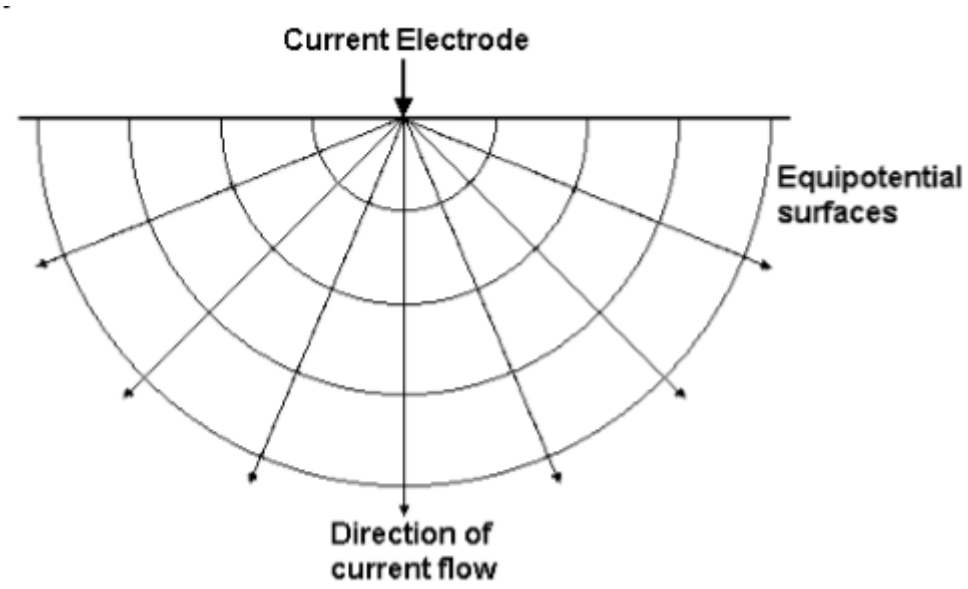

(M. Loke & Lane, 2004)

Figure 6 Flow of current from a point source with resulting potential distribution

Having a pair of electrodes distorts the field somewhat, but the potential lines remain symmetrical when the space is homogenous, see Figure 7.

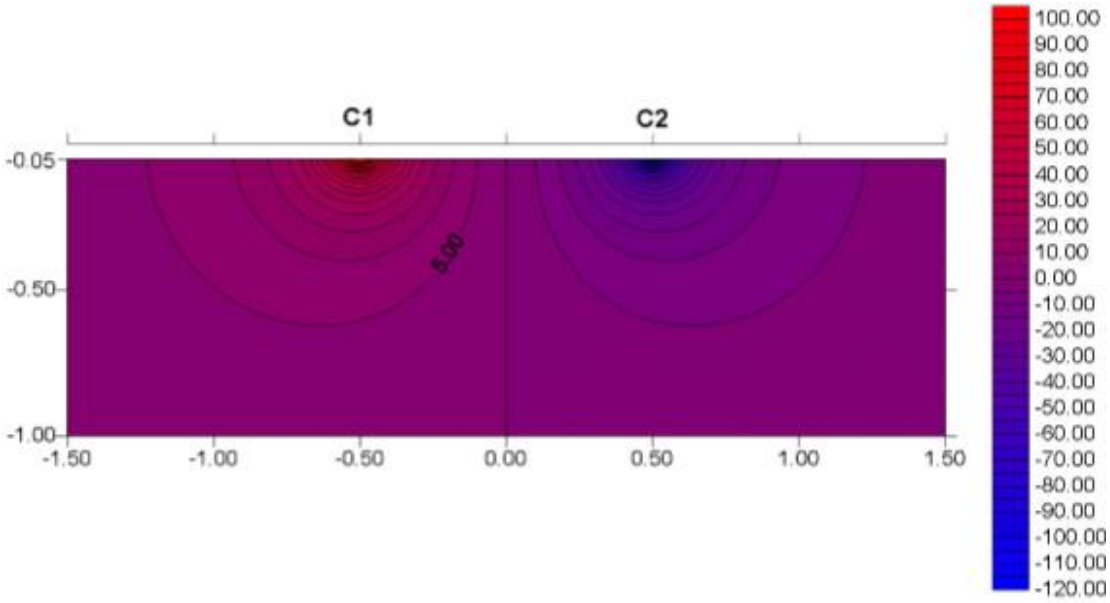

(M. Loke & Lane, 2004)

Figure 7 Distribution from two electrodes with 1 ampere of current and resistivity of 1 Ω.m

The numerical solution of equation (5) models how the potential is distributed out from a point source. In most surveys, the standard electrode configuration is two current electrodes (C1 and C2) that induce the current, and two potential electrodes (P1 and P2) that measure the voltage drop. They are arranged as displayed, Figure 8.

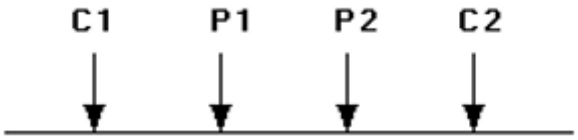

Figure 8 Standard electrode configuration

As equation (5) models the potential distribution, the potential at a specific point is found by manipulating the width between the electrodes. The wider they are, the deeper the resulting potential will be from the surface. When using a four electrode array, the calculation for the potential difference is as follows

$$\Delta\Phi = \frac{\rho I}{2\pi}\left(\frac{1}{r_{C1P1}} - \frac{1}{r_{C2P1}} - \frac{1}{r_{C1P2}} + \frac{1}{r_{C2P2}}\right) \tag{6}$$

Where

$$\Delta\Phi = Potential\ Difference$$
$$\rho = Medium\ Resistivity$$
$$r = distance\ between\ electrode\ combination$$

The limitation of equation (6) is that the potential difference found is on the assumption of a homogenous medium (M. Loke & Lane, 2004). As the majority of situations will undoubtedly be heterogeneous, the equation is changed to calculate the apparent resistivity.

$$\rho_a = k\left(\frac{\Delta\Phi}{I}\right) \tag{7}$$

Where

$$k = \frac{2\pi}{\left(\frac{1}{r_{C1P1}} - \frac{1}{r_{C2P1}} - \frac{1}{r_{C1P2}} + \frac{1}{r_{C2P2}}\right)}$$

k is the geometric configuration of the electrodes so it only needs to be calculated once for each trial, hence the allocation of it to a constant. k can also be calculated from a simpler approach for a given protocol. In this project, the Wenner protocol is used.

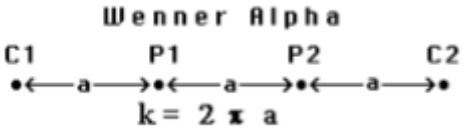

(M. Loke & Lane, 2004)

Figure 9 Calculation of geometric configuration constant

The Terrameter itself measures an apparent resistance value R which according to Ohm's law, is equal to $\frac{\Delta\Phi}{I}$ as seen in equation (7). This means that in a real world application, the more difference there is in electric potential, such as a rock compared to water, the more apparent resistivity the machine will measure. This measurement occurs over the 651 electrode combinations available, to produce a pseudosection of the apparent resistivity when compared with other points in the same soil profile. A specific reading does not necessarily mean a certain soil characteristic, i.e a reading of 10 ohm.m does not always mean dry sand, there are a range of factors that influence that apparent resistivity reading. This is where calibration and data inversion become important to ensure the recorded data is converted into an actual resistivity measurement that is representative of the soil conditions in the sample. Without these processes, the apparent resistivity reading is not useful for any type of interpretation or analysis.

It is in this ground proof calibration and data inversion where soil water can be identified. As this experiment is conducted over the period of one day, it is unlikely that the soil characteristics will change during that time. Texture, structure, salinity and geological features all take many years to change as these are on a geological time scale, therefore any change in the apparent resistivity reading within one day can be directly attributed to the soil moisture as it is introduced by an external irrigation source. Ground proofing the initial soil moisture via the traditional method of oven drying allows

a baseline measurement for apparent resistivity, and any changes from this baseline measurement at depth represent a change in soil moisture.

For different experimental locations, the baseline apparent resistivity will not be the same, as it is unlikely that a second soil profile will have identical features to the first. The apparent resistivity for rock, sand and clay, compacted and uncompacted, and water all differs, depending on the features of the specific sample. Some example ranges of apparent resistivity have been identified by (Samouëlian, Cousin, Tabbagh, Bruand, & Richard, 2005) in Figure 10, and lie on a logarithmic scale.

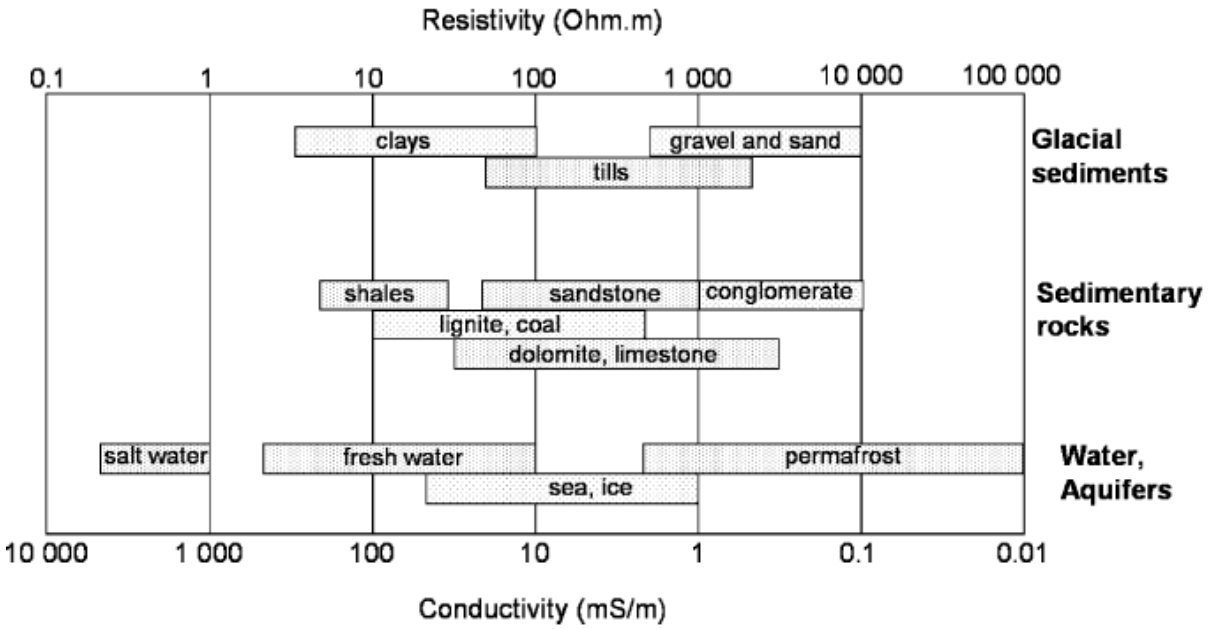

Figure 10 Resistivity of various soil features

2.4.5 Summation and discussion of all methods

Geophysical techniques as a whole can be classed into two main categories: those that measure subsurface responses to artificially-induced electrical, seismic and electromagnetic signals, referred to as active measurement techniques; and passive techniques that measure the earth's natural magnetic, electrical and gravitational fields (Caputo & Carlo, 2011). In this way, it is much the same concept as the comparison of direct and indirect measurement techniques that have previously been discussed.

Oven drying cannot be used to monitor soil moisture change over time as each point requires soil removal and this destruction means anything more than instantaneous soil moisture is impossible. However the use of oven drying soil samples is important in order to establish a baseline measurement for initial soil moisture across a transect, and down to depth. In this regard, the use of oven drying is useful when used in conjunction with the other infiltration measurement techniques. Within this project, it is used for calibrating the Terrameter in accordance with the initial moisture conditions.

In situations where the direct measurement techniques are not applicable, the indirect method of capacitance probes and time-domain reflectometry offer a suitable

alternative, however these measure volumetric moisture content as they are actually reading the electrical properties of the soil. In order to convert this back to a gravimetric reading for direct comparison with oven drying, the bulk density of the soil must be known. The use of a capacitance probe is most prevalent in agricultural irrigation systems where the user will place it in the soil, take some bulk density readings for calibration, and leave it for the entire season to record on a fixed time interval. This allows relatively real time moisture readings which are vital for irrigation scheduling. Currently, there is interest in using remote sensing techniques for broad scale soil moisture measurement which could potentially limit the use of a capacitance probe moving forward, however for the time being, the capacitance probe will likely remain the measurement technique of choice in agriculture due to its proven historical performance. In other applications, the limitations of both frequency and time-domain reflectometry exist when used in dry cracking clay where there are air gaps immediately around the sensor, or in stony or shaly soil profiles. Any soil feature that will change the electrical properties will cause the probe to become unreliable.

The alternative to the probe for long term soil moisture is the use of satellite or other remote sensing instruments, and appropriate hydrologic models. The combination of the sensor and model is critical, since each technique can be inaccurate (Fang et al., 2016). Systems such as ASMR-E, RFID, SAR, and many others have been developed in the past decade to facilitate the large scale measurement of soil moisture. The development has been driven by researchers from a large array of fields, all with their own ambitions for the technology, making the progression of sensor and model systems a very interesting and rapidly advancing area of development. One area of this advancing research is in-situ based sensors, such as ERT.

2.5 2D measurement of soil infiltration using ERT

The method of ERT lends itself to a repeatable measurement on the same location as the electrodes are fixed. This enables the ERT to be run and re-run in successive events throughout a single day, as each measurement sequence takes a fixed amount of time (93min for the settings discussed in Chapter 3). If there is the ability to measure the same set of 651 points repeatedly, then changes at each of these points can be monitored through a time-lapse sequence. The changes at each point can be quantified as anomalies through the following equation;

$$\Delta\rho_t = \frac{\rho_t - \rho_0}{\rho_0}$$

$$Where \qquad \rho_0 = initial\ resistivity\ reading$$
$$\rho_t = resistivity\ from\ temporal\ measurement$$

This is a simple equation, yet if $\Delta\rho_t$ equals anything other than 0, there has been a change in the resistivity reading. For this project, the intention is that as the wetting front moves downwards, it changes the resistivity reading for each depth it reaches due to the conductivity properties of water being markedly different to the conductivity properties of soil and rock. If the variation in resistivity is captured by the above equation, the time between the recordings is known, and the location (vertical and

horizontal) of each measurement is known for distance measurement, then the rate at which the resistivity variation moves downwards, can be correlated to the rate at which the wetting front moves through the profile. This concept provides the grounds for infiltration rate measurement, which can be interpreted into a number of methods, ultimately coming to the quantification of the hydraulic conductivity.

The use of ERT in temporal measurement has been done in a number of studies (Cassiani, Bruno, Villa, Fusi, & Binley, 2006; French & Binley, 2004; P. Jackson et al., 2002; Slater et al., 2002), in a range of conditions with different experimental outcomes. The difference of this project is the time-lapse is occurring over a number of hours, rather than months as was seen in the literature.

2.6 Limitations of ERT

ERT provides very useful information in regards to the features of a soil profile, however if the interpretation or collection of the information is not correct, then the data becomes misleading. There are a number of limitations that exist with this technology that must be considered when taking measurements and inverting data.

a) Poor electrode ground contact

Soil/electrode contact is crucial when attempting to put current into the soil. If the computer is putting a fixed amount of current into the electrode and it cannot transfer the prescribed amount to the soil, due to the soil being stony, shaly, or dry, then there will be an incorrect reading of the voltage drop into the potential electrode. This is overcome by placing a salt and bentonite mixture with the electrode to increase the transferability of current.

b) Poor current penetration

If there is a high resistivity layer in the top part of the profile, then the current will have difficulty penetrating through to the lower part of the profile. This happens in reverse as well, with a low resistivity top layer, the current can become trapped and not be accurate in the lower layer. There is no solution for this. When there is a highly contrasting layer in the data consideration of said limitation should be applied. This contrast can also happen when there is a gravelly surface, with a clay or saline subsoil, for example.

c) Not letting current charge decay

As there is quite high current being put into the soil, it takes time for it to dissipate through mechanisms of equilibration in the soil. If there is a case where an electrode is used as a current electrode, then immediately used as a potential electrode in the following measurement, an error could occur. Current decay may cause problems in this project as the order of measurement is rewritten so that the electrodes are sequentially used. A test using the conventional protocol, and the modified protocol will determine whether there is any variability in results caused by this.

d) Limited by laws of physics

As the resistivity measurement gets deeper in the later parts of the protocol, the inaccuracy, or more specifically the clarity, of objects decreases. It is commonly understood that an object of 1m width, would be 'blurred' at a depth of 10m. This is because the principles on which ERT is based, assume a homogenous medium for the calculation of apparent resistivity. The wider the electrodes become to achieve greater depths, the larger the area that is assumed to be homogenous, making measurement at depth, less defined and potentially less accurate.

3.0 Terrameter Function and Protocol Development

As suggested earlier, the Terrameter is, in its most basic form, a computer that allocates current to selected electrodes known as current electrodes, and records the resistance that is created by the soil medium through other electrodes known as potential electrodes. With this in mind, it is important to have a thorough understanding of how it works to ensure there are no incorrect assumptions when analysing the data. Therefore, this chapter will first report on how the Terrameter actually works, what each of the settings control, and detail how the Terrameter performs a measurement. Then using this knowledge, a new set of protocols will be coded for the specific application of infiltration measurement in order to maximise the potential that ERT brings to soil water dynamics. These new protocols will be designed with ERT limitations in mind as to minimise the potential errors that were documented in the previous section. It is also intended that they will be universally compatible with other ERT platforms, not just the brand that is used for this project.

This chapter is crucial to developing appropriate strategies for using ERT in this application, and should not be confused as methodology; it is original work. ERT is not specifically designed to monitor short interval time-lapse, so a thorough understanding of how it can be manipulated to do this, is important. It is also important that a document be developed so if the work is to be repeated, the user can comprehensively understand the implications of using manipulated protocols, and possibly obtain an understanding of how protocols can be written to suit other applications.

3.1 Terrameter settings

The Terrameter comes with a variety of configurations and protocol settings that allow the machine to be used in a wide range of situations. For this project there is a requirement for a repeatable measurement on a fixed time interval. Measurement is also required to be relatively shallow given that infiltration measurement is traditionally performed from the surface. With this in mind, a 2X32 cable configuration is used (2 cables with 32 take-outs on each cable), with a Wenner array used for resistivity measurement. However, the Wenner array protocol itself will be re-coded to suit the application.

There are two stages of computer setup that need to be completed before measurement can begin. They take a reasonable amount of time to complete, however all the settings can be saved as a template in the Terrameter's memory to be called upon each time the machine is rebooted. The method for this will be discussed further in this section. The menu system on the Terrameter is quite intuitive so it is assumed that the user is familiar with moving between menus and selecting options throughout the Terrameter's interface.

What follows is the best set of machine settings determined for the particular task:

1. Receiver Settings
   - Measure mode to 'RES'.
   - Min Stackings to 3.

- Max Stackings to 3.
    - This value is the number of times each measurement cycle is repeated for accuracy of the average.
- Error to 0.01.
    - The measurement cycle will repeat until either this tolerance is reached, or the maximum stackings number is reached.
    - This number is redundant as the min stackings = max stackings.
- Delay time to 0.3 seconds.
    - Recommended to allow current to stabilise before measurement begins.
- Acquisition time to 0.5 seconds (500ms = 25 samples @ 50Hz).
- Record full waveform.
    - To be used for the first experiment to optimise the signal to noise ratio, then can be switched off.
- Powerline frequency to 50Hz.

2. Transmitter Settings
    - Minimum and Maximum current set to site conditions.
        - Aim to achieve a good signal-to-noise ratio.
    - Max power to 250W.
    - Allowed power loss to 50W.
    - Max output voltage to 600V.
    - Focus one on
        - To be used for initial test to determine electrode contact.
    - Bad and Fail electrodes.
        - Thresholds for acceptable electrode contact.
        - Leave default.
    - Electrode test current to 20mA.

There are a further two machine setting sections, but these refer to using Induced Polarization and Borehole measurement techniques and are not applicable to this project. Hence, these need not be parameterised and the default parameters set for these will not interfere with the task at hand.

To save the above settings as a template, enter the settings as normal and create the task. Once the task is created, highlight the task name and press ‘options’. There will be the opportunity to ‘save as template’. To use this template, highlight over the template name and press ‘options’, and select ‘new from’.

3.2 Taking a measurement

The following process describes the method of how to deal with the results that electrode initial testing produces, if ‘Focus one’ was turned on in the Terrameter Setup section.

- Navigate to ‘Measure/Progress’
- Selected ‘Start Measuring’

- The electrode test will begin, if every electrode is found to have sufficient contact, the measuring will begin automatically, if not, it will wait for operator instruction.
    - Navigate to the Measure/Electrode view (the picture of an electrode with a cable), and select 'Opt' on an electrode with no contact to exclude it singularly or exclude them all. The operator also has the option to fix the contact issue before re-running the test. The method of doing this involves physically resetting the pin into the ground to achieve better contact. The troubleshooting section of the operations manual describes a process for achieving the required contact.
- Occasionally the Terrameter will detect a problem with its data recording; things such as recording a negative resistivity will trigger this alert. Incorrect data can be remeasured by pausing the measurement process, highlighting the row in the progress list that is the first that needs to be remeasured, press 'options', delete measurements after MXXXX (the measurement ID). Then press 'continue measuring'.

Once the 'Focus One' test is complete, the measuring will begin. The protocol includes the prescribed order in which the actual measurements are taken. This order changes for each different configuration and protocol selection, so the development of a number of different orders of measurement will be performed and used as templates for various situations.

3.3 Order of measurement

The order of measurement for a 2X32 array with a manipulated Wenner protocol is controlled by a script file (.xml format) that instructs the computer on which electrodes to put DC current through, and which to measure the resistance with. The default protocol was supplied directly from ABEM, and was manipulated to measure in an order that suits simple data analysis for the time-lapse situation encountered in this project; i.e. sequential depth measurement throughout the wetted zone. For the purpose of testing, there were three different protocol files developed with slightly different orders of measurement.

The development of protocols created a map of the 2 dimensional transect that visually showed the order and location in which the computer recorded measurements. This map is known as a psuedosection and has the sole purpose of assisting the reader to understand the method in which the Terrameter collects resistivity data.

The actual process of creating a protocol involves the use of a program that is capable of editing .xml files. The program used for this project was 'XML Marker 2'. The script file itself was written as follows.

```
<?xml version="1.0" encoding="UTF-8" ?>
<Protocol>
<Name> Protocol_1 </Name>
```

<Description> Wenner measuring on spread with 64 electrodes </Description>
<Arraycode> 1 </Arraycode>
<SpreadFile> 4X16.xml </SpreadFile>
<SpreadFile> 2X32increasing.xml </SpreadFile>
<SpreadFile> 2X32mirrored.xml </SpreadFile>

<Sequence>

<Measure>
<Tx> 1 4 </Tx>
<Rx>
2 3
</Rx>
</Measure>

The introduction allocates the name, in this case 'Protocol_1', a brief description, and the spreadfiles that the protocol will be associated under. When starting a new task, the first selection is the spreadfile which dictates how many take-outs (electrodes) are available, and the cables that are being used, i.e, 2 cable sets of 32 take-outs each, or 4 cable sets of 16 takeoutes each.

After this introduction the sequence begins, where the current and potential electrodes are assigned. Each electrode in the array is assigned a number from 1 to 64 in ascending order. In the above example, the electrodes 1 and 4 are 'Tx', meaning transmission, and electrodes 2 and 3 are 'Rx' meaning receiving. This piece of code represents the first electrode combination and will be repeated three times as per the 'Stackings' settings that were previously selected.

The exercise of writing the protocol involves typing this section of code for each electrode combination required, and placing them in sequential order to dictate the order of measurement, for instance the first three electrode combinations are as follows.

<Measure>
<Tx> 1 4 </Tx>
<Rx>
2 3
</Rx>
</Measure>

<Measure>
<Tx> 2 5 </Tx>
<Rx>
3 4
</Rx>
</Measure>

<Measure>
<Tx> 3 6 </Tx>
<Rx>

4 5
</Rx>
</Measure>

This pattern progresses through the entire 64 electrodes, then is proceeded to start at the next depth, by selecting electrodes one increment further apart. The transition of that occurs as follows.

<Measure>
<Tx> 61 64 </Tx>
<Rx>
62 63
</Rx>
</Measure>

<Measure>
<Tx> 1 7 </Tx>
<Rx>
3 5
</Rx>
</Measure>

This method is repeated until the maximum depth is reached, by selecting transmission electrodes as 1 and 64. The graphical representation of this process is displayed as a pseudosection and is shown in Figure 11. There are 651 electrode combinations that must be written to cover the entire analysis space.

The reason for rewriting the code is so that the time-lapse of recorded measurements can be followed logically. The water application occurs over the full width of the transect in a uniform fashion, while the ERT recording occurs sequentially as per the protocol. Having the recordings occur from one side to the other in a sequential order, rather than jumping in increments of 3 (as the standard Wenner protocol does) means that there is the ability to correct each data point for lagged infiltration in the future.

Consider a homogenous medium subject to a constant infiltration rate for the entire transect width. As the first measurement is taken, the water may be just in the top millimetres, but by the time the measurement reaches the far end of the transect distance, the water may be a number of centimetres into the profile, giving an incorrect impression that the infiltration rate at the far end is much faster than it is at the beginning; i.e. the time lag in the measurement process affords more time for each subsequent measurement given the uniform irrigation and the fact it commences at a single point in time (not with each measurement). If the recording occurs sequentially, and each takes 8.7 seconds (to be explained in Section 3.4), each data point can be corrected since the time and distance of each data point is known and follows logically. There were three different protocol arrangements written for comparison. Their pseudosection's are shown in Figures 11, 12, and 13.

3.3.1 Protocol 1

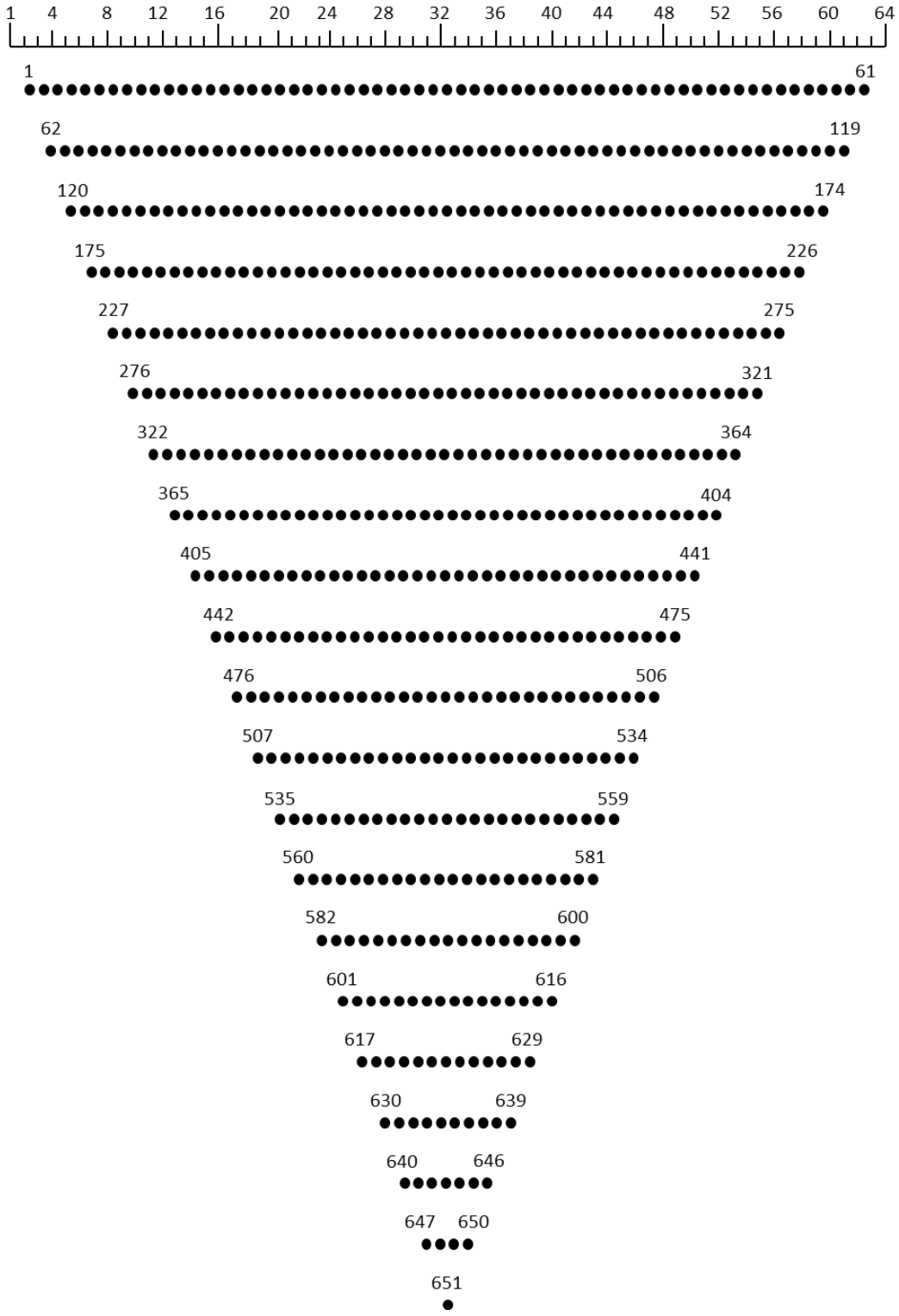

Figure 11 Pseudosection for Protocol 1; axis=electrodes; data point numbers represent order of measurement.

3.3.2 Protocol 2

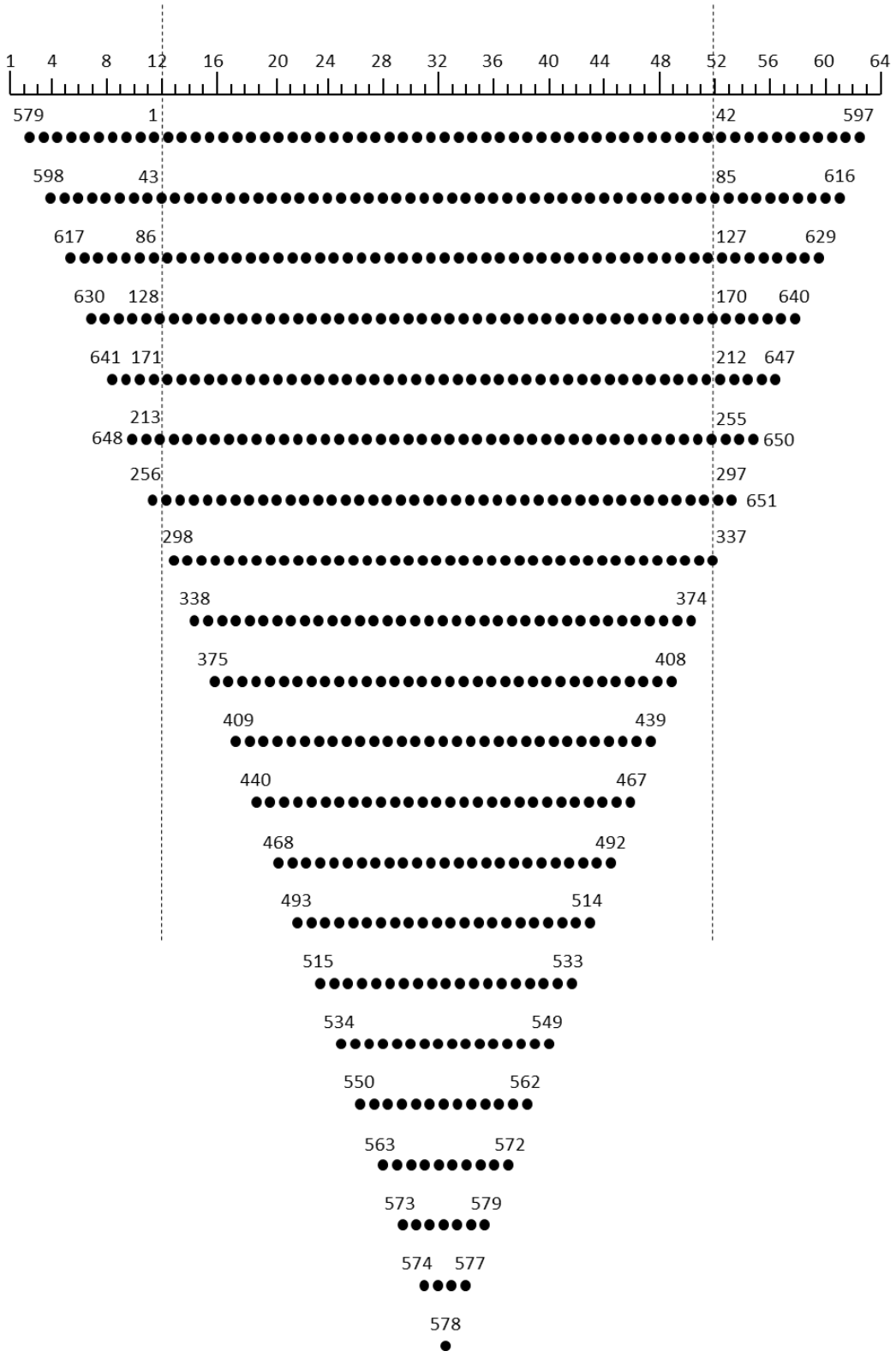

Figure 12 Pseudosection for Protocol 2; axis=electrodes; data point numbers represent order of measurement; hashed lines represent nominal transect boundaries to define a central sequential depth.

3.3.3 Protocol 3

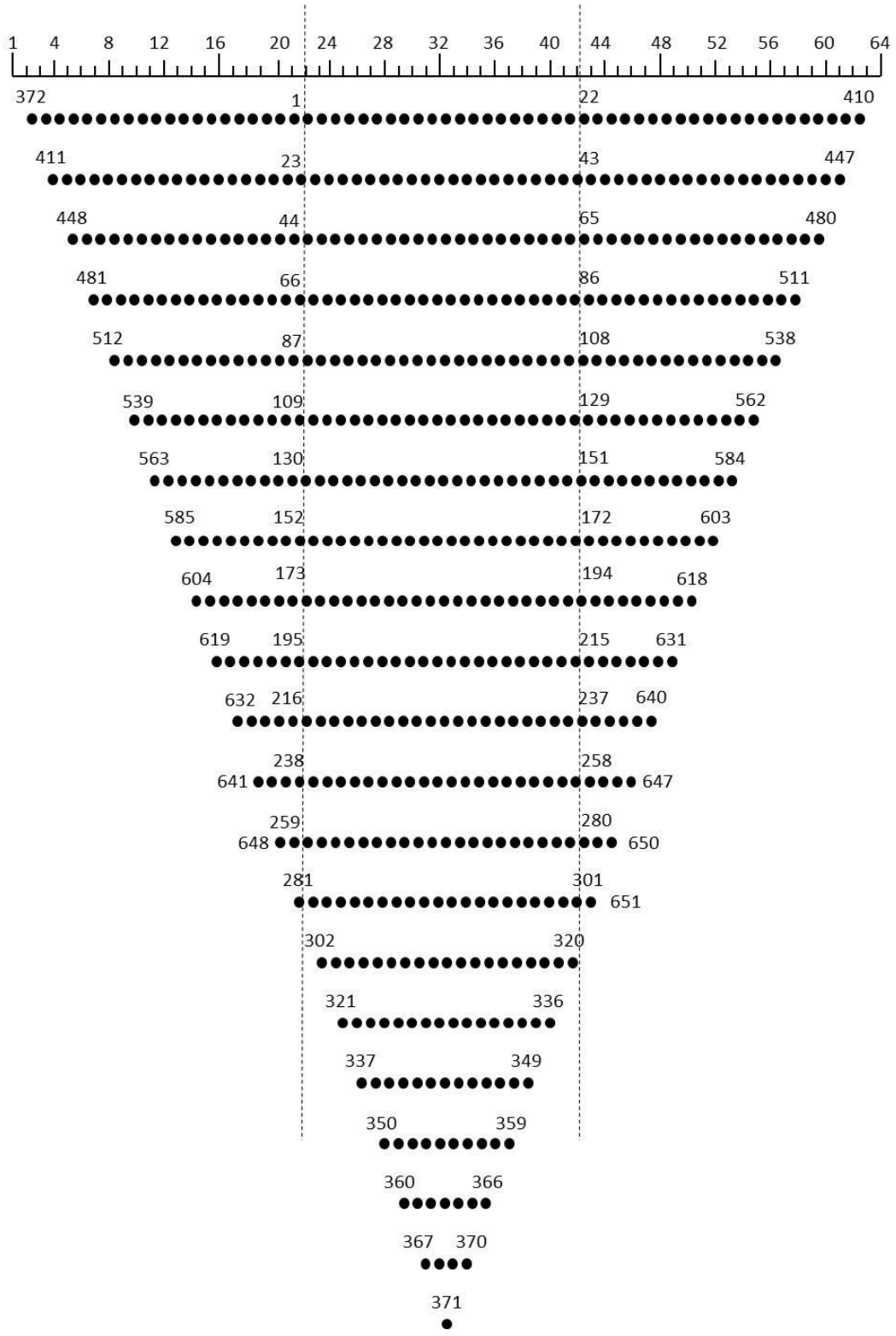

Figure 13 Pseudosection for Protocol 3; axis=electrodes; data point numbers represent order of measurement; hashed lines represent nominal transect boundaries to define a central sequential depth.

In Protocol 2, the dotted lines represent a 10m section of the transect. The irrigation occurs over 5m in the centre of the transect so a 10m width was selected to collect data outside the irrigation to visually assist the operator to see what effect the soil water had on the resistivity readings, while reducing the time of measurement by eliminating the recording of values at the very edge.

Protocol 3 had the dotted lines at 5m wide, in order to only collect data that will be impacted by the changing water content. This is done to completely minimise the time of measurement, but as a trade-off, the visual benefit of seeing data not impacted by water is removed.

3.4 Time of measurement

Time for each measurement is dependent on the settings discussed in the Terrameter setup section above. One measurement pulse consists of one positive, followed by two negatives and then one positive, each being a period of current. This is shown visually in Figure 14.

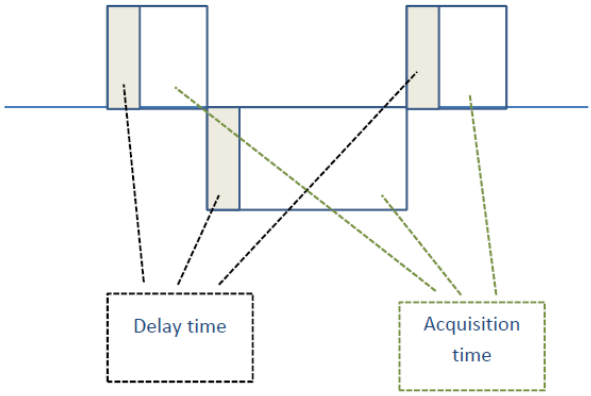

Figure 14 Terrameter measurement procedure; delay time is when current is applied but not recorded to allow current stabilisation, acquisition time is when voltage drop is recorded (ABEM, 2012)

The delay time and acquisition time are set as 0.3 and 0.5 seconds respectively in the settings section, but can be changed as the situation requires. With these numbers, the measurement time for one pulse, looking at Figure 11, will be 2x(0.3+0.5)+(0.3+(2x0.5)) = 2.9 sec. However, the measurement is not complete until stackings and error are taken into account. To achieve an accurate result, the maximum stackings should be set so that the above pulse is repeated until this arbitrary number is reached, or until the variance in the results is below the value set as the error. For instance, if the maximum stackings is set as 3, and error as 0.01, then the above pulse will take place twice (2.9x2 = 5.8 seconds) and average, and if the variance between these results is less than 0.01 then the ERT will record the average as the correct result and move to the next electrodes. However if the variance is greater than 0.01 then the third stacking (third measurement) will be completed, and the average of the three will be recorded as the correct result, regardless of the variance between all results. Therefore if each electrode combination requires all 3 stackings, then the total time will become 3x2.9 = 8.7 seconds. It is more accurate to have a large number of stackings and a low error,

however as each pulse takes 2.9sec, each extra measurement adds significant time to the total measurement time over 651 different electrode combinations. Hence, there becomes a trade-off between accuracy and the ability to record infiltration sequentially, where for infiltration, the measurement time is best minimised, but this compromises accuracy.

4.0 Methodology

This methodology was developed in order to critically evaluate the potential of ERT to measure the variability parameters of infiltration rate in an array of soil environments. The project, and subsequently the methodology, will be split into two sections. Firstly, running the ERT continuously over a relatively homogenous soil while irrigating at a slow rate. This allows infiltration rate and the ERT's potential to measure this, in a simple environment, to be evaluated. From this, the methodology can be readjusted based on the evaluation. The second methodological approach will be to create a variable soil environment (anthropogenic profile: Anthroposol) and run the ERT with the previous**ly** adjusted method. Subsequently, the results will be critically evaluated.

4.1 Irrigation design

The irrigation equipment is to be designed to minimise the loss of irrigation water from solar and wind evaporation. A preliminary drawing is provided as Appendix A1. The irrigation rate was arbitrarily selected as the slowest commercially available rate and pressure limited dripper. Drippers of 2 L hr^{-1} were used at spacing of 50 cm in a grid arrangement, with 20 drippers delivering 2 L hr^{-1} each, within the 5x2 m frame. This infiltration rate was assessed as suitable given the soil conditions (granitic parent material).

The 'frame' for this project was required to be transported to and from different experiment sites in order to assess a range of different soil types and soil uses. Therefore it was suggested that it be able to be flat packed by dismantling and reassembling in a simple and timely manner for each use; using pins and slotted PVC to avoid needing to carry a toolbox. The dimensions were limited to the length of the dual axle trailer provided by the NCEA, made to be the maximum length possible that is still legal to tow behind a vehicle. With this in mind, the length was in multiples of approximately 5 m. Making the frame into two, 5 m sections, provided a total of 10 m, or 40 electrodes of the 2X32 array that was used. The frame was capable of being either 10 or 5m long by 2m wide, depending on the requirements of the protocol and the experimental situation. It was designed to have a peaked roof with a canvas cover and eyelets through which the Terrameter electrodes are inserted. Below the roof was a network of cross sections that are set up to support the irrigation drip line so that it is off the ground, ensuring the required flow is met from each nozzle, without the drippers being blocked by soil.

In terms of material, the internal cross sections can be made from metal, but needed to be arranged so they were not in contact with the Terrameter electrodes. The edge pieces are required to be insulated from the ground as the current from the electrodes would use a metal edge as the path of least resistance, creating errors in the results. Flat plastic was chosen as most desirable, although manufacturing costs were too expensive for this project. Instead, PVC tubing was be used (it should be noted this is not the most eloquent solution). The PVC provided a non-conductive material keeping the irrigation equipment off the ground. It was simple and cost-effective to put together and able to be transported.

For each experiment, a water tank mounted on a trailer was set up nearby to provide a pressure head to initiate the drippers. The drippers delivered 40 L per hour, so a standard 1000 L shuttle sufficed for all experiments. The initiation of each experiment began by turning on the water and priming each dripper; once primed, the ERT begins to measure. Priming volume was captured in plastic containers beneath drippers, which also allowed irrigation uniformity to be assed. A schematic of the dripper arrangement is provided in Figure 15.

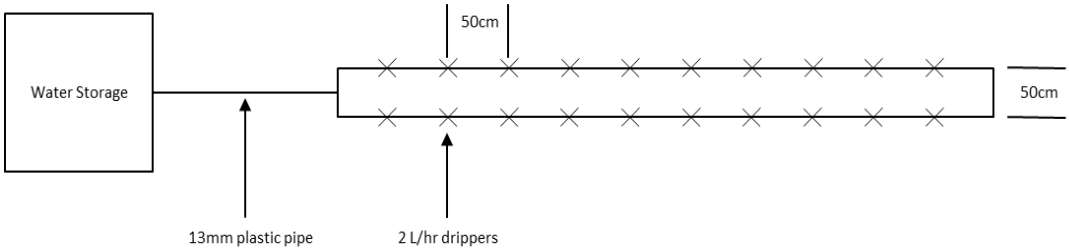

Figure 15 Schematic of irrigation layout

In this schematic, the water storage is at approximately 1.7 m higher than the drippers to ensure a pressure head at the drippers that will allow them to deliver 2 L/hr over the entire experimental area. The electrodes for each experiment were placed down the centre of the irrigation arrangement, so water was applied 25 cm either side of measurement zone. As the electrodes have a 3-dimensional sphere of influence, they picked up the soil water at this distance, and the water was not close enough to touch the electrodes on the surface causing an error in the readings. The 13 mm plastic pipe was flexible and approximately 15m long between the drippers and water storage. This allowed the water storage to be positioned off to the side so that it was not in the line of electrodes, as may b**e** interpreted from the Figure 15.

4.2 Optimisation of Terrameter settings

The optimisation of the Terrameter is important as the electrical signals are sensitive to foreign influences such as nearby powerlines and electronically powered railways (ABEM, 2012); the latter not an issue for the rural setting used in the experiment. The procedure in Chapter 3.0 was followed closely to set up the Terrameter correctly, but for the first run period, the setting 'Record full waveform' was turned on. This allowed far more detailed information of the data to be analysed. The first run of the machine was the baseline data and the time of measurement was thus not of importance to infiltration results, as no irrigation occurred. The 'LS Toolbox' software allowed each measurement to be investigated to evaluate the signal to noise ratio, which was important to reduce the disruption of background electrical interference. If the waveform data showed that there was a poor ratio, the minimum and maximum current settings could be changed to suit the conditions. This was done experimentally until the optimal settings were found to minimise the signal to noise ratio; once they were set, they were suitable for all experiments conducted at that site.

It did not matter which of the manipulated Wenner protocols were used in this optimisation approach, as the influential element of the protocol was the sequential nature, which they all contained.

4.3 Modified protocol comparison

As there were two protocols to be compared in this project, each of them had to be run on a dry soil to address discrepancies between. Hence, both were run on the same profile, and the data was inverted for direct comparison. The process of this inversion will be detailed further in the methodology.

Once the existing resistivity status was known, each protocol was run under irrigation events immediately adjacent to one another, as demonstrated in Figure 13. This ensured that the natural infiltration variability in the soil was minimised, as opposed to testing the protocols on completely separate soils. Each of the protocols was run continuously with the same Terrameter settings, so that direct comparison could be made. The objective of the comparison was to evaluate whether recording the measurements immediately under irrigation first, as in protocol 3, and completing the dry zone at the end of the measurement procedure would create a different result from recording with all 64 electrodes in a conventional fashion, as in protocol 1; or whether Protocol 2 was suitable for a balance of visual data interpretation and time of measurement minimisation.

Neither of these protocols was expected to provide false data or misleading information. The defining factor for protocol selection was the ease of interpretation, defined as protocol efficiency in quantifying variability.

The layout of the plot will be set out as in .

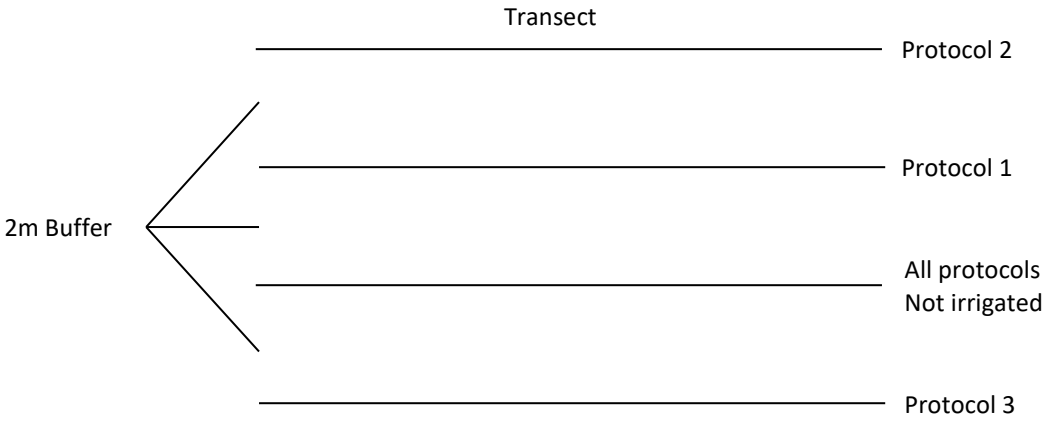

Figure 16 Plot layout

4.4 Infiltration data collection and measurement procedure

4.4.1 Site selection

The site selection process was driven by soil texture. The site was selected near Inverell, NSW, with a soil texture of sandy loam to sand, located relatively close to a waterway.

The geography of the area suggest it was once a deep valley that has been filled up via weathered and transported gravel and sand. These are known as 'sand slugs' and are quite common in the district as it is in the head waters of Myall Creek, meaning the heavier particles such as sand and gravel have dropped out of the water while clay and silt have remained in suspension and have been carried downstream towards Bingara where the Myall Creek joins the Gwydir River. At the site, there was a sloping hillside onto a flat (slope less than 1%), arable area approximately 200 m wide before it reaches the waterway. The 200 m wide flat was where the experiments were undertaken.

The chosen site was approximately 25km south west of Inverell, NSW, where the well-drained sandy river flat had been sown to Lucerne some years ago. There was a known underground water source with a bore (<1 y.o.). When the bore was being sunk, the drilling rig extracted samples of the subsurface soil and it appears to be well drained at depth beyond what was required for this project. The site has not been land formed or cultivated in the past 5 years, but has been grazed by livestock. Given the relatively even elevation, lateral flow of soil water was not anticipated to affect results, nor was observed to.

4.4.2 Experimental procedure

The experimental procedure for this project consisted of ERT transect lines with a 2 m buffer between them. Then setting the task on the Terrameter with the appropriate measurement settings (identified in Section 3.1) and running each protocol on the appropriate transect line. The process of setting up the Terrameter was as follows:

1. Place electrodes in the ground in straight line at 25cm increments.
2. Roll out the cable and connect to the electrodes with the jumper cables as seen in Figure 14. With '1' on the left of the schematic, and '64' on the right.
3. Connect cables to the Terrameter in the correct socket, as detailed on the side of the machine.
4. Connect external power supply.
5. Switch on with the power button.
6. The 'STOP' button must be released before measurement can begin.

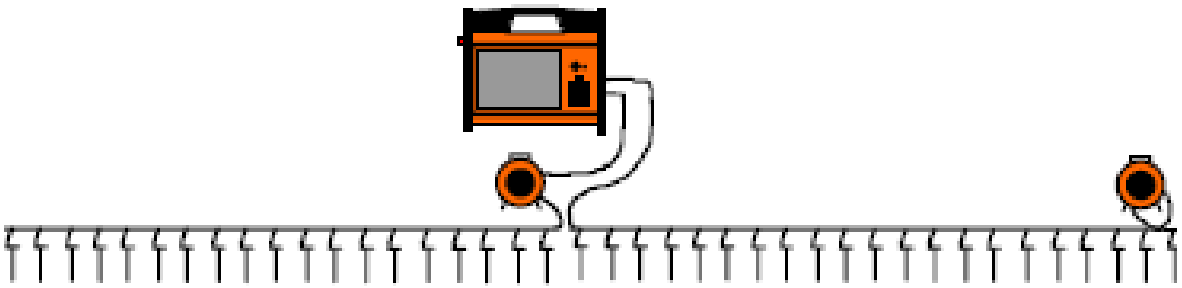

Figure 17 2x32 cable layout (ABEM, 2012)

This first measurement collected the full waveform data for settings optimisation, and for the soil moisture benchmarking. When the irrigation was introduced, the pipe and dripper network was set up as follows:

1. Set up frame of irrigation support with internal beams in place.
2. Lay pipe network across the internal beams and connect to the external water source.
3. Roll canvas roof over the frame and place electrodes through the eyelets and along the rest of the transect outside the irrigation zone.
4. Proceed as per step '2' in previous steps.
5. Turn the irrigation on as the Terrameter begins its measurement procedure.

The procedure outlined in Section 3.2 was then followed to begin the measurement procedure. Each time the Terrameter was moved to a new transect line, the data was saved to a specific task within the project. Therefore, the data from each transect remained in the Terrameter's memory for the duration of the day, to be downloaded at the conclusion of experimentation.

Data transfer

Transferring this data onto a PC was completed either by a USB, or Ethernet connection. The transfer of full waveform data was to be performed via Ethernet due to the size of the file, however regular, individual tasks were performed and collected with a USB device. The Terrameter allows data export to be completed in the form of a number of files, namely DAT, TXT, LAS, or USF. The most recognised by the inversion software is DAT so this is what was used. The process of exporting data was to navigate to Project/Task List, highlight Task, press 'options', and select export task as the selected format preference. This can also be performed more efficiently through the LS Toolbox.

4.4.3 Variability trials

In this trial, a variable Anthroposol soil profile was constructed in advance by digging a hole ≈5 m wide and burying a large rock with a flat top surface at a recorded location, as well as a series of logs, again recorded in terms of location. A compacted region was created in the middle of the plot with machinery and hand tools (as soil was replaced back into the pit), and the location recorded, as demonstrated in Figure 3. Once the Anthroposol was constructed, the same ERT setup and measurement processes were followed as for the initial experimentation.

Figure 18 Variability trial with features exposed

Figure 19 Variability trial buried with electrodes

In both Figures 18 and 19, it can be seen that there are two distinct soil types based on colour, where the yellow soil was the subsoil of the initial profile. The texture of this yellow subsoil was heavy clay, and the black topsoil a very coarse sandy loam. The

excavation of clay indicated that the site selection was different to the initial experimental site, with the high clay subsoil associated with being closer to the hillside. However as the site had been excavated and reformed to be anthropogenic, the inclusion of a high clay content subsoil was not considered a confounding issue. In fact, this texture contrast is useful as it allows a 4th element of variability in the system, alongside the rock, logs and compaction in the centre. As suggested above, and most important to visual interpretation of data, the locations and dimensions of all soil features were recorded using a measuring tape. This allowed electrode location to directly associate with zones of variability that had been imposed. Hence, visual examination of infiltration changes due to the soil features, registered by the ERT, were able to be directly made from inverted pseudosections.

4.5 Inversion processes

Once the data was collected and was in the LS Toolbox, it was put through the inversion software RES2DINV. This process produced the 2D transect map of resistivity by depth, and as the Terrameter was run continuously a new map was produced approximately every hour. The hypothesis being that resistivity changes with depth in each subsequent map will indicate change in soil moisture due to a clear wetting front progressing through a drier soil profile.

The inverted data layers were inverted independently of each other, meaning that an instance was processed and taken out of the software before the subsequent data set was imported. Loke (1999) demonstrated that a joint inversion technique – where the initial data set is used as a set of constraints for the inversion of the second and subsequent – produced a much better correlation of the change in resistivity. This was consistent with the aim of all time-lapse measurement experiments undertaken. Hence the method of Loke (1999) was to initiate constraints for subsequent data sets (constrained by each other). This allowed production of a variation map.

Another benefit of using the joint inversion technique was the ability to produce a map of the variation between data sets, using a percentage change method, much the same as that discussed in Section 2.5. This map of change takes out the visual issue of seeing the resistivity of a range of soil features, and just shows what has changed between the data sets. This can be done with a traditional inversion method, however the accuracy will not be as high as is if the data sets are constrained together (Loke 1999).

Barker and Moore (1998) further demonstrated the use of a percentage change map in a groundwater recharge experiment, which is presented here as an example of the process. They applied 10 h of irrigation and assessed the changes in resistivity. In Figure 20, 10 h worth of irrigation water is not overly apparent in the data. It may be evident if placed beside the initial data set, however there is such a range in resistivity values that the colour scheme is very busy. In contrast, Barker and Moore also plotted the percentage change maps (Loke 1999) for various time intervals (Figure 21).

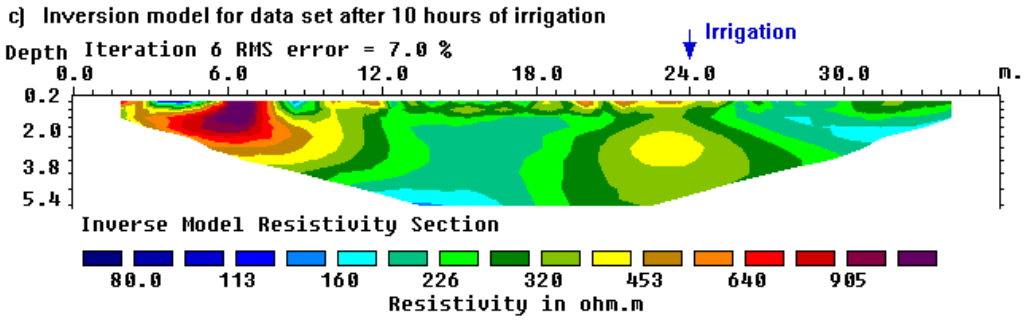

(Barker and Moore, 1998)

Figure 20 Normally inverted data set

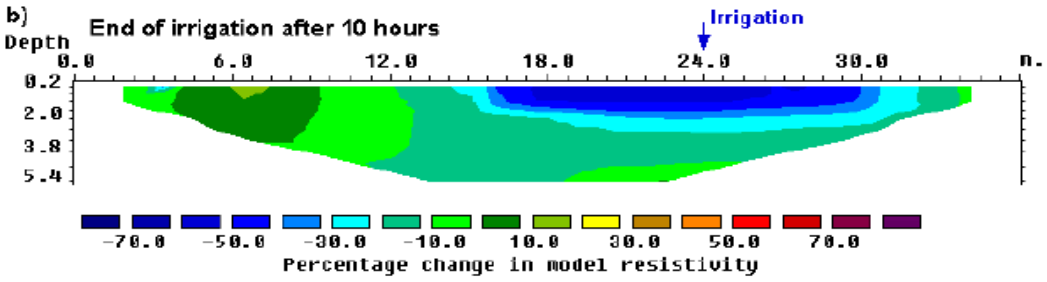

(Barker and Moore, 1998)

Figure 21 Percentage change in model resistivity

Where the joint inversion techniques have been used, the change in resistivity when compared with the initial data set, for the same 10 h time interval as Figure 20, is very apparent. From this, the benefits of using a map of the percentage change in resistivity vs simply comparing the plainly inverted data can be clearly seen.

The joint inversion method and mapped percentage change was therefore used to display the wetting front as it progressed downwards, each hour. This percentage change map also limited the requirement for calibration with actual moisture data measured from coring as it is a map of what has directly changed between the time intervals. Thus, for the purpose of investigating infiltration front detection potential of the ERT, the relative differences are appropriate. However, for conversion to infiltration and hydraulic conductivity results in future work, coring would still be required.

One significant assumption of the inversion process, is that the potential distribution (discussed in section 2.4.4) is originating from a point source. However, in reality, the current is induced as a point source but the voltage drop is read as a line source. This line source comes from the use of flux in Ohm's laws. The flux is a measure of the flow of current through a fixed cross sectional area with respect to time; i.e. for a simplified ideal situation, the current will move through a cylinder that joins the current and potential electrodes. It is assumed that this cylinder has a homogenous medium within it, which is another assumption and the cause of why clarity of resistivity decreases with depth. As flux is fundamental to the calculation of apparent resistivity from a voltage

drop, it must be used, and subsequently, so must the assumption that the current is a line source rather than a point source.

In the inversion software, the line source assumption is not accounted for, and the inversion process proceeds with the use of a point source for modelling between blocks. In this project, this error can be ignored because the intention is to model relative difference; i.e. the change from one time-lapse to the next in the same soil profile. The limitation this brings is that a calculated resistivity (post processing) reading of x in one profile, cannot be compared with a calculated resistivity reading of x in another profile. The calculated resistivity from the model was only useful for monitoring changes within the same exact soil profile. For the purpose of this work, that is sufficient and the resistiveity data is not proximally converted to soil moisture. However, in future work, the resitivity will likely need to be converted to soil moisture, and thus means to deal with the assumption issue will have to be developed.

5.0 Results

As was identified in the project objectives, the use of ERT as an approach to measure infiltration rate in variable and complex environments is hinged on the resolution of relative resistivity. Thus, a method of data analysis that quantified the changes between the time-lapsed resistivity readings was required; in this case joint inversion. Quantification of these changes is then required both spatially and temporally, to relate the resistivity changes with a dynamic soil wetting front. This section presents the results based on this approach for the initial investigation and refinement, as well as the variable Anthroposol environment.

5.1 Protocol 2 –Homogenous profile

Protocol 2 was run over a profile with very little variability to gauge the preliminary ability of the ERT to capture changing resistivity. Figure 22 and Figure 23 demonstrates a clear change in the top, centre of the profile (decreased resistivity) consistent with where the irrigation took place. In this trial, a further experimental limitation was encountered. There was a heavily gravelled top layer in the profile. This appeared to limit the feasibility of subsoil resistivity readings, due to gravel being naturally resistive. It did serve well in demonstrating that moisture causes a clear reduction in resistivity.

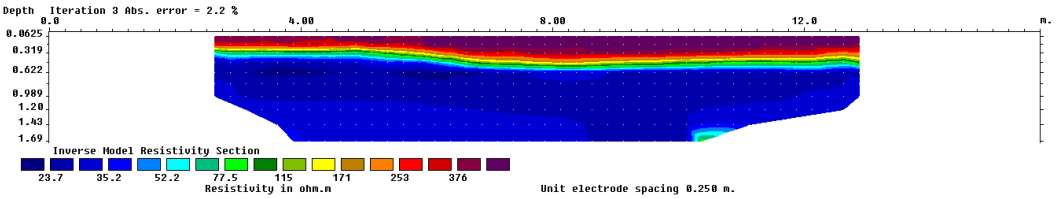

Figure 22 Protocol 2 - Homogenous profile - Initial

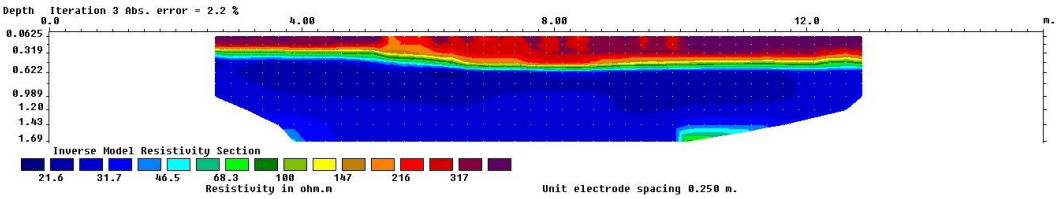

Figure 23 Protocol 2 - Homogenous profile - 4hrs

Figures 22 and 23 were inverted using default settings in RES2DINV, meaning that direct comparison will not be the highest level of accuracy due to the inversion processes being independent of each other. This inversion process is done as a least squares regression, with enough iteration until an error threshold is reached. In this case, that threshold was 5%.

Figure 24 shows the time-lapse inversion as a percentage change using the joint inversion technique. These results were then plotted as the difference between each location, as a percentage change between the calculated apparent resistivities.

Figure 24 shows each hour, compared to the initial reading before water was introduced. It can be seen that the biggest change of -49.6% in the final interval (Figure

24e), is much more change than the -28.6% in the first time-lapse (Figure 24a), but this is not visually evident due to individual colour schemes. With this in mind, the blue is increasing in intensity as the time draws on. A decreasing percentage change, as Figure 24 demonstrates for the irrigated zone, indicates the later profile is less resistive, or more conductive than the initial profile, which is due to water changing the conductivity of the soil. The large increase in resistivity, identified as red and purple, below the infiltration zone is presumed an artefact of the gravel layer, previously mentioned, where current movement through the gravel layer is retarded.

Figure 25 shows the data sets of Figure 24, in the form of graphed resistivity change. The inverted data set is exported from the model as an .xyz file which can be viewed in excel as the actual numbers that were calculated. In Figure 22, the difference between the calculated apparent resistivity, at the location of the data points from the pseudo section, are displayed for each hour increment. It is interpreted as a resistivity change if the line for a particular depth is anything except zero. After 2 hours (Figure 25b), there is a data artefact distorting the data between 4 and 6 metres. However, the line at 0.39m indicates reduced resistivity, which is consistent the water reaching this depth at the end of 2hrs. At 4 hours (Figure 25d) there is a slight change at 0.65m meaning the water has reached that depth, but not 0.78m after 4hrs.

A further option for analysing the data is by plotting the resistivity value of each model block, as opposed to plotting at the pseudo section data point. This provides more control over the depth of each data layer and is determined by the inversion model parameters. The minimum block thickness that the inversion software will read is half the pseudo section depth, and the location of the reading will be given in the centre of each block, meaning the first depth displayed is (0.13/2 /2 = 0.0325 m). In actuality, the data is displayed as 0.031 m and increases in increments of 0.063 m. It is presumed this is due to rounding errors contained in the software or measurement equipment. When the data is graphed from model blocks, there are 2 blocks between each data point meaning there is a level of rounding and averaging across the blocks as the model iterates and recalculates the block boundaries. These data are depicted in Figure 26.

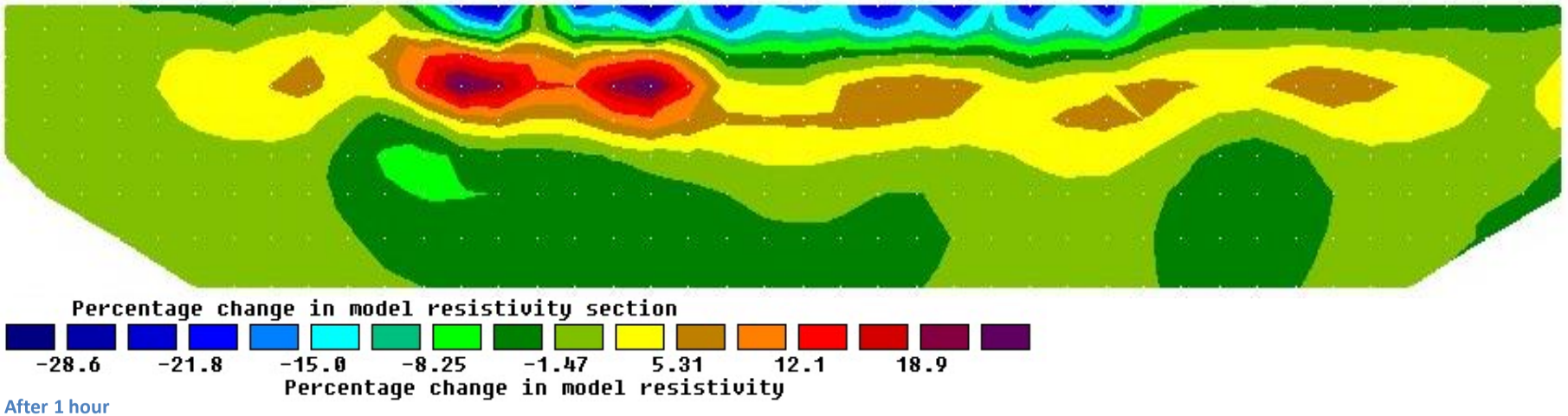

After 1 hour

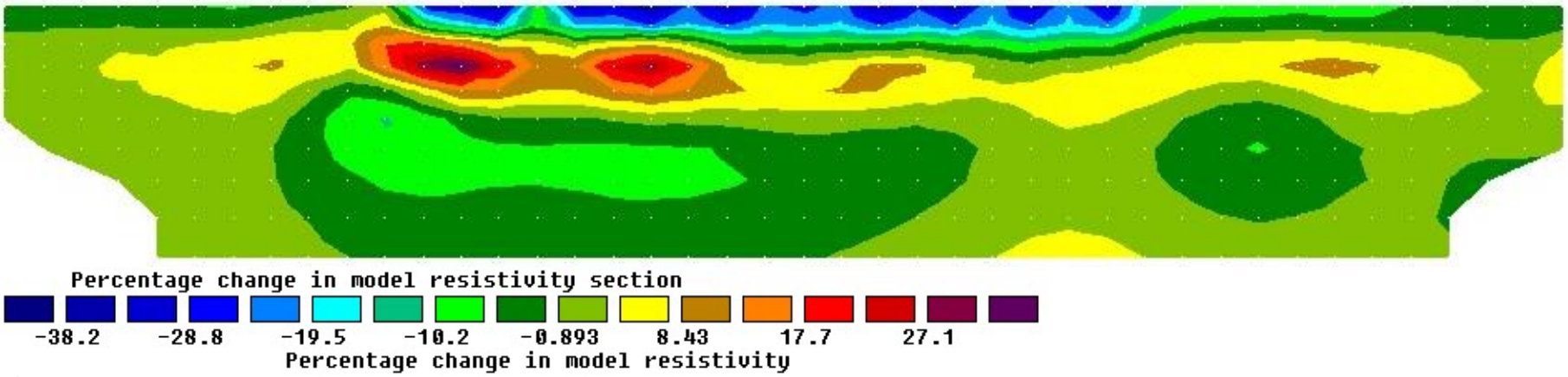

After 2 hours

Figure 24 Homogenous profile - hourly time-lapse percentage change

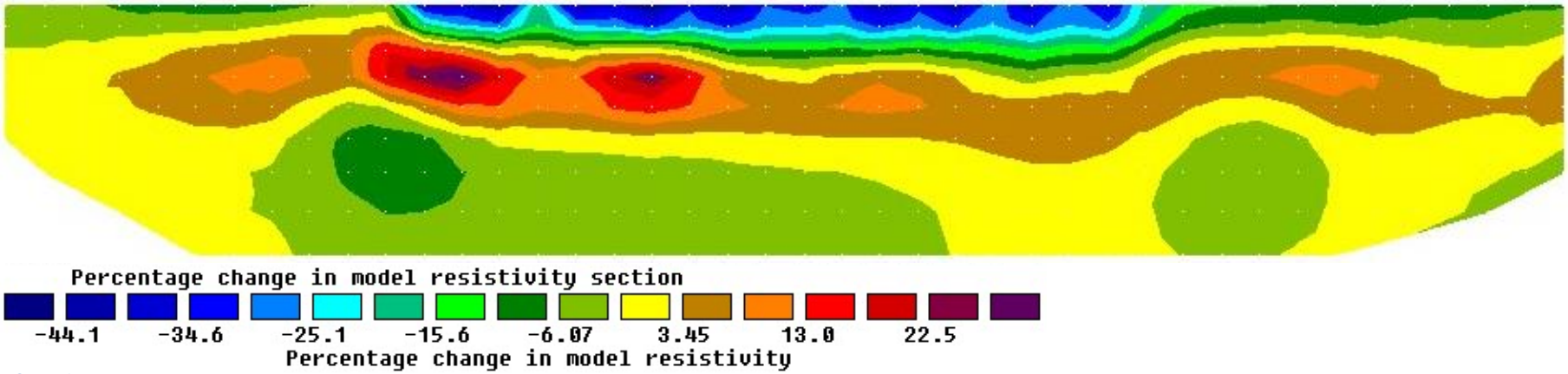

After 3 hours

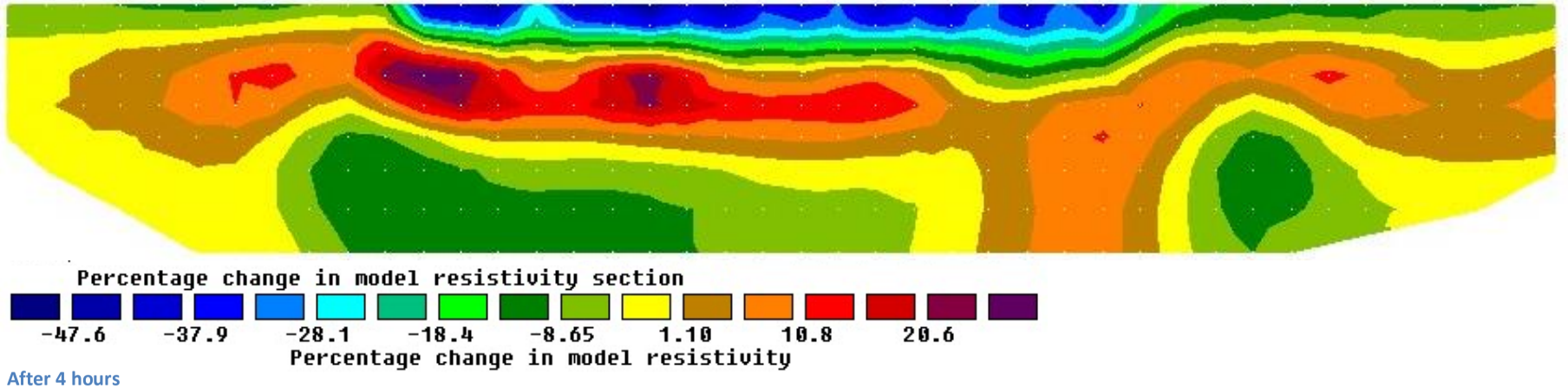

After 4 hours

Figure 24 (Cont.) Homogenous profile - hourly time-lapse percentage change

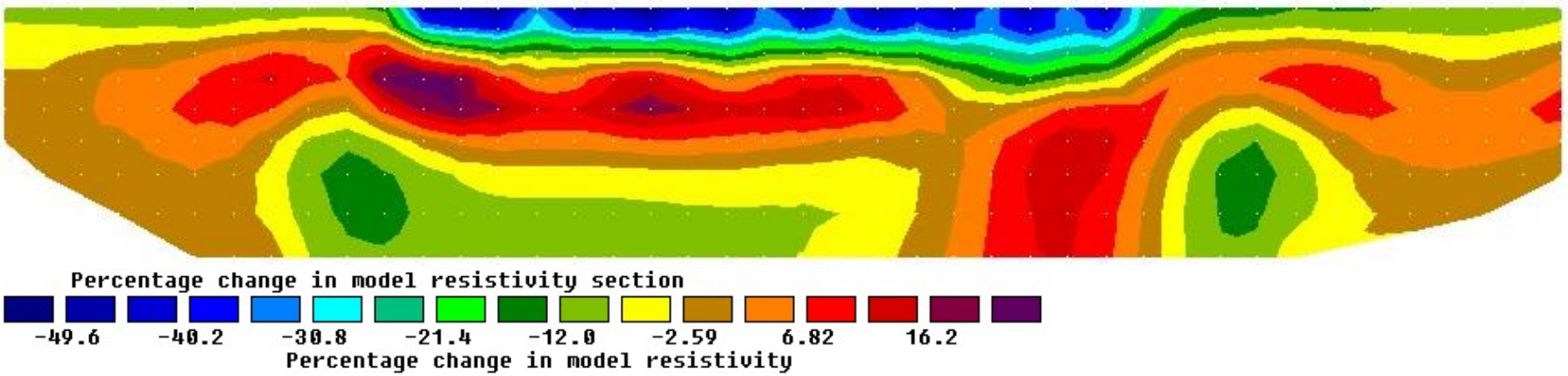

After 5 hours

Figure 24 (Cont.) Homogenous profile - hourly time-lapse percentage change

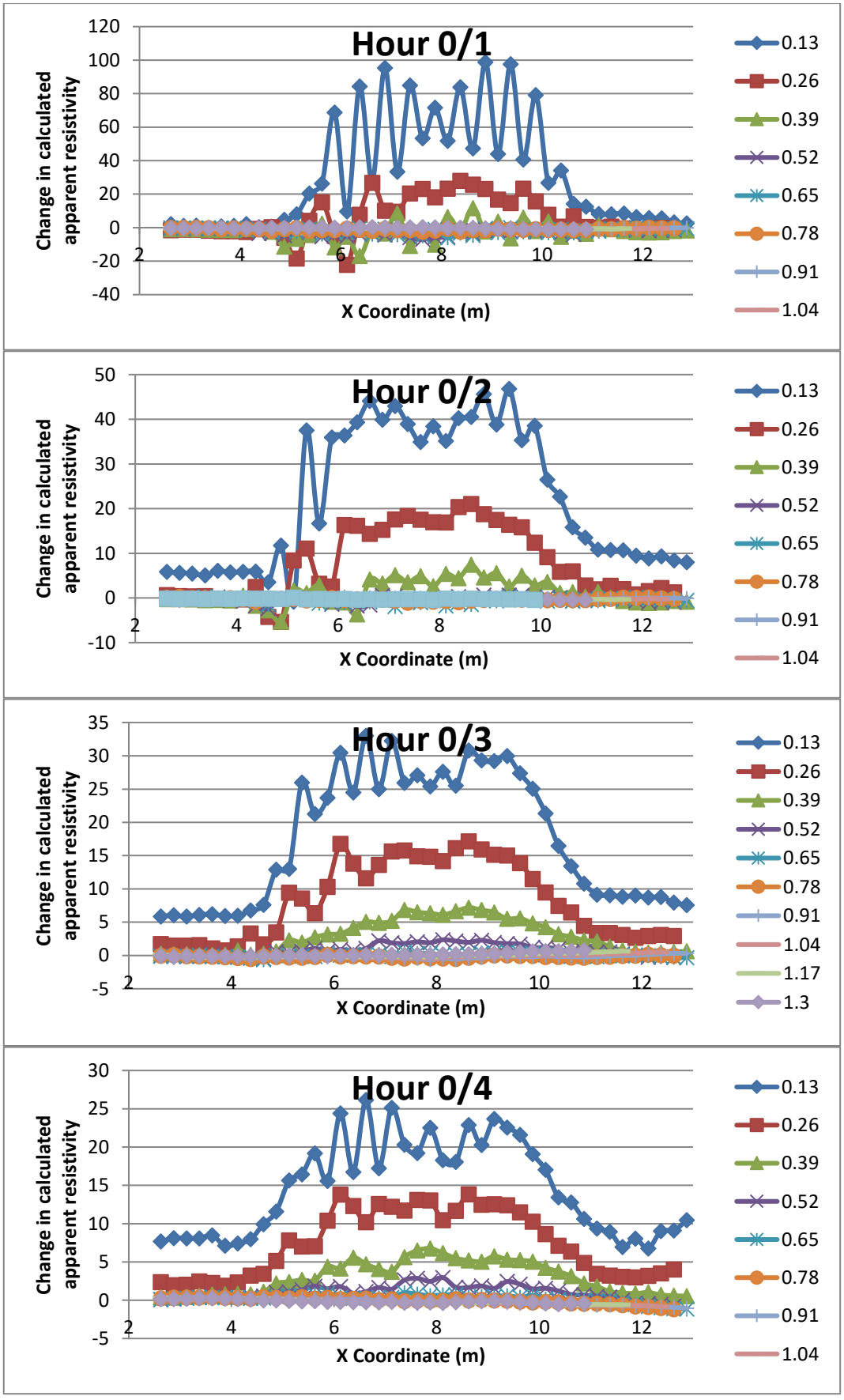

Figure 25 Change in calculated apparent resistivity (ohm m^{-1}) after (a) 1, (b) 2, (c) 3 and (d) 4 hours of irrigation from the baseline inversion constraints (time 0)

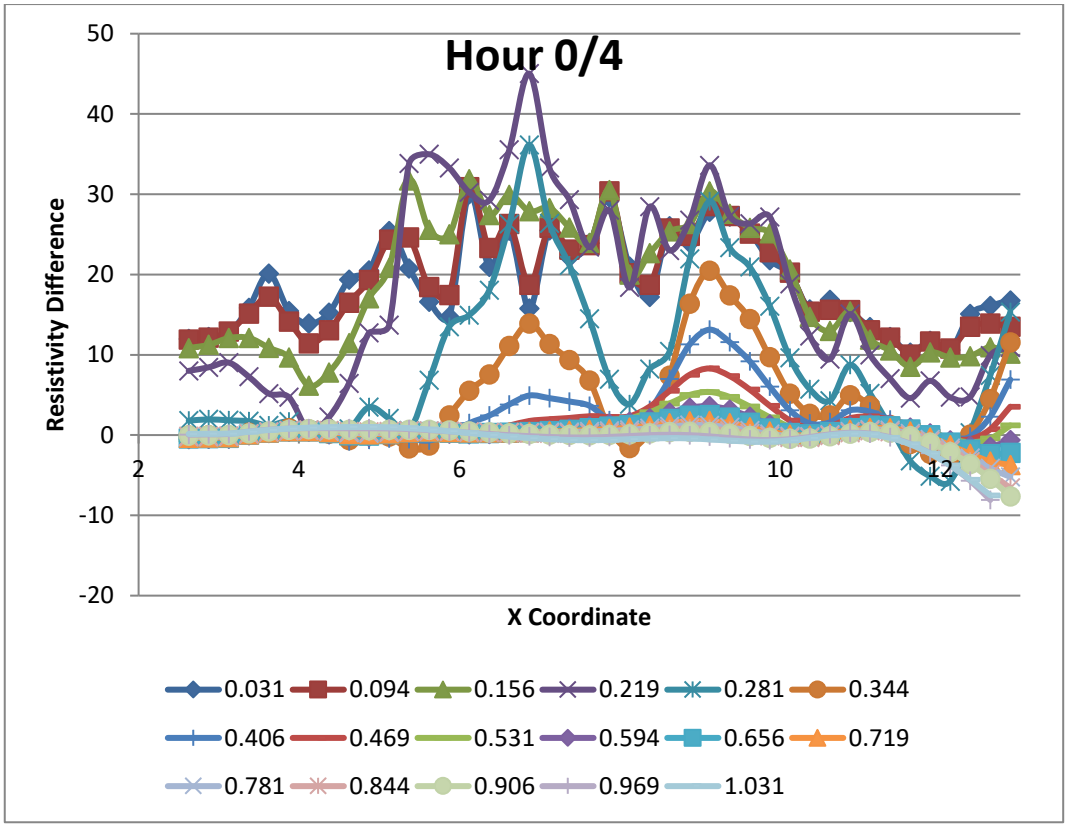

Figure 26 Resistivity of model blocks (ohm m^{-1}) after 4 hours of irrigation from the baseline inversion constraints (time 0)

From Figure 26, it is observed that there is a high density of data at the deeper depths between 8 and 10 m. However it should be noted that in each of the layers presented, there was a resistivity change recorded indicating water had infiltrated to that depth, contrary to what the plot of the pseudo section data (Figure 24d) had displayed. This is due to the iterative nature of recalculating boundaries between each model block and essentially creating a smoothed average between actual recorded data points, as would occur in the pseudo section. Figure 26 also shows a negative resistivity change, which indicates a reduction in conductivity, around 6m, 8m, and 12m, which are artefacts of the inversion process.

5.3 Protocol 3 – Homogenous profile

Protocol 3 was not able to be completed due to Terrameter malfunction. The experiment was run, but the machine failed to store the data. Once this malfunction had occurred, an older model ABEM Terrameter SAS4000 was used to complete the project. The protocol manipulation for this machine had to occur within the software package supplied, not by writing the code into an .xml file and loading it onto the machine as was the case for the Terrameter LS (a severe limitation of the SAS400, and great improvement for the LS). Due to time constraints, only Protocol 2 was re-written into the sequential format. By doing this, the variable profile could still be collected and compared with the same measurement procedure as the homogenous profile.

The justification for not writing the third protocol for comparison is that the preliminary results from Protocol 2 suggest the infiltration measurement is limited to ±13cm in depth for each hour time-lapse. The purpose of Protocol 3 was to refine the time of measurement by half to increase temporal accuracy, however Protocol 3 will not address the ±13cm constraint, meaning it would have no clear benefit over Protocol 2 in terms of spatial accuracy when locating infiltration variability. If anything, Protocol 2 would be more suitable as it includes an unirrigated section either side of the examined transect, which is useful for visualisation of the extent of infiltration at each time-lapse, giving the experiment 'control' for graphical interpretation.

5.4 Protocol 2 – Variable profile

The variable profile data was captured with the SAS4000 from ABEM. This machine is the older version of the Terrameter LS, and is quite different in its settings. It was used because the LS malfunctioned and was unable to be repaired via the remote diagnostics service from ABEM in time for final experimentation. The actual measurement method is the same as the LS, being a Wenner based protocol with DC current supplied to the soil and voltage drop measured, however the setup to take this measurement including all the settings and protocol input is quite different. As a result of this, the time of measurement could not be restricted to one hour as was the case with the LS, the full protocol had to be run. This procedure took two hours determining the temporal measurement of infiltration as two hours.

Figure 27 shows the variable profile data as a percentage change map (joint inversion) when compared to the initial data set, before irrigation had begun. The variable features that were placed in this profile to cause stochastic infiltration, depicted in Figure 18, were placed between -2.5m and 2.5m, as read from the plots in Figure 27. After 2 hours, and 4 hours, there is a reduction in resistivity at the surface between these points, which is attributable to the irrigation water, however in none of the plots, do the features placed in the profile show up clearly.

During the inversion of this data, a warning was given from the RES2DINV software that the model block width should be refined due to large variations in the apparent resistivity near the surface. This is not an error of measurement, but because the profile being examined was designed to be variable, the inversion software makes recommendations to improve the model results. In this instance, the model was run twice for comparison and the decreased width of model blocks failed to make any significant changes to what is seen in Figure 27.

As there are no clear decreases in resistivities when comparing each data set to the initial constraints, and the decreases observed occur uniformly (not as would be expected given the known variability the inversion was undertaken a second time comparing each data set to the time-lapse immediately prior. For this inversion approach, changes in resistivity occurring in the specified 2hr time space are displayed as a percentage change map. The inversion was completed under the same inversion settings, which were slightly different to the homogenous profile settings and are

available in Appendix B2. The differences were to account for a model block thickness previously discussed.

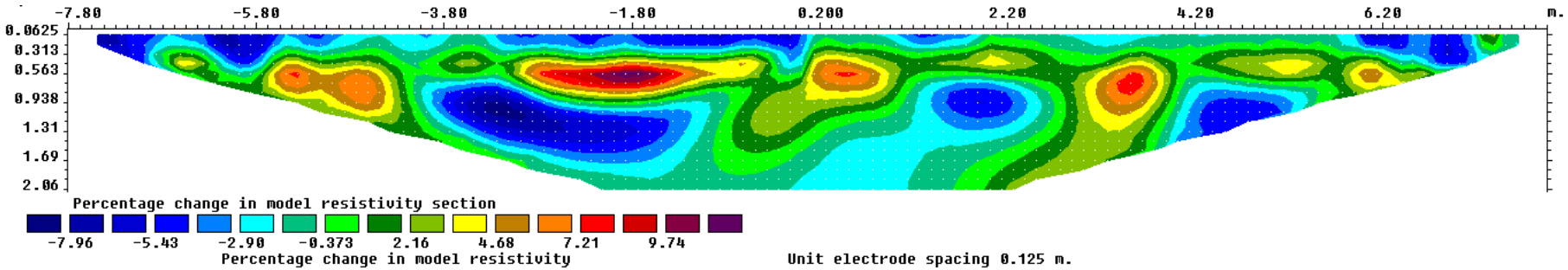

After 2 hours

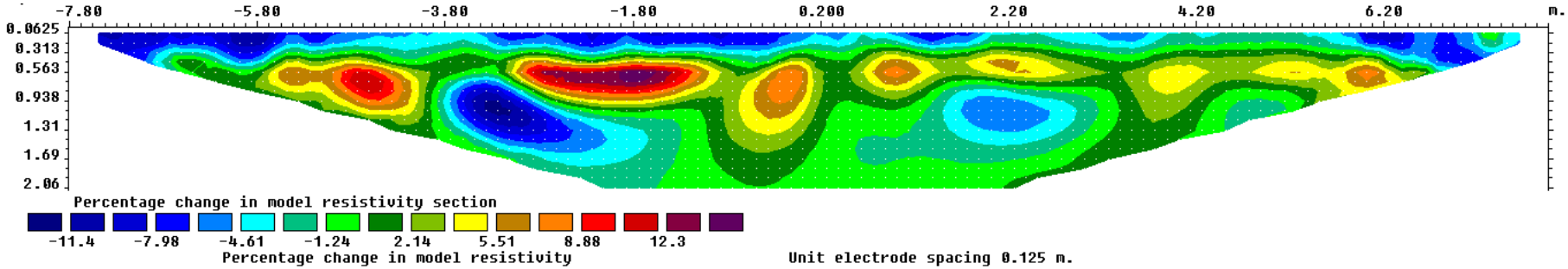

After 4 hours

Figure 27 Variable profile – two hour time-lapse

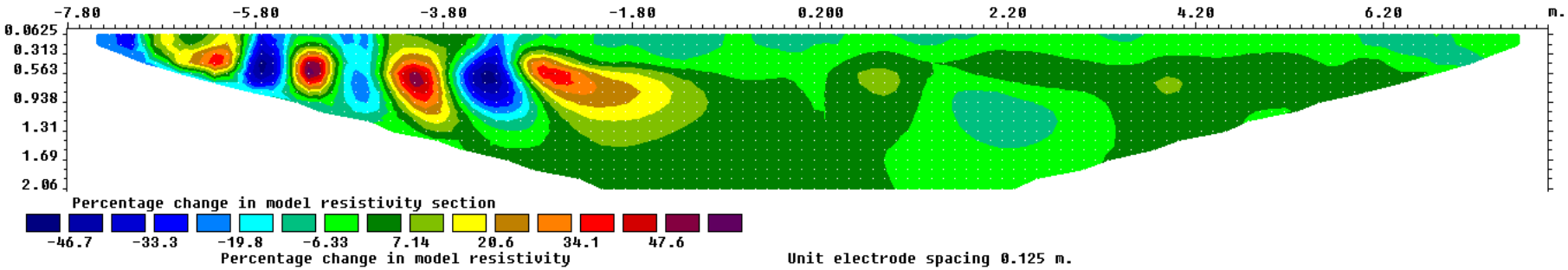

After 6 hours

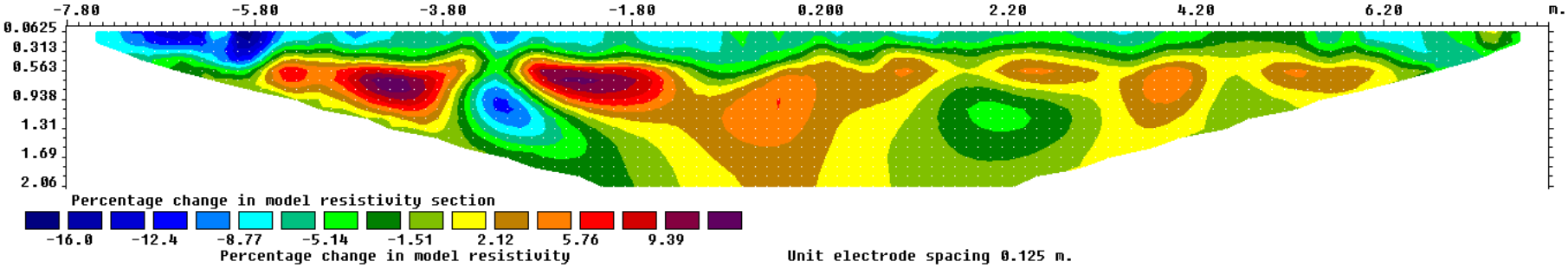

After 8 hours

Figure 27 (Cont.) Variable profile – two hour time-lapse to initial comparison

Figure 27 shows the variable profile data as a percentage change map when compared to the initial data set, before irrigation had begun. The variable features that were placed in this profile to cause stochastic infiltration, as seen in Figure 18, were placed between -2.5m and 2.5m, as read from the plots in Figure 27. After 2 hours, and 4 hours, there is a reduction in resistivity at the surface between these points, which is attributable to the irrigation water, however in none of the plots, do the features placed in the profile show up clearly.

During the inversion of this data, the warning was given from the RES2DINV software that the model block width should be refined due to large variations in the apparent resistivity near the surface. This is not an error of measurement, but because the profile being examined was designed to be variable, the inversion software makes recommendations to improve the model results. In this instance, the model was run twice for comparison and the decreased width of model blocks failed to make any significant changes to what is seen in Figure 27.

As there are no clear decreases in resistivity's when comparing each data set to the initial and what decreases are there, don't show any variability as would be expected given the soil features that were placed and created in this profile, the inversion was undertaken a second time comparing each data set to the time-lapse immediately prior. In this inversion, the changes that occurred in that 2hr time space only would be displayed as a percentage change map. The inversion was completed under slightly different inversion settings to the homogenous profile settings and are available in Appendix C2. The differences were to account for a model block thickness previously discussed.

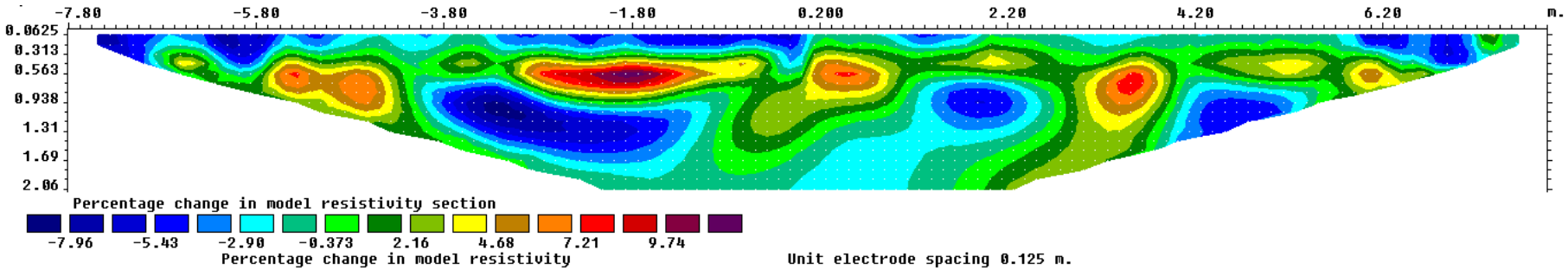

Initial to 2 hours

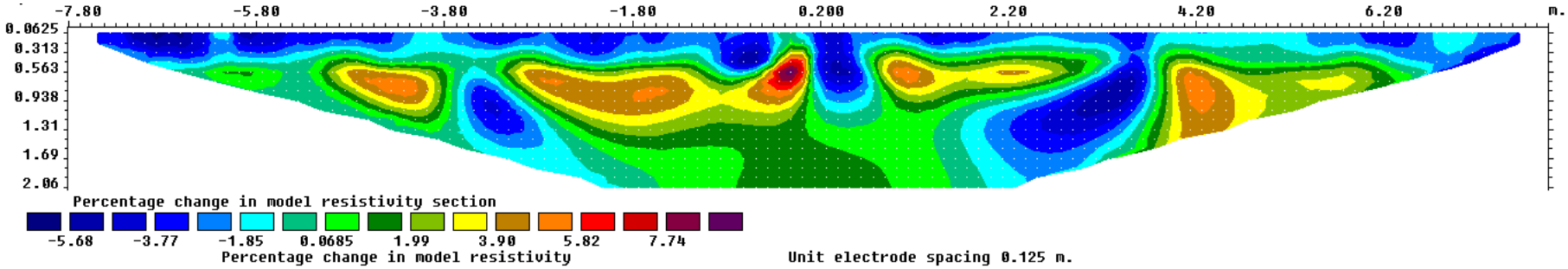

2 hours to 4 hours

Figure 28 Variable profile – two hour time-lapse intervals

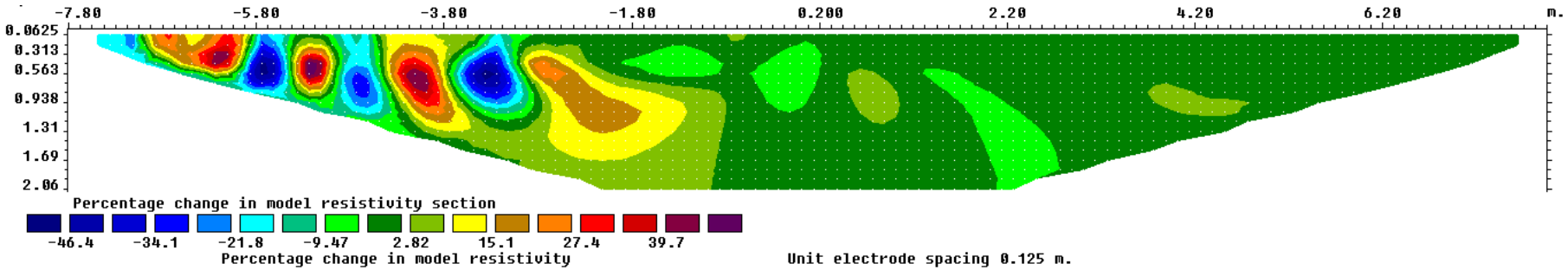

4 hours to 6 hours

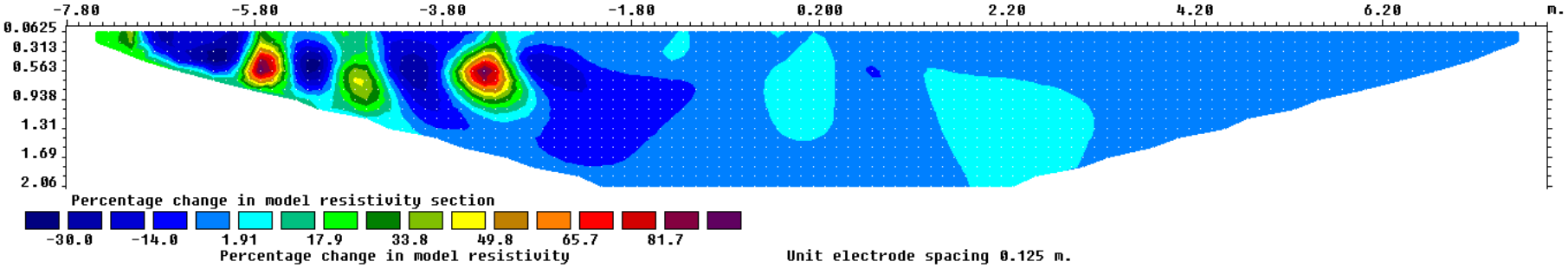

6 hours to 8 hours

Figure 28 (Cont.) Variable profile – two hour time-lapse intervals

The results in Figure 28 are again, not obvious as to the extent of infiltration, apart from the time interval of two to four hours. In the variable profile, the anthropogenic variability features were placed at the following locations, measured from the western side of the pit, that being -2.5m on the SAS4000 images:

- Logs: 0.7 – 1.6 m, 30cm below surface
- Compaction: 2.3 – 3.0 m, 40cm below surface
- Rock: 3.3 – 4.5 m, 50cm below surface

On the transect map produced by the SAS4000, these measurements equate as follows:

- Logs: -1.8 – -0.9 m
- Compaction: -0.2 – 0.5 m
- Rock: 0.8 – 2 m

These features line up remarkably well with the changes in resistivity between hours two and four (Figure 29).

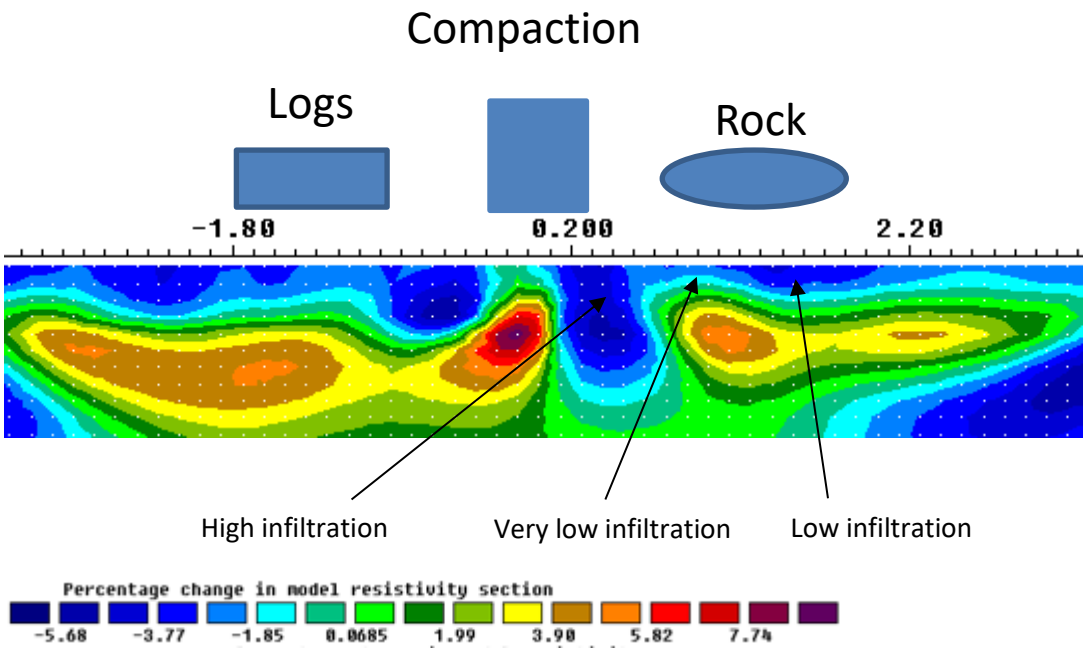

Figure 29 Correlation of infiltration with soil features

Figure 29 displays the visual correlation between the profile anthropogenic variability features, and the relative differences identified by the ERT. A similar visual result was obtained from the initial to two hours' data set, where it shows an infiltration response over the logs, but not the rock. This makes logical sense as the logs were buried with a gravel, while the rock buried with clay. In the first two hours, there was no noticeable impact on the clay.

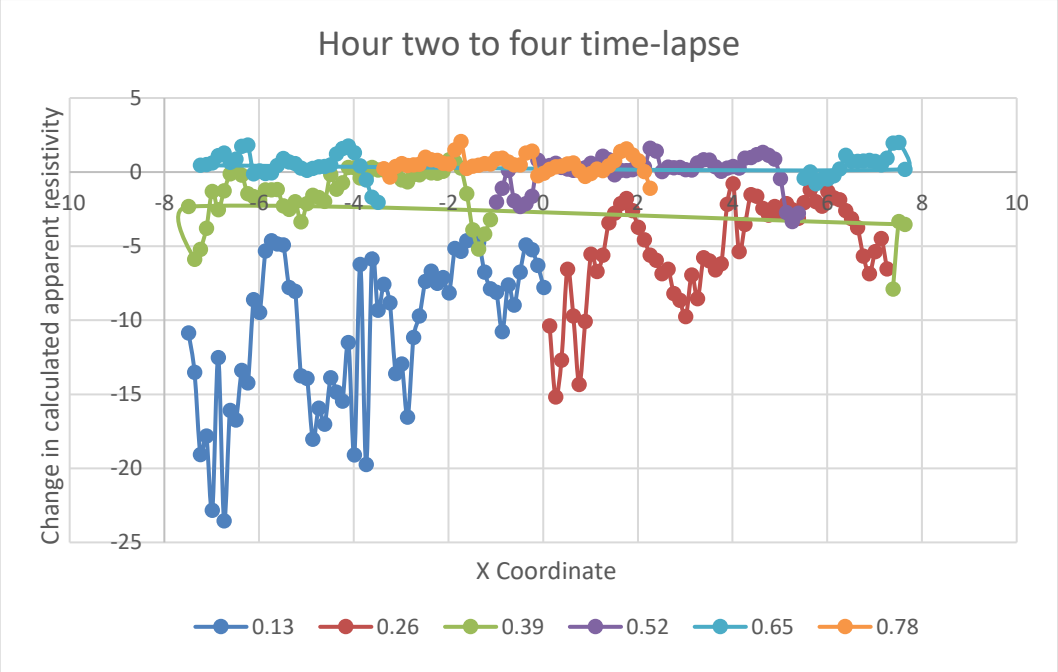

Figure 30 Variable profile - change in calculated apparent resistivity

Figure 30 is the same style data as was presented in the homogenous profile in order to determine the depth at which the water was influencing the resistivity measurements. However, in this data set, the use of the SAS4000 has caused issue with graphing in the exact same manner. While the protocol used was the same, the SAS4000 has a setting for identifying the midpoint of the electrode array. This is entered as a set of coordinates to be between electrodes 32 and 33, as this is the geometric midpoint. This setting however influences the protocol procedure and it does not follow the direct, sequential order laid out by the protocol. Instead, it measures the first depth with electrodes on one side of the midpoint, then the next depth with electrodes on the other side of the midpoint. By doing this, there is not a recorded value for every x coordinate, at every depth.

It is not split directly in half either. Because the ERT measures what looks like an inverted triangle, the number of recordings on each depth layer decreases, causing the midpoint staggering to begin to overlap. This is seen in Figure 30 where the depth 0.39m has data on both sides of the midpoint.

6.0 Discussion

This section builds on the results previously presented and discusses these against the initial aims and objectives. In general, the ERT approach has shown significant potential to help inform soil profile infiltration variability and complexity. However, there are a number of identified limitations and modifications of procedure that will be important in moving towards parameterising stochastic variation in infiltration models, and in converting resistivity data to apparent infiltration data.

6.1 Capability of electrical resistivity tomography to inform infiltration

The initial experiment was conducted over a homogenous profile with no obvious soil factors that would create infiltration variability. This was done so the settings of the inversion software could be optimised to reduce the noisy data and eliminate artefacts cause by the inversion process or errors read by the machine. The process of optimisation involved manipulating the imbedded settings within the software and running the model to identify which parameters gave the lowest root mean square (RMS) error and created the least visual variability on the pseudo section plots. With the settings optimised, and available for viewing in Appendix C1, the data can be viewed in RES2DINV as an image, or exported as an .xyz file. The .xyz file is imported into excel for viewing and graphing. In Figure 25, each depth is graphed across the transect as the change in resistivity between the inverted data sets. It is not a change in resistivity as read from the percentage change maps displayed in Figure 24; it is a straight comparison of the calculated apparent resistivity readings from one data set to the next, after an hour time-lapse. This graph indicates at which depth the change in resistivity is occurring, or in simpler terms, at what depth the water is influencing the resistivity readings.

It can be seen in Figure 25 that in the final time-lapse after four hours of applied irrigation, there has been a resistivity change registered at 0.65m, but not for the entire profile. Closer examination of the figure shows that at some locations along the transect, 0.65m showed no change while it showed a change of 2 Ohm.m in other parts. This potentially indicates that even in the homogenous profile, there is a variability of soil water dynamics being identified by the ERT. This is reinforced by the visualisation of the Figure 24 plots themselves, namely each depth layer not having a smooth curve. This is indicating that at each point above the wetting front, that is, the soil theoretically approaching saturation and located between the wetting front and the ground surface, there is varying volumes of water present. This is an accurate assumption given that volumetric water content is a function of porosity, and the distribution, shape, and size of the pore network will never be identical, even in two sections of the same soil profile. Therefore, varying levels of resistivity change indicate that there is in fact natural variability present within this profile.

6.1.1 Low resistivity layers

A low resistivity layer was identified in the naturally occurring (homogeneous) soil profile, which was presumed to have been cause by a high gravel content, whereby this

facilitated numerous voids. The presumption is extended that these voids filled with air and likely to drain rapidly when not saturated, such as under unsaturated hydraulic conductivity conditions like those imposed under drip irrigation (Philip, 1957). This is suggesting that conductivity has been reduced, which could only happen by removing water from the profile. The more likely cause of this increased resistivity is due to an error outlined in section 2.6, whereby the current couldn't penetrate into the subsoil due to the coarse nature of the surface horizon. In the time 0 measurement, the profile is dry meaning the highly resistive gravelly soil at the top of the profile prevents the current from reaching a depth below the top soil to record any measurement in the subsoil. However, by hour 4, the gravelly top soil is saturated and the current is able to use the water as a conductive medium to reach into the subsoil and register a reading that is accurate, but different to the initial reading. As this is different, it is calculated as a percentage change and displayed on the image accordingly.

This raises the issue of whether a negative resistivity change at the wetting front as interpreted by the ERT data, are changes due to the direct influence of soil water, or are a result of the error that has been described and is a measure of the actual soil properties that couldn't be read with an unsaturated top soil. This measurement error will occur again if the situation is reversed, in the case of a resistive, say gravelly subsoil, the current penetrates into it, but it cannot move back out for measurement by the potential electrodes at the surface. The error wouldn't occur in a profile without a large texture and coarse fragment contrast, however as anthropic or variable soils are likely to be highly contrasting in nature, a potential solution to this error would be performing the inversions in reverse. That is, collecting the irrigation data as done in the original method, but instead of using the initial data set as the constraints for the subsequent data sets, using the completely saturated profile, which is more likely to have captured the profile resistivity as it actually is, as the constraining data set and looking for any decreases in resistivity between the individual data sets. As all of the time based parameters are known, there is no reason why showing the influence of soil water in reverse and back calculating the extent of infiltration for each time interval, wouldn't be a viable option.

6.2 Informing stochastic variability

As the variable profile data was collected with an older model Terrameter SAS4000, it is difficult to directly implement the methods developed from the homogenous profile experiment and validate them on the variable profile, given that the measurement procedures were not identical. That said, the variable profile still showed a reasonable result in one of the time-lapse intervals. Figure 29 show's good correlation with the underground soil features that can be seen in Figure 18. The data to the left of the midpoint where the logs buried in gravelly soil were the feature, show a quite even infiltration depth. This would be expected as the logs were not sealed meaning that as the wetting front reached them, lateral flow caused the water to continue downwards, moving around and between the logs. That is, the water would not reach the logs and completely stop to eventually cause a ponded head, it would gravimetrically find its way

around without having to laterally flow more than 0.2m, being the approximate radius of the logs.

The opposite situation occurs to the right of the midpoint, where the rock was completely sealed and has a large surface area. The rock also had a depression in the middle and was placed to be somewhat bowl shaped, which if sat above ground would hold any water that was poured onto it. This same principle applies when the rock is underground, any water that infiltrates to the rock surface would take a long time to move laterally around the rock. The mechanism for this movement is the matric potential and osmotic potential, which must overcome the downward forces of the gravimetric and pressure potentials in order to move upwards and over the lip of the rock. As there is irrigation underway, the pressure of the water applied is enough to overcome the matric and osmotic potentials, so the water within the boundary of the rock, remains within the boundary and any additional water applied will infiltrate until soil saturation is realised and a ponded head builds. The volume of water applied to reach this ponded head status is significant and was not applied in this experiment. There will come a point in which the pressure caused by the ponded head will cause the saturated section of the profile to infiltrate water laterally, moving water outside the boundary of the rock which allows downward infiltration once again. However, the water moving out of plane, that is, the water moving perpendicular to the transect line, is out of the range of influence of the ERT measurement as it is the third geometric dimension. In this regard, saturated flow around impermeable soil features cannot be monitored by the ERT. As part of this three-dimensional saturated flow, there will be lateral flows that are parallel with the ERT transect, however, these will not influence the infiltration rate if the soil is at saturation. For instance, looking at Figure 29, water that is not infiltrating at the 'no infiltration' label may laterally flow to the left into the soil where there is a high infiltration rate. In this high infiltration rate, it is not possible to determine the proportions of water that have come from irrigation directly above, and from lateral flow from the rock. As mentioned, if the soil in the high infiltration rate section is at saturation, then it is the same concept as a double ring infiltrometer and the water above the rock will be restricted to moving out of plane, rather than into the high infiltration zone, as driven by pressure gradients. If saturation has not yet been achieved however, there will be water moving laterally from the rock, at a rate dependent on the pressure gradient.

With this said, the identification of which section of irrigation is delivering water to which infiltration zone is out of the scope of this project. The important fact here is that the ERT recognises that water has infiltrated to a significantly deeper depth between the compaction and the rock, than it has over the top of these features, and this is a successful parametrisation of stochastic variability.

From Figures 28 and 29, there can be a number of rate of infiltration categories described, each with the geometric amount of profile they are representative of, with respect to both width and depth. Figure 29 alone does not provide the grounds for giving an explicit infiltration rate, as it is only a single time interval. It can be said that in the high infiltration zone, the water is impacting to approximately 0.94m, after 4 hours,

implying an infiltration rate of 235mm/hr. This is extraordinarily high, but given that the profile was excavated and reburied, with no compaction or time allowed for natural settling, it is likely that the soil is unusually well aerated which would accommodate for infiltration rates of this magnitude. By the same logic, it is said that the low infiltration rate zone above the rock has infiltrated approximately 0.31m in the same 4 hours, indicating an infiltration rate of 77.5mm/hr. This is a very different result to the high infiltration rate zone, but the soil placed on top was the same for both. It is likely that the soil on top of both had a very similar infiltration rate, however the water above the rock reached the rock surface well before 4 hours and hadn't moved since. This indicates that shorter time lapses would be useful in determining the actual infiltration rate of the section of the profile above the rock.

For the purpose of this project however, the important aspect is that a difference is shown in the infiltration rate, spatially. In the industry application of this technology, the fact that the rock has completely stopped infiltration in its section, is more important than what the infiltration rate of the soil within that section actually is. This allows the categorisation or zoning of the infiltration variability. With this, the following zones of infiltration can be read from the pseudo section in Figures 28 and 29.

Table 1 Stochastic infiltration rate categories

Infiltration zone	Percent of transect	Infiltration (four hours)	Infiltration rate
-2.5m to -0.8m	34%	0.46	115 mm/hr
-0.8m to -0.2m	12%	0.6	150 mm/hr
-0.2m to 0.1m	6%	0	0 mm/hr
0.1m to 0.6m	10%	0.94	235 mm/hr
0.6m to 2.5m	38%	0.31	77.5 mm/hr

The data presented in Table 1 is simply read from Figure 29, it is not calculated as a statistically significant difference of calculated resistivity, which although would be more accurate, would not improve the accuracy of the actual zoning due to the fact the data is limited to ±13cm/hr anyway.

The infiltration zone that registered zero was that recorded above the compaction zone. The compaction zone itself, recorded an increase in resistivity between these data sets, with the resistivity calculated to be in excess of 2000 Ohm.m. This is clearly an unreasonable results given the range of the other readings in the profile were from 0 to approximately 600 Ohm.m. As this value for resistivity becomes larger, the sensitivity of the display as a percentage change becomes larger, that is, the model is more likely to incorrectly predict the resistivity at higher values and considering the RMS error is already relatively high, model convergence when the resistivity is abnormally different to the rest of the profile, is unlikely. As a result of this, the section which recorded an infiltration rate of 0 would be excluded from inclusion with a HYDRUS model, for instance.

Without the infiltration rate of 0, parametrisation of stochastic variability has been largely successful, albeit, without an accurate and specific infiltration rate. In an industry

application, the ERT has provided the means to locate the infiltration variability and distinguish between areas of high and low variability. If this method was to be used in an actual industry application, then it would be recommended that the zones of similar infiltration be obtained from the ERT data, and actual infiltration rates measured with infiltrometers to obtain values for input into hydrologic models. As per a standard limitation of the infiltrometer, this will only give the result of infiltration from the surface, not at depth. Combining the traditional technique with the methods developed here using ERT, there is significant ability to accurately identify and zone infiltration variability, and obtain actual infiltration rates for each of these zones.

6.3 Inversion processes

The inversion process is highly influential in the quality of the output of the experimental data. The spatial resolution of the data with respect to depth is determined by the electrode spacing, but can be processed at a more detailed thickness by creating model blocks that are smaller than the electrode depths. In this regard, the spatial resolution can essentially be selected, but the more detailed it is, the more smoothing and averaging is performed, which limits accuracy and creates over populated plots. The mechanism of creating model blocks to increase the spatial resolution is controlled by the model discretization settings within RES2DINV software. When model blocks are made to match the pseudo section data points, the grid looks like Figure 31.

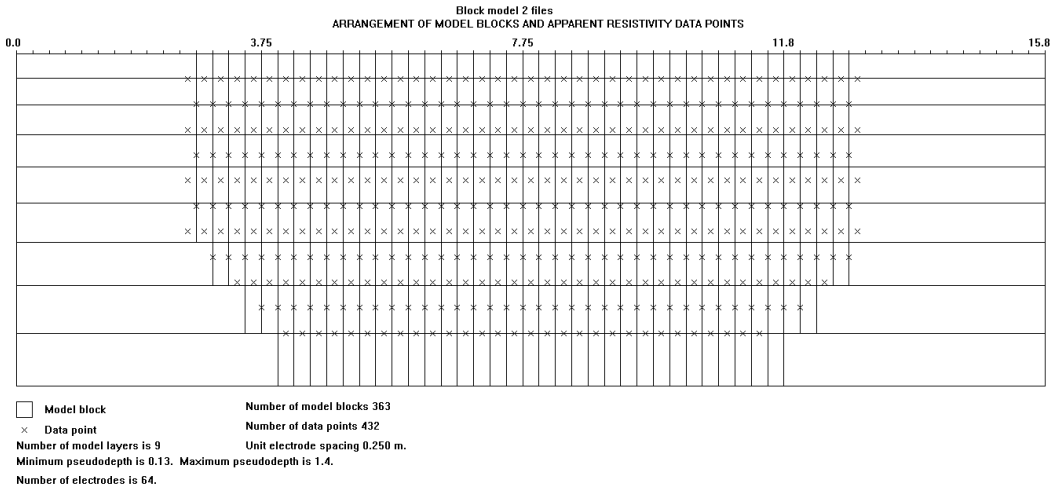

Figure 31 Model blocks matching pseudo section data

It should be noted that not every pseudo section data point matches up with a boundary on a model block. This is because the software is defaulted to increase the model block thickness by a factor of 1.05 with each layer. This can be changed, however there is no accuracy to be gained from reducing it as the sensitivity of resistivity measurements at depth is reduced as per point d, of section 2.6 regarding the laws of physics limiting accuracy at depth, whereby the assumed homogenous section for the measurement of apparent resistivity, is larger at depth due to wider electrode spacing. It should also be noted that plotting the calculated apparent resistivity is done at the location of the pseudo section data point for this experiment, not the centre of the model block. This is significant because the graphed change in calculated apparent resistivity at the pseudo

section points showed a more reasonable result, albeit at larger increments between each recorded depth, than plotting at the centre of each model block where the result of averaging and the recalculation of boundaries caused the data to be smoothed at the cost of clarity.

Figure 32 displays the increased spatial resolution when the model blocks are set to less than the pseudo section data depth. In this instance, the software iterates and calculates the apparent resistivity for each block in the pseudo section, but uses the data recorded at the pseudo section cross to do this. Figure 32 visually shows that many model blocks exist without an actual recorded data point within its boundaries, meaning the value of a model block, is determined as the average of surrounding blocks, by the method of finite difference modelling.

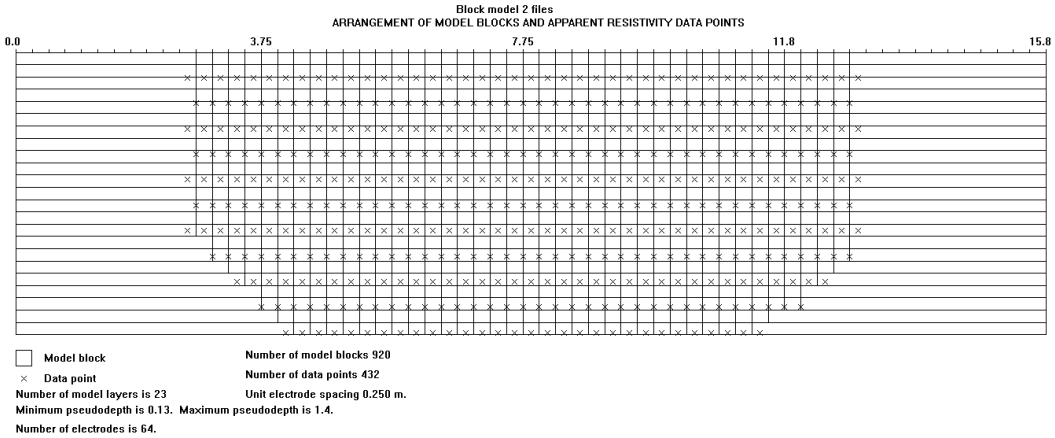

Figure 32 Model blocks for higher spatial resolution

Data inverted using the higher spatial resolution, when plotted using excel, loses the distinct change that occurs in the actual data. For instance the wetting front may actually be at a depth of 0.4 m, but the forward modelling has created two blocks below 0.4 m (0.406 m and 0.469 m) that were subjected to iterative averaging as they approached the next pseudo section data point at 0.52 m, and consequently show a slight resistivity change at 0.469 m which doesn't actually exist. By using the lower resolution, it would be seen that at the pseudo section point at 0.39 m there was a resistivity change, but not at 0.52 m, which is the next depth. Therefore there is confidence that the wetting front is somewhere between 0.39 m and 0.52 m, while the higher resolution indicates that it may lie between 0.469 m and 0.52 m, which although is a smaller range, is potentially incorrect. One of the primary limitations of ERT technology in informing infiltration is clearly the depth based b spatial resolution. There cannot be an accurate infiltration estimation made when the confidence range is 0.39 m to 0.52 m, in an hour time-lapse. However, for the purpose of determining highly differential environments, this is perhaps not important, and the resolution sufficient to inform further modelling. The intent of the work was not to produce a highly accurate discrete measure of infiltration, but to vital characteristics of stochastic function key parameters (e.g. max, min and frequency).

6.4 Limitations of approach

6.4.1 Terrameter SAS4000 versus Terrameter LS

The project was split into two phases, the first being the protocol testing and inversion development on a homogenous profile, and the second being testing on a variable profile that was purpose built with the locations of underlying features recorded for comparison with data obtained from the ERT.

Initially, there were to be two protocols written and tested, which restricted measurement to 10m and 5m respectively in order to best maximise the temporal accuracy by reducing the time it takes to capture each data set. Due to an unforeseen malfunction of the Terrameter LS that was used in the project, an older model Terrameter SAS4000 was borrowed. With this machine, the input options for the control protocols are limited to designing the protocol in the supplied software, rather than a universal method such as writing code into an .xml file format. As this takes extensive amounts of time, only the protocol of 10 m (Protocol 2) was rewritten to allow direct comparison between the homogenous profile and the variable soil environment. The measurement procedure was run continuously while the irrigation was underway, and at the completion of each protocol, the data was saved and recorded as a standalone image for that specific time interval. Subsequently, the changes between these images is what is important to capture changes in the soil hydraulic system.

As these are standalone images, they each must be inverted to actual resistivity readings and compared with one another. The simplest approach to examining differences in time-lapse data sets is to invert each with existing RES2DINV software, and compare them as a percentage change map, that is, the percentage of difference at each location between each time-lapse. However, this opens up the entire analysis to data noise from both the initial and subsequent data sets due to the iterative nature of a finite differencing model, that is, the boundaries used throughout the model that are recalculated until convergence will be different between two data sets. This noise will create artefacts in the resistivity data that will show up on a percentage change map as a variation that does not really exist in the soil profile (Hayley, Pidlisecky, & Bentley, 2011). In order to combat this, it is recommended that a joint inversion or a simultaneous inversion program is implemented in order to constrain each dataset to the same set of initial boundary conditions, so that there is a point of reference for beginning each inversion. This joint inversion program exists as part of the RES2DINV software and was used for the inversion of all data sets.

6.4.2 Depth based data intensity

In conjunction with the discussion of natural variability in the homogenous profile, there is of course another interpretation of the changes identified at 0.65m. That is, that the spatial accuracy of the ERT at this depth is not as great as it is at the surface and it is simply an error of measurement or an error of the inversion process. The raw, apparent resistivity reading, as discussed, includes the assumption that the soil medium between the current and potential electrodes is homogenous. Assume a point ‘x’ that exists within the profile at a depth of 0.65m. From the pseudo section, there could be up to 50

electrode combinations that include the point ‘x’ in its apparent resistivity calculation, depending on the location of ‘x’. As each of these readings will be slightly different, given they’re each measuring a different section of the profile, it is the role of the inversion process to deduct what each electrode combination is calculating the apparent resistivity value at point ‘x’ to be, and make a calculation through finite differencing of what the most likely actual value at ‘x’ is, with the supplied data. With this information, it can be interpreted that as depth increases, the longer the assumed ‘homogenous’ sections become and the more inaccurate the finite differencing technique becomes. It doesn’t become inaccurate in its calculations; it becomes inaccurate due to the quality of data decreasing.

6.5 Further work

Within this project, only the measurement format of a Wenner protocol was investigated. There are a range of different measurement styles, as well as induced polarisation methods. While the Wenner was selected as it is a well-established protocol for a range of situations, the other protocol arrangements each have their strengths and weaknesses regarding temporal and spatial parameters. Research into how other protocols, particularly dipole-dipole resistivity work would be recommended for further work in infiltration.

Additionally, the RES2DINV software provides a host of settings to enable a large variety of data manipulation. Further investigation into how the software works would provide an invaluable benefit to maximising the potential that the Terrameter data offers.

Finally, the use of 12 channel Terrameter’s or other brands of ERT measuring devices would be of use as extra channels, and other machine designs offer various levels of temporal manipulation.

7.0 Conclusion

7.1 Fulfilment of project aims

This research project was conducted to determine the potential that ERT technology brings to quantifying the infiltration variability that commonly exists in a highly variable and complex soil environment. It was determined that these environments will become increasingly common as mine site rehabilitation becomes a pressing environmental and social issue moving forward. The ability to monitor changes in these complex and variable environments has traditionally been a difficult task because the subsoil complexities are completely stochastic, making classical methods of infiltration measurement highly inefficient. The primary project objective for this research was to develop a measurement method that enabled infiltration variability to be located. In order to begin the development of this method, there was a requirement to thoroughly understand the manner in which the Terrameter LS performs a measurement so that both the order and time of measurement could be manipulated to accommodate the post-processing of time-lapse data sets.

The investigation of the Terrameter LS instigated the creation of a standalone and original measurement protocol that confined the measurement of raw data points to within a 10m section. This refined the time of measurement to 60min in order to achieve better temporal resolution through faster measurement. This new protocol was accompanied with prescribed settings to the Terrameter LS itself. It is important that the settings identified are always selected when performing work with this protocol as they were selected to assist in the accuracy. Without the prescribed settings, the new protocol is subject to a range of potential errors.

This new protocol was run over a homogenous profile in order to collect data that could be used to optimise the inversion software that is required to invert raw apparent resistivity data from the Terrameter LS, into values of actual resistivity. For this development, it was required that there be able to be direct comparison between time-lapse intervals, hence a joint inversion technique was implemented where a single set of constraints were used as a modelling reference point. This allowed the data to be plotted as a map of percentage change, that is, at a point ‘x’ on the time 0 data set, the same point, ‘x’ on the time 1 data set could be compared and calculated as a percentage difference. With this process performed across the entire two-dimensional transect, it can be seen at what depth there has been a decrease in resistivity, which indicates the introduction of water, given that water is more conductive than soil. This measurement technique on the homogenous profile encountered some errors, however was largely successful at showing that as water reaches a depth measured by the ERT, it can be realised as a change in resistivity. Subsequently, as the water changed a resistivity value at a specific depth, the time was known to within an hour. This was the grounds for measuring a specific infiltration rate (depth/time), however due to the depth intervals of the Terrameter LS being 13cm, and the time-lapse at an hour, it was not possible to give an infiltration rate as accurately as the traditional methods.

The variable profile had the same measurement technique run, however with a different ERT measuring device, that being the SAS4000, an older model Terrameter which was used due to malfunction of the Terrameter LS. These data sets, after having undergone a similar inversion process, showed that on the percentage change map there was a visual correlation that indicated that the ERT technology had identified and two-dimensionally located the variable soil features that had been placed in the profile. Again, an accurate infiltration rate could not be allocated, however the locating of stochastic infiltration variability largely fulfils the primary aim of this project.

7.2 Application to industry

From this project, the application of ERT technology in industries where the monitoring of soil water dynamics is important, contains significant potential. The results from the variable profile showed that with the appropriate data cleaning and inversion techniques, the ERT has the capacity to identify where in the profile that the infiltration rate changes, how much of the profile is represented by various infiltration rates, and is able to show a rate of infiltration to a $\pm$13cm/hr accuracy. Although this is a very inaccurate infiltration rate for science and research purposes, it is useful in determining infiltration variability as when there are coarse fragments in the profile, the infiltration rate may become zero, while in a clay section there will be slow movement, and high infiltration rates in the coarsely textured sections. The purpose of this project was to identify infiltration variability in complex and variable soil environments, to which it was successful in locating variability, and marginally successful in allocating an actual infiltration rate. The most prominent environment for these variable conditions is mine site rehabilitation where the burial of waste rock has created an environment that is statistically random and difficult to predict. The prediction of where the variability is located, and the parameterisation of the minimum, maximum, average and distribution is very useful for improving the accuracy of hydrologic models which are commonly used to predict how water moves through a landscape. If these models, such as HYDRUS, are used without an understanding of the underground variability, then water may not infiltrate as expected which could cause significant run off issues in extreme cases. The use of ERT technology in this research project has shown that there is indeed potential to use and build on the methods developed here, to better optimise the Terrameter's performance, and subsequently, optimise current hydrologic models so that they may be used to better predict the behaviour of water in complex and variable soil environments.

List of References

ABEM. (2012). *Instruction Manual: Terrameter LS*. Sweden: ABEM Instrument AB.

Afshar, A., Abedi, M., Norouzi, G.-H., & Riahi, M.-A. (2015). Geophysical investigation of underground water content zones using electrical resistivity tomography and ground penetrating radar: A case study in Hesarak-Karaj, Iran. *Engineering Geology, 196*, 183-193. doi:http://dx.doi.org/10.1016/j.enggeo.2015.07.022

Australia, S. A. o. (1990). Determination of the Moisure Content of a Soil: Oven Drying Method (Standard Method) (Vol. AS 1289 B1.1-1977).

Barker, R., & Moore, J. (1998). The application of time-lapse electrical tomography in groundwater studies. *Leading Edge (Tulsa, OK), 17*(10), 1454. Retrieved from http://www.scopus.com/inward/record.url?eid=2-s2.0-0032188422&partnerID=40&md5=005e4687f5b19e5b0014299b12cc5b3c

Brady, N. C., & Weil, R. (1984). The natural and properties of soils: Macmillan, New York.

Brebbia, C. A., & Walker, S. (2013). *Boundary element techniques in engineering*: Elsevier.

Brouwer, C., Prins, K., Kay, M., & Heibloem, M. (1988). *Irrigation Water Management: Irrigation Methods (Training Manual No. 5)*. Rome.

Caputo, M. C., & Carlo, L. D. (2011). *Field Measurement of Hydraulic Conductivity of Rocks*. Bari, Italy: InTech.

Cassiani, G., Bruno, V., Villa, A., Fusi, N., & Binley, A. M. (2006). A saline trace test monitored via time-lapse surface electrical resistivity tomography. *Journal of Applied Geophysics, 59*(3), 244-259. doi:http://dx.doi.org/10.1016/j.jappgeo.2005.10.007

Chan, C. Y., & Knight, R. J. (1999). Determining water content and saturation from dielectric measurements in layered materials. *Water Resources Research, 35*(1), 85-93.

Clément, R., Descloitres, M., Günther, T., Ribolzi, O., & Legchenko, A. (2009). Influence of shallow infiltration on time-lapse ERT: Experience of advanced interpretation. *Comptes Rendus Geoscience, 341*(10–11), 886-898. doi:http://dx.doi.org/10.1016/j.crte.2009.07.005

Daily, W., Ramirez, A., LaBrecque, D., & Nitao, J. (1992). Electrical Resistivity Tomography of Vadose Water Movement. *Water Resources Engineering, 28*(5), 1429 - 1442.

Dey, A., & Morrison, H. (1979). Resistivity modelling for arbitrarily shaped two-dimensional structures. *Geophysical Prospecting, 27*(1), 106-136.

Dirksen, C. (1999). *Soil physics measurements*: Catena Verlag.

Douglas, J., & Crawford, C. (1993). The response of a ryegrass sward to wheel traffic and applied nitrogen. *Grass and Forage Science, 48*(2), 91-100.

Fang, L., Hain, C. R., Zhan, X., & Anderson, M. C. (2016). An inter-comparison of soil moisture data products from satellite remote sensing and a land surface model. *International Journal of Applied Earth Observation and Geoinformation, 48*, 37-50. doi:http://dx.doi.org/10.1016/j.jag.2015.10.006

Fox, R. L., Phelan, J. T., & Criddle, W. D. (1956). *Design of subirrigation systems*: American Society of Agricultural Engineers.

French, H., & Binley, A. (2004). Snowmelt infiltration: monitoring temporal and spatial variability using time-lapse electrical resistivity. *Journal of Hydrology, 297*(1–4), 174-186. doi:http://dx.doi.org/10.1016/j.jhydrol.2004.04.005

Garré, S., Coteur, I., Wongleecharoen, C., Hussain, K., Omsunrarn, W., Kongkaew, T., . . . Vanderborght, J. (2013). Can We Use Electrical Resistivity Tomography to Measure Root Zone Dynamics in Fields with Multiple Crops? *Procedia*

Environmental Sciences, 19, 403-410. doi:http://dx.doi.org/10.1016/j.proenv.2013.06.046

Ghosh, R. K. (1980). Modeling infiltration. *Soil Science, 130*(6), 297-302.

Gifford, G. F. (1976). Applicability of some infiltration formulae to rangeland infiltrometer data. *Journal of Hydrology, 28*(1), 1-11.

Greacen, E., Correll, R., Cunningham, R., Johns, G., & Nicolls, K. (1981). Calibration *Soil water assessment by the neutron method*.

Greacen, E. L. (1981). Soil water assessment by the neutron method.

Greve, A., Acworth, R., & Kelly, B. (2008). Design, construction and testing of 3D borehole resistivity tomography equipment to measure deep drainage and soil moisture changes. *Sydney, Australia: UNSW-CWI*.

Hanson, B. R., & Peters, D. (2000). Soil type affects accuracy of dielectric moisture sensors. *California Agriculture, 54*(3), 43-47.

Hayley, K., Pidlisecky, A., & Bentley, L. (2011). Simultaneous time-lapse electrical resistivity inversion. *Journal of Applied Geophysics, 75*(2), 401-411.

Herman, R. (2001). An Introduction to Electrical Resistivity in Geophysics. *American Journal of Physics, 69*(9), 943 - 952.

Hillel, D. (1980). *Applications of Soil Physics*. New York, USA: Academic Press.

Hillel, D. (2003). *Introduction to environmental soil physics*. Academic press.

Hoekstra, P., & Delaney, A. (1974). Dielectric properties of soils at UHF and microwave frequencies. *Journal of geophysical research, 79*(11), 1699-1708.

Holtan, H. (1971). *USDAHL-70 Model of Watershed Hydrology*. Washington DC: Agricultural Research Service.

Hornung, U., & Messing, W. (1981). Simulation of two-dimensional saturated/unsaturated flows with an exact water balance. *Flow and transport in porous media. Balkema, Rotterdam, The Netherlands*, 91-96.

Horton, R. (1941). An approach toward a physical interpretation of infiltration-capactiy. *Soil Science Society of America Journal, 5*(C), 399-417.

Huisman, J. A., Snepvangers, J. J. J. C., Bouten, W., & Heuvelink, G. B. M. (2002). Mapping spatial variation in surface soil water content: comparison of ground-penetrating radar and time domain reflectometry. *Journal of Hydrology, 269*(3–4), 194-207. doi:http://dx.doi.org/10.1016/S0022-1694(02)00239-1

Huisman, J. A., Sperl, C., Bouten, W., & Verstraten, J. M. (2001). Soil water content measurements at different scales: accuracy of time domain reflectometry and ground-penetrating radar. *Journal of Hydrology, 245*(1–4), 48-58. doi:http://dx.doi.org/10.1016/S0022-1694(01)00336-5

Jackson, P., Northmore, K. J., Meldrum, P. I., Gunn, D. A., Hallam, J. R., Wambura, J., . . . Ogutu, G. (2002). Non-invasive moisture monitoring within an earth embankment — a precursor to failure. *NDT & E International, 35*(2), 107-115. doi:http://dx.doi.org/10.1016/S0963-8695(01)00030-5

Jackson, R. D. (1982). Soil moisture inferences from thermal-infrared measurements of vegetation temperatures. *Geoscience and Remote Sensing, IEEE Transactions on*(3), 282-286.

Jackson, T. J. (1990). Laboratory evaluation of a field-portable dielectric/soil-moisture probe. *Geoscience and Remote Sensing, IEEE Transactions on, 28*(2), 241-245.

Kachanoski, R. G., Wesenbeeck, I. J. V., & Gregorich, E. G. (1988). ESTIMATING SPATIAL VARIATIONS OF SOIL WATER CONTENT USING NONCONTACTING ELECTROMAGNETIC INDUCTIVE METHODS. *Canadian Journal of Soil Science, 68*(4), 715-722. doi:10.4141/cjss88-069

King, K. W., Arnold, J., & Bingner, R. (1999). Comparison of Green-Ampt and curve number methods on Goodwin Creek watershed using SWAT. *Transactions of the ASAE, 42*(4), 919.

Kirkham, D. (1972). *Advanced Soil Physics*. New York: Wiley.

Kostiakov, A. N. (1932). *On the dynamics of the coefficient of water-percolation in soils and on the necessity of studying it from a dynamic point of view for purposes of amelioration*. Paper presented at the 6th Congress of International Soil Science Society, Moscow.

Kutilek, K., Haverkamp, Rendon, Parlange. (1988). On extrapolation of algebraic infiltration equations. *Soil Technology, 1*(1), 47-61.

Loke, M., & Lane, J. (2004). Inversion of data from electrical imaging surveys in water-covered areas. *ASEG Extended Abstracts, 2004*(1), 1-4.

Loke, M. H. (1999). *Time-lapse resistivity imaging inversion.* Paper presented at the 5th EEGS-ES Meeting.

Lunt, I. A., Hubbard, S. S., & Rubin, Y. (2005). Soil moisture content estimation using ground-penetrating radar reflection data. *Journal of Hydrology, 307*(1–4), 254-269. doi:http://dx.doi.org/10.1016/j.jhydrol.2004.10.014

Marthaler, H., Vogelsanger, W., Richard, F., & Wierenga, P. (1983). A pressure transducer for field tensiometers. *Soil Science Society of America Journal, 47*(4), 624-627.

Martinez, A., & Byrnes, A. P. (2001). *Modeling dielectric-constant values of geologic materials: An aid to ground-penetrating radar data collection and interpretation*: Kansas Geological Survey, University of Kansas.

Mays, L. (2010). *Water Resources Engineering* (2nd ed.): Wiley.

Merrill, S., & Rawlins, S. (1972). FIELD MEASUREMENT OF SOIL WATER POTENTIAL WITH THERMOCOUPLE PSYCHROMETERS. *Soil Science, 113*(2), 102-109.

Mohammadzadeh-Habili, J., & Heidarpour, M. (2015). Application of the Green–Ampt model for infiltration into layered soils. *Journal of Hydrology, 527*, 824-832. doi:http://dx.doi.org/10.1016/j.jhydrol.2015.05.052

Morin, J., & Benyamini, Y. (1977). Rainfall infiltration into bare soils. *Water Resources Research, 13*(5), 813-817.

Naeth, M., Chanasyk, D., & Bailey, A. (1991). Applicability of the Kostiakov equation to mixed prairie and fescue grasslands of Alberta. *Journal of Range Management*, 18-21.

Nations, U. (2015). *World Population Prospects, The 2015 Revision*. New York: United Nations.

Neuman, S. P. (1973). Saturated-unsaturated seepage. *J. Hydraul. Div., Am. Soc. Civ. Eng.;(United States), 99*.

Njoku, E. G., & Li, L. (1999). Retrieval of land surface parameters using passive microwave measurements at 6-18 GHz. *Geoscience and Remote Sensing, IEEE Transactions on, 37*(1), 79-93.

Oades, J. M. (1984). Soil organic matter and structural stability: mechanisms and implications for management. *Plant and soil, 76*(1-3), 319-337.

Organization, W. M. (2014). Measurement of evaporation, humidity in the biosphere and soil moisture *Measurement of Soil Moisture* (Vol. 72). Geneva, Switzerland: WMO.

Ortiz-Reyes, T. (1979). Experimental evaluation of infiltration using Holtan, Philip, and Mein and Larson equations.

Owe, M., De Jeu, R., & Walker, J. (2001). A methodology for surface soil moisture and vegetation optical depth retrieval using the microwave polarization difference index. *Geoscience and Remote Sensing, IEEE Transactions on, 39*(8), 1643-1654.

Pan, L., Warrick, A., & Wierenga, P. J. (1996). Finite element methods for modeling water flow in variably saturated porous media: Numerical oscillation and mass-distributed schemes. *Water Resources Research, 32*(6), 1883-1889.

Philip, J. R. (1957). The theory of infiltration: 4. Sorptivity and algebraic infiltration equations. *Soil Science, 84*(3), 257-264.

Powers, M. H. (1997). Modeling frequency-dependent GPR. *The Leading Edge, 16*(11), 1657-1662.

Rawls, W. J., Ahuja, L. R., Brakensiek, D. L., & Shirmohammadi, A. (1993). *Handbook of Hydrology*: McGraw Hill, Inc.

Redinger, G., Campbell, G., Saxton, K., & Papendick, R. (1984). Infiltration rate of slot mulches: measurement and numerical simulation. *Soil Science Society of America Journal, 48*(5), 982-986.

Reynolds, J. M. (2011). *An introduction to applied and environmental geophysics*: John Wiley & Sons.

Reynolds, W. D., Bowman, B. T., Drury, C. F., Tan, C. S., & Lu, X. (2002). Indicators of good soil physical quality: density and storage parameters. *Geoderma, 110*(1–2), 131-146. doi:http://dx.doi.org/10.1016/S0016-7061(02)00228-8

Richards, L. A. (1931). Capillary Conduction of Liquids Through Porous Mediums. *Journal of Applied Physics, 1*(5), 318-333.

Ross, P. (1990). Efficient numerical methods for infiltration using Richards' equation. *Water Resources Research, 26*(2), 279-290.

Ryan, J., Monroe, G., Kacemi, M., & Monem, M. A. (1990). *Compaction of a clay soil: Impact on infiltration and related physical parameters*.

Samouëlian, A., Cousin, I., Tabbagh, A., Bruand, A., & Richard, G. (2005). Electrical resistivity survey in soil science: a review. *Soil and Tillage Research, 83*(2), 173-193. doi:http://dx.doi.org/10.1016/j.still.2004.10.004

Schneider, D. (2016). The Potential Use of the EM38 for Soil Water Measurements.

Simunek, J., Huang, K., & Van Genuchten, M. T. (1998). The HYDRUS code for simulating the one-dimensional movement of water, heat, and multiple solutes in variably-saturated media. *US Salin. Lab. Res. Rep, 144*.

Singer, M. J., & Munns, D. N. (2006). *Soils: An Introduction*. Upper Saddle River, NJ: Pearson Prentice Hall.

Slater, L., Binley, A., Versteeg, R., Cassiani, G., Birken, R., & Sandberg, S. (2002). A 3D ERT study of solute transport in a large experimental tank. *Journal of Applied Geophysics, 49*(4), 211-229. doi:http://dx.doi.org/10.1016/S0926-9851(02)00124-6

Susha Lekshmi, S. U., Singh, D. N., & Shojaei Baghini, M. (2014). A critical review of soil moisture measurement. *Measurement, 54*, 92-105. doi:http://dx.doi.org/10.1016/j.measurement.2014.04.007

Topp, G., Davis, J., & Annan, A. P. (1980). Electromagnetic determination of soil water content: measurements in coaxial transmission lines. *Water Resources Research, 16*(3), 574-582.

Turner, E. (2006). *Comparison of infiltration equations and their field validation with rainfall simulation.* (Master of Science), University of Maryland.

Van Dam, R. L., & Schlager, W. (2000). Identifying causes of ground-penetrating radar reflections using time-domain reflectometry and sedimentological analyses. *Sedimentology, 47*(2), 435-449.

Varado, N., Braud, I., Ross, P. J., & Haverkamp, R. (2006). Assessment of an efficient numerical solution of the 1D Richards' equation on bare soil. *Journal of Hydrology, 323*(1–4), 244-257. doi:http://dx.doi.org/10.1016/j.jhydrol.2005.07.052

Visvalingam, M., & Tandy, J. (1972). The neutron method for measuring soil moisture content—A review. *Journal of Soil Science, 23*(4), 499-511.

Walker, W. R. (1989). *Guidelines for designing and evaluating surface irrigation systems*. (45). Rome, Italy: Publications Division, Food and Agriculture Organisation of the United Nations.

Wang, J., Engman, E. T., & Ungar, S. G. (2010). *Soil Moisture Transect Data (FIFE)*.

Werner, H. (1995). *Irrigation Management Using Electrical Resistance Blocks to Measure Soil Moisture*. Brookings, South Dakota: College of Agriculture & Biological Sciences.

Youngs, E. (1968). AN ESTIMATION OF SORPTIVITY FOR INFILTRATION STUDIES FROM MOISTURE MOMENT CONSIDERATIONS. *Soil Science, 106*(3), 157-163.

Zarba, R. L., Bouloutas, E., & Celia, M. (1990). General mass-conservative numerical solution for the unsaturated flow equation. *Water Resources Research WRERAQ, 26*(7), 1483-1496.

Zhang, F. (2011). *Climate Change Assessment for the Southeastern United States.* (Doctor of Philosophy), Georgia Institute of Technology.

Zhenghui, X., Fengge, S., Xu, L., Qingcun, Z., Zhenchun, H., & Yufu, G. (2003). Applications of a surface runoff model with Horton and Dunne runoff for VIC. *Advances in Atmospheric Sciences, 20*(2), 165-172.

Zienkiewicz, O., & Parekh, C. (1970). Transient field problems: Two-dimensional and three-dimensional analysis by isoparametric finite elements. *International Journal for Numerical Methods in Engineering, 2*(1), 61-71.

Appendix A: Project Specification

ENG4111/4112 Research Project

Project Specification

For: Ned Skehan

Title: Towards two-dimensional infiltration measurement in complex and variable soil environments

Major: Agricultural engineering

Supervisor: Dr. John Bennett

Sponsorship: NCEA

Enrolment: ENG4111 – ONC S1, 2016 ENG4112 – ONC S2, 2016

Project Aim: To develop a method of quantifying infiltration variability using two-dimensional Electrical Resistivity Tomography in highly variable soil environments.

Programme: Issue A, 16th March 2016

1. Research the current uses of Electrical Resistivity Tomography in soil science as well as geophysical measurement situations.

2. Research the current two-dimensional infiltration measurement techniques and interpret the current level of model development.

3. Develop an understanding of how the ABEM Terrameter performs a resistivity measurement and manipulate the order of measurement to suit the project.

4. Design a simple irrigation system that drip irrigates a controlled volume of water while preventing evaporation influences.

5. Run Terrameter continuously throughout an irrigation event on a homogenous soil at a convenient location and ground proof results to determine accuracy of measuring infiltration rates with resistivity.

6. Use calibrated machine on a heterogeneous soil and perform statistical analysis on the likelihood of recording the absolute maximum and absolute minimum infiltration rates.

If time and resources permit:

7. Use the variability parameters in an existing model such as HYDRUS to examine if the accuracy is improved for general infiltration predictions

Appendix B: Experimental Design and Planning

B.1 Irrigation frame design

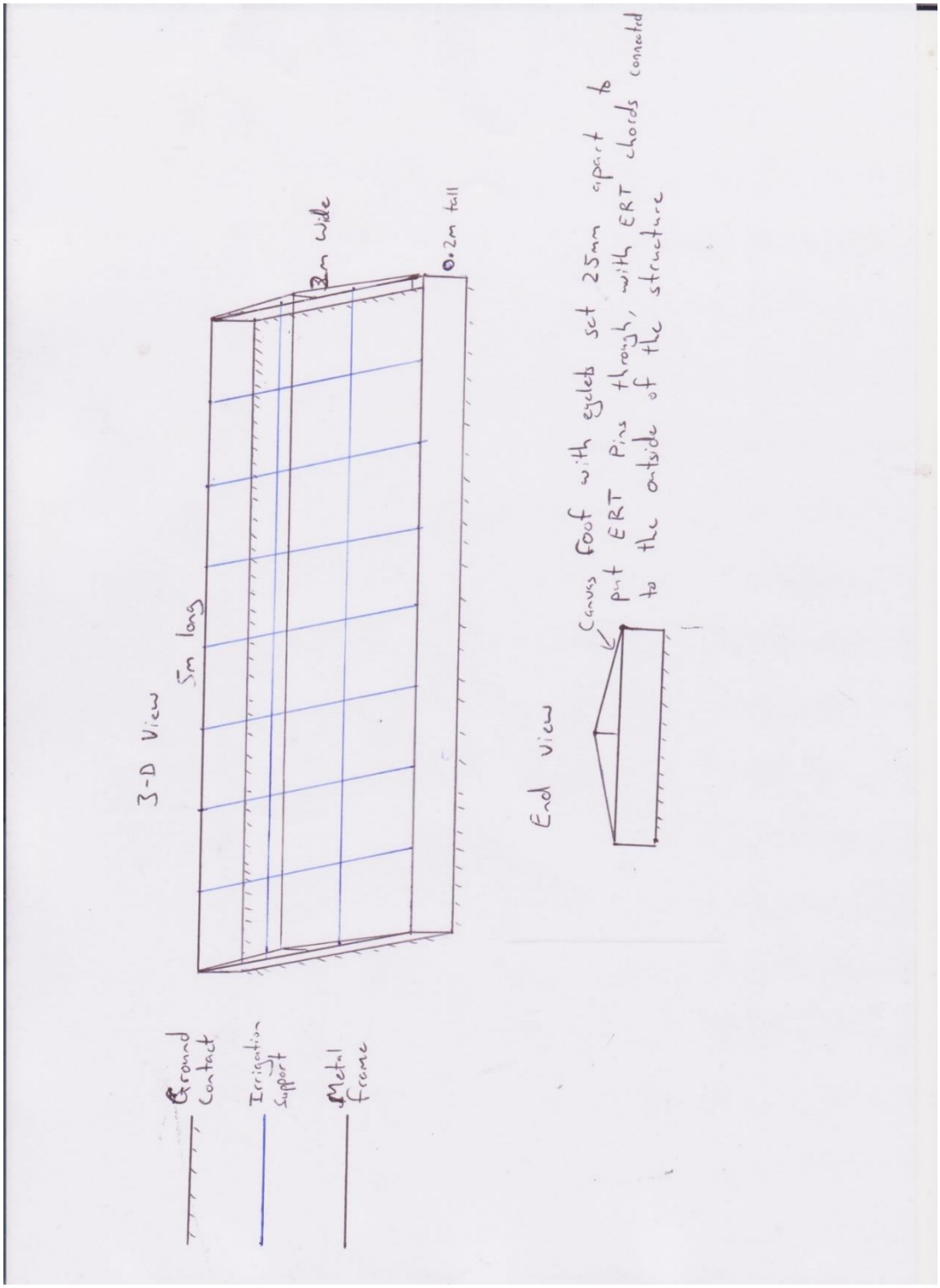

Figure 33 Irrigation frame design

B.2 Risk assessment

The way this risk assessment is structured will be based around the key which matches the likelihood of occurrence with the consequence, to give each activity a coded rating. The risks that will be undertaken are broken into categories, those that influence the personal safety of people involved, and those risks that threaten the quality of the project. The key to these different risks is provided in Table A1.

Table A1 Personal risk rating table

		Consequence			
		A Minor First aid or some medical attention	B Moderate Increased medical attention	C Major Severe health outcome or injury	D Extreme Intensive care or death
Likelihood of Occurrence	1 Rare	A1	B1	C1	D1
	2 Unlikely	A2	B2	C2	D2
	3 Likely	A3	B3	C3	D3
	4 Almost Certain	A4	B4	C4	D4

Table A2 Personal hazards

Task	Hazard	Risk	Minimisation
1	Car accident on the way to site	D1	Obey road rules. Drive to road conditions.
2	Electrocution from ERT	C1	Undertake training with appropriate instructor. Leave power supply cut off until ready to record data.
3	General injury on the trial site	B2	Wear appropriate PPE.

Table A3 Project hazards

Task	Hazard	Risk	Minimisation
1	Receive unprecedented rainfall on site to jeopardise initial moisture recordings.	Medium	Observe weather patterns and perform testing in dry conditions. Cover test site with rain

			protection.
2	Unable to source ERT from the NCEA.	Low	Give plenty of notice to technical staff as to when it will be required.
3	Unable to access trial site.	Low	Remain in consultation with landowners for the timeframe for intended work.

ERT Equipment

The ERT equipment involves the use of electricity, it comes from a 12V battery source, however the hazard comes from the direct current that is used for measuring, it is enough to cause significant health concerns should electrocution occur. The means for minimising this risk involves following the warnings that are included with the machine. Before testing is to begin, there is a warning on the Terrameter's user interface that warns of electric shock if the electrodes are touched. It must be read in full to appreciate the circumstances in which electric shock will occur, and its guidelines followed to avoid contact. There is a built in cut-off button on the side of the machine that can be pressed to immediately stop all electricity that is flowing to the electrodes. Pressing this will not delete or create errors in the data, it simply stops all in an instant, and therefore if there is a dangerous situation arising, pressing it should be the first step to averting the risk.

Irrigation Equipment

The project requires a large volume of water to be supplied through a pipe network that must be constructed as part of the experimental design. This requires cutting plastic pipe with a sharp blade which introduces a risk of personal injury. PPE such as thick gloves are to be worn when using the blade to avoid cutting hands. The gloves will not completely negate the risk as they have to be thin enough to allow mobility, so care must still be taken to keep body parts away from the sharp edge.

The irrigation design also requires the use of a large volume of water to be transported to the site from a nearby storage tank. This introduces the risk of transport where incorrect operation of vehicles may lead to personal injury. Appropriate signage on the vehicle to keep bystanders at a safe distance, and appropriate chains and trailer attachments must be used to prevent the trailer from disconnecting and rolling on its own. Persons with appropriate licencing must only be involved with vehicle operation.

The water from the tank also creates an equipment risk as although the Terrameter is water proof, getting it wet may damage the hardware which requires expensive repairs. Another risk is the combination of electricity and water, as water is an efficient conductor of electricity, keeping the water in the tank and away from the electrodes until the trial begins is an important step to reducing risk of electrocution. The irrigation is to be a drip system releasing a slow rate of water to avoid a ponded head on the surface. If the pipe network is damaged by a dripper coming loose or a pipe bursting, there is a higher risk of a person suffering a more intense electric shock when the cables

and electrodes are wet. To avoid this, properly engineered pipe fittings must be selected to ensure they are able to handle the conditions. If there is damage to the pipe network during the trial, the emergency shut off switch on the Terrameter must be pressed to cease all electricity.

B.3 Resource requirements

The preliminary list of equipment that is expected to be required is shown below with the quantity, source and cost.

Table A4 Equipment requirements

Item	Quantity	Source	Cost
ERT	One	NCEA	Nil
Computer Software	One	NCEA	Nil
Water Storage	One	Landowner	Nil
Building and Plumbing Materials	One	Student	≈$150

Additional equipment will be required for the experimental procedure as follows.

- Spare external, deep cycle 12V batteries.
- Hammers for electrodes.
- Saltwater and bentonite solution for poor electrode contact.
- Measuring tape at least 16m long.
- Spray paint and marking pegs.
- Tool kit including multimeter to monitor batteries, and equipment to repair irrigation plumbing.
- Stationary.

B.4 Timeline

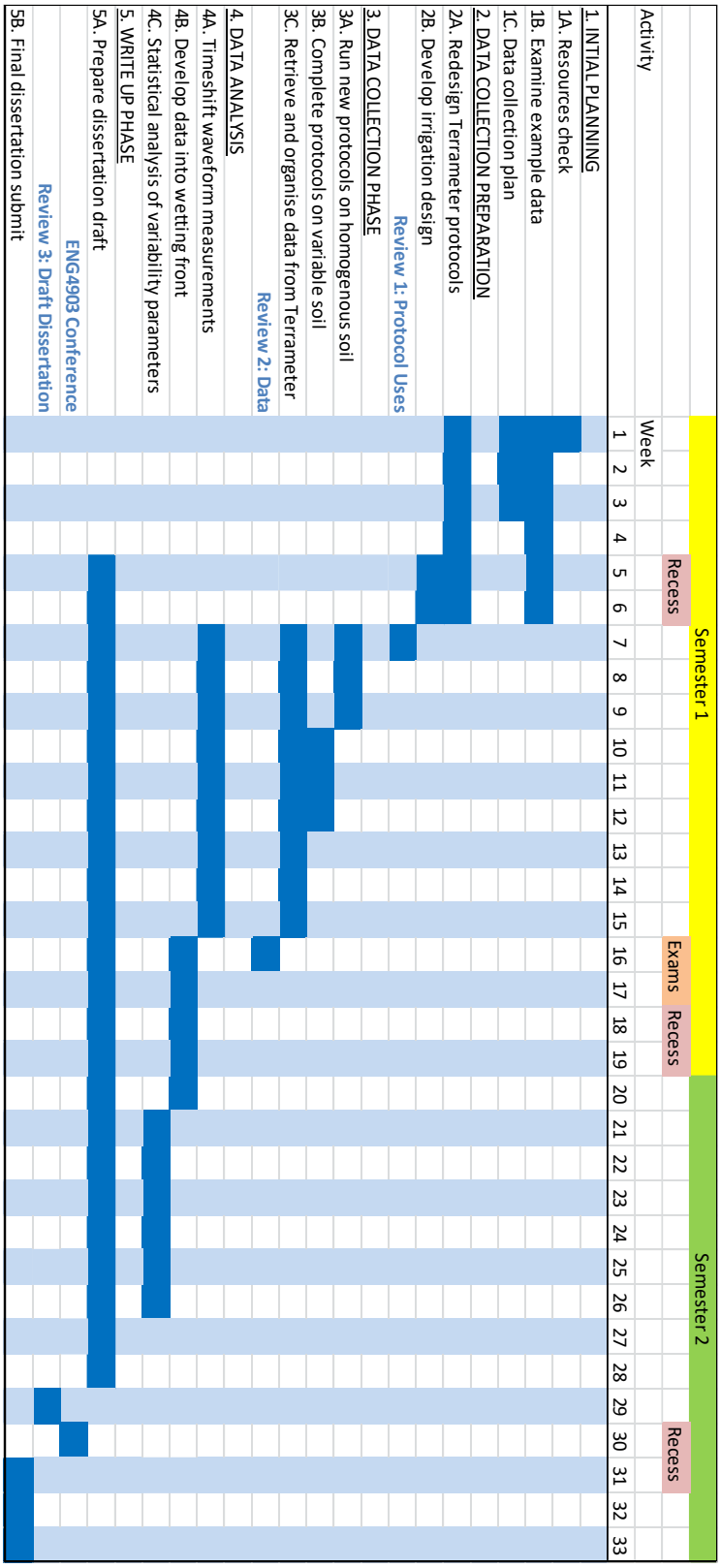

Figure 34 Project timeline

Appendix C: Experimental results

C.1 Inversion settings – homogenous profile

Inversion settings
Initial damping factor (0.01 to 1.00)
0.1500
Minimum damping factor (0.001 to 0.75)
0.0200
Local optimization option (0=No, 1=Yes)
1
Convergence limit for relative change in RMS error in percent (0.1 to 20)
2.0000
Minimum change in RMS error for line search in percent (0.5 to 100)
0.5000
Number of iterations (1 to 30)
15
Vertical to horizontal flatness filter ratio (0.25 to 4.0)
1.0000
Model for increase in thickness of layers(0=default 10%, 1=default 25%, 2=user defined)
2
Number of nodes between adjacent electrodes (2 or 4)
4
Flatness filter type, Include smoothing of model resistivity (0=model changes only,1=directly on model)
1
Reduce number of topographical data points? (0=No,1=Yes. Recommend leave at 0)
0
Carry out topography modeling? (0=No,1=Yes)
1
Type of topography trend removal (0=Average,1=Least-squares,2=End to end)
2
Type of Jacobian matrix calculation (0=Quasi-Newton, 1=Gauss-Newton, 2=Mixed)
1
Increase of damping factor with depth (1.0 to 2.0)
1.0500
Type of topographical modeling (0=None, 1=No longer supported so do not use, 2=uniform distorted FEM, 3=underwater, 4=damped FEM, 5=FEM with inverse Swartz-Christoffel)
4
Robust data constrain? (0=No, 1=Yes)
0
Cutoff factor for data constrain (0.0001 to 0.1))
0.0500
Robust model constrain? (0=No, 1=Yes)
0
Cutoff factor for model constrain (0.0001 to 1.0)
0.0050
Allow number of model parameters to exceed data points? (0=No, 1=Yes)
1
Use extended model? (0=No, 1=Yes)
0

Reduce effect of side blocks? (0=No, 1=Slight, 2=Severe, 3=Very Severe)
2
Type of mesh (0=Normal,1=Fine,2=Finest)
1
Optimise damping factor? (0=No, 1=Yes)
1
Time-lapse inversion constrain (0=None,1&2=Smooth,3=Robust)
1
Type of time-lapse inversion method (0=Simultaneous,1=Sequential)
0
Thickness of first layer (0.25 to 1.0)
0.2500
Factor to increase thickness layer with depth (1.0 to 1.25)
1.0000
USE FINITE ELEMENT METHOD (YES=1,NO=0)
0
WIDTH OF BLOCKS (1=NORMAL WIDTH, 2=DOUBLE, 3=TRIPLE, 4=QUADRAPLE,
5=QUINTIPLE)
1
MAKE SURE BLOCKS HAVE THE SAME WIDTH (YES=1,NO=0)
1
RMS CONVERGENCE LIMIT (IN PERCENT)
0.100
USE LOGARITHM OF APPARENT RESISTIVITY (0=USE LOG OF APPARENT RESISTIVITY,
1=USE RESISTANCE VALUES, 2=USE APPARENT RESISTIVITY)
0
TYPE OF IP INVERSION METHOD (0=CONCURRENT,1=SEQUENTIAL)
0
PROCEED AUTOMATICALLY FOR SEQUENTIAL METHOD (1=YES,0=NO)
0
IP DAMPING FACTOR (0.01 to 1.0)
0.250
USE AUTOMATIC IP DAMPING FACTOR (YES=1,NO=0)
0
CUTOFF FACTOR FOR BOREHOLE DATA (0.0005 to 0.02)
0.00010
TYPE OF CROSS-BOREHOLE MODEL (0=normal,1=halfsize)
0
LIMIT RESISTIVITY VALUES(0=No,1=Yes)
0
Upper limit factor (10-50)
50.000
Lower limit factor (0.02 to 0.1)
0.020
Type of reference resistivity (0=average,1=first iteration)
0
Model refinement (1.0=Normal,0.5=Half-width cells)
1.00
Combined Combined Marquardt and Occam inversion (0=Not used,1=used)
0
Type of optimisation method (0=Gauss-Newton,2=Incomplete GN)

0
Convergence limit for Incomplete Gauss-Newton method (0.005 to 0.05)
0.005
Use data compression with Incomplete Gauss-Newton (0=No,1=Yes)
0
Use reference model in inversion (0=No,1=Yes)
1
Damping factor for reference model (0.0 to 0.3)
0.01000
Use fast method to calculate Jacobian matrix. (0=No,1=Yes)
0
Use higher damping for first layer? (0=No,1=Yes)
1
Extra damping factor for first layer (1.0 to 100.0)
5.00000
Type of finite-element method (0=Triangular,1=Trapezoidal elements)
1
Factor to increase model depth range (1.0 to 5.0)
1.000
Reduce model variations near borehole (0=No, 1=Yes)
0
Factor to control the degree variations near the boreholes are reduced (2 to 100)
5.0
Factor to control variation of borehole damping factor with distance (0.5 to 5.0)
1.0
Floating electrodes survey inversion method (0=use fixed water layer, 1=Incorporate water layer into the model)
1
Resistivity variation within water layer (0=allow resistivity to vary freely,1=minimise variation)
1
Use sparse inversion method for very long survey lines (0=No, 1=Yes)
0
Optimize Jacobian matrix calculation (0=No, 1=Yes)
0
Automatically switch electrodes for negative geometric factor (0=No, 1=Yes)
1
Force resistance value to be consistant with the geometric factor (0=No, 1=Yes)
0
Shift the electrodes to round up positions of electrodes (0=No, 1=Yes)
0
Use difference of measurements in time-lapse inversion (0=No,1=Yes)
0
Use active constraint balancing (0=No,1=Yes)
0
Type of active constraints (0=Normal,1=Reverse)
0
Lower damping factor limit for active constraints
0.4000
Upper damping factor limit for active constraints
2.5000

Water resistivity variation damping factor
8.0000
Use automatic calculation for change of damping factor with depth (0=No,1=Yes)
0
Type of I.P. model transformation (0=None, 1=square root, 3=range)
1
Model Chargeability Lower Limit (mV/V) for range
0.00
Model Chargeability Upper Limit (mV/V) for range
900.00
Use I.P. model refinement (0=No, 1=Yes)
1
Weight for I.P. data (1 to 10)
1.00
I.P. model damping factor (0.05 to 1.0)
0.25
Use program estimate for I.P. model damping factor (0=No, 1=Yes)
0
Type of I.P. smoothness constraint (1=Same as resistivity, 0=Different)
1
Joint or separate I.P. inversion method (1=Separate, 0=Joint)
0
Apparent I.P. cutoff value (300 to 899 mV/V)
899.00
Use diagonal filter (0=No, 1=Yes)
0
Diagonal filter weight (0.2 to 5.0)
1.00
Limit range of data weights from error estimates? (0=No, 1=Yes)
0
Lower limit of data weights (0.2 to 0.5)
0.30
Upper limit of data weights (2.0 to 5.0)
3.00
Use same data weights from error estimates for different time series? (0=No, 1=Yes)
0
Calculate model resolution? (0=No, 1=Yes)
0
Use L curve method? (0=No, 1=Yes)
0
Use same norms in L curve method? (0=No, 1=Yes)
0
Allow damping factor in increase in L curve method? (0=No, 1=Yes)
1
Type of borehole damping method (0=Horizontal distance from nearest borehole,
1=Distance from nearest active electrode)
0

C.2 Inversion settings – variable profile

Inversion settings
Initial damping factor (0.01 to 1.00)
0.1500
Minimum damping factor (0.001 to 0.75)
0.0200
Local optimization option (0=No, 1=Yes)
1
Convergence limit for relative change in RMS error in percent (0.1 to 20)
2.0000
Minimum change in RMS error for line search in percent (0.5 to 100)
0.5000
Number of iterations (1 to 30)
15
Vertical to horizontal flatness filter ratio (0.25 to 4.0)
1.0000
Model for increase in thickness of layers(0=default 10%, 1=default 25%, 2=user defined)
2
Number of nodes between adjacent electrodes (2 or 4)
2
Flatness filter type, Include smoothing of model resistivity (0=model changes only,1=directly on model)
1
Reduce number of topographical data points? (0=No,1=Yes. Recommend leave at 0)
0
Carry out topography modeling? (0=No,1=Yes)
1
Type of topography trend removal (0=Average,1=Least-squares,2=End to end)
2
Type of Jacobian matrix calculation (0=Quasi-Newton, 1=Gauss-Newton, 2=Mixed)
1
Increase of damping factor with depth (1.0 to 2.0)
1.0500
Type of topographical modeling (0=None, 1=No longer supported so do not use, 2=uniform distorted FEM, 3=underwater, 4=damped FEM, 5=FEM with inverse Swartz-Christoffel)
4
Robust data constrain? (0=No, 1=Yes)
0
Cutoff factor for data constrain (0.0001 to 0.1))
0.0500
Robust model constrain? (0=No, 1=Yes)
0
Cutoff factor for model constrain (0.0001 to 1.0)
0.0050
Allow number of model parameters to exceed data points? (0=No, 1=Yes)
1
Use extended model? (0=No, 1=Yes)
0
Reduce effect of side blocks? (0=No, 1=Slight, 2=Severe, 3=Very Severe)
2

Type of mesh (0=Normal,1=Fine,2=Finest)
1
Optimise damping factor? (0=No, 1=Yes)
1
Time-lapse inversion constrain (0=None,1&2=Smooth,3=Robust)
1
Type of time-lapse inversion method (0=Simultaneous,1=Sequential)
0
Thickness of first layer (0.25 to 1.0)
1.0000
Factor to increase thickness layer with depth (1.0 to 1.25)
1.0000
USE FINITE ELEMENT METHOD (YES=1,NO=0)
0
WIDTH OF BLOCKS (1=NORMAL WIDTH, 2=DOUBLE, 3=TRIPLE, 4=QUADRAPLE,
5=QUINTIPLE)
1
MAKE SURE BLOCKS HAVE THE SAME WIDTH (YES=1,NO=0)
1
RMS CONVERGENCE LIMIT (IN PERCENT)
0.100
USE LOGARITHM OF APPARENT RESISTIVITY (0=USE LOG OF APPARENT RESISTIVITY,
1=USE RESISTANCE VALUES, 2=USE APPARENT RESISTIVITY)
0
TYPE OF IP INVERSION METHOD (0=CONCURRENT,1=SEQUENTIAL)
0
PROCEED AUTOMATICALLY FOR SEQUENTIAL METHOD (1=YES,0=NO)
0
IP DAMPING FACTOR (0.01 to 1.0)
0.250
USE AUTOMATIC IP DAMPING FACTOR (YES=1,NO=0)
0
CUTOFF FACTOR FOR BOREHOLE DATA (0.0005 to 0.02)
0.00010
TYPE OF CROSS-BOREHOLE MODEL (0=normal,1=halfsize)
0
LIMIT RESISTIVITY VALUES(0=No,1=Yes)
0
Upper limit factor (10-50)
50.000
Lower limit factor (0.02 to 0.1)
0.020
Type of reference resistivity (0=average,1=first iteration)
0
Model refinement (1.0=Normal,0.5=Half-width cells)
0.50
Combined Combined Marquardt and Occam inversion (0=Not used,1=used)
0
Type of optimisation method (0=Gauss-Newton,2=Incomplete GN)
2
Convergence limit for Incomplete Gauss-Newton method (0.005 to 0.05)

0.005
Use data compression with Incomplete Gauss-Newton (0=No,1=Yes)
0
Use reference model in inversion (0=No,1=Yes)
1
Damping factor for reference model (0.0 to 0.3)
0.01000
Use fast method to calculate Jacobian matrix. (0=No,1=Yes)
0
Use higher damping for first layer? (0=No,1=Yes)
1
Extra damping factor for first layer (1.0 to 100.0)
5.00000
Type of finite-element method (0=Triangular,1=Trapezoidal elements)
1
Factor to increase model depth range (1.0 to 5.0)
1.000
Reduce model variations near borehole (0=No, 1=Yes)
0
Factor to control the degree variations near the boreholes are reduced (2 to 100)
5.0
Factor to control variation of borehole damping factor with distance (0.5 to 5.0)
1.0
Floating electrodes survey inversion method (0=use fixed water layer, 1=Incorporate water layer into the model)
1
Resistivity variation within water layer (0=allow resistivity to vary freely,1=minimise variation)
1
Use sparse inversion method for very long survey lines (0=No, 1=Yes)
0
Optimize Jacobian matrix calculation (0=No, 1=Yes)
0
Automatically switch electrodes for negative geometric factor (0=No, 1=Yes)
1
Force resistance value to be consistant with the geometric factor (0=No, 1=Yes)
0
Shift the electrodes to round up positions of electrodes (0=No, 1=Yes)
0
Use difference of measurements in time-lapse inversion (0=No,1=Yes)
0
Use active constraint balancing (0=No,1=Yes)
0
Type of active constraints (0=Normal,1=Reverse)
0
Lower damping factor limit for active constraints
0.4000
Upper damping factor limit for active constraints
2.5000
Water resistivity variation damping factor
8.0000

Use automatic calculation for change of damping factor with depth (0=No,1=Yes)
0
Type of I.P. model transformation (0=None, 1=square root, 3=range)
1
Model Chargeability Lower Limit (mV/V) for range
0.00
Model Chargeability Upper Limit (mV/V) for range
900.00
Use I.P. model refinement (0=No, 1=Yes)
1
Weight for I.P. data (1 to 10)
1.00
I.P. model damping factor (0.05 to 1.0)
0.25
Use program estimate for I.P. model damping factor (0=No, 1=Yes)
0
Type of I.P. smoothness constraint (1=Same as resistivity, 0=Different)
1
Joint or separate I.P. inversion method (1=Separate, 0=Joint)
0
Apparent I.P. cutoff value (300 to 899 mV/V)
899.00
Use diagonal filter (0=No, 1=Yes)
0
Diagonal filter weight (0.2 to 5.0)
1.00
Limit range of data weights from error estimates? (0=No, 1=Yes)
0
Lower limit of data weights (0.2 to 0.5)
0.30
Upper limit of data weights (2.0 to 5.0)
3.00
Use same data weights from error estimates for different time series? (0=No, 1=Yes)
0
Calculate model resolution? (0=No, 1=Yes)
0
Use L curve method? (0=No, 1=Yes)
0
Use same norms in L curve method? (0=No, 1=Yes)
0
Allow damping factor in increase in L curve method? (0=No, 1=Yes)
1
Type of borehole damping method (0=Horizontal distance from nearest borehole,
1=Distance from nearest active electrode)
0